

Wylfa Newydd Project

**6.4.81 ES Volume D - WNDA Development App
D12-2 - Sediment Regime**

PINS Reference Number: EN010007

Application Reference Number: 6.4.81

June 2018

Revision 1.0

Regulation Number: 5(2)(a)

Planning Act 2008

Infrastructure Planning (Applications: Prescribed Forms and Procedure) Regulations 2009

[This page is intentionally blank]



JACOBS™

Sediment Regime

Wylfa Newydd Project

Environmental Statement

Appendix D12-2

February 2018

**DOCUMENT CONTROL**

Version History					
Version	Date	Prepared by	Reviewed by	Approved by	Approved as
V01	27/06/2017	JP/MRW/KB	MRW	KB	Draft
V02	07/07/2017	JP/MRW/KB	MRW	KB	Draft
V03	24/07/2017	JP	MRW	KB	Draft
V04	13/10/2017	JP/MRW/KB	MRW	KB	Draft
V05	11/01/2018	JP	MRW	MRW	Draft
V06	15/01/2018	JP	MRW	MRW	Draft
V07	14/02/2018	JP	MRW	MRW	Final

Changes from the Previous Version	
n/a	Original version
V02	Revised following comment from Lucy Shuker and Andrew Brookes (Jacobs)
V03	Revised following Client comment. Received from Zoe Crutchfield (20/07/2017)
V04	Revised following comment from Professor Ken Pye, additional data reported.
V05	Revised following comments received from NRW and IC (Zoe Crutchfield)
V06	Revised following comments received from Alistair Davis (Jacobs)
V07	Revised following specific request received from Rob Bromley (Jacobs)

Recipient	Distribution Method		
	Paper (copies)	PDF	Online
Dr Andrew Brookes (Jacobs), Alistair Davis (Jacobs)		x	
<i>Holders of controlled copies will automatically be provided with subsequent approved versions of this document when they become available.</i>			



EXECUTIVE SUMMARY

Partrac has undertaken a comprehensive baseline sediment regime investigation as an integral part of the Environmental Impact Assessment (EIA) associated with the proposed future development of the facility at the Wylfa Newydd Project site. The scope of the investigation was defined within a series of meetings with the EIA consultant (Jacobs UK Ltd) and further enhanced by consultation with National Resources Wales (NRW). The aim of the study is to establish a comprehensive description, using available data sources, of the coastal sediment (transport) regime at the site. The approach to the work has involved a combination of qualitative assessments of site data, empirical evaluation, detailed site modelling and application of professional judgement. Assessments have been made over a range of spatial scales according to the marine processes involved. This report provides a description of the sediment (transport) regime and includes the following:

- The area of investigation;
- The general nature and form of the coastal physiography;
- The distribution of water depths and associated sediment cover;
- The nature of the tidal and wave regimes, including extremes thereof; and
- A synthesis of the sediment regime, including a conceptual understanding.

Wylfa Newydd Project site is located on the northern coastline of Anglesey (Gwynedd), a low-lying hard rock coastline interrupted by numerous embayments. It is within coastal sub-cell 10b according to the categorisation by Motyka & Brampton (1993). Sediments within the region derive from marine erosion of Devensian Till and various coastal and fluvially derived deposits. Sand and gravel lag deposits have been swept into the heads of the embayments by rising (antecedent) sea levels and form the sediments within the major bays (Cemlyn and Cemaes). Sub-tidally, a patchy veneer of variable thickness (~ 1 – 5m) and comprising a mix of coarse grain sediments (sand and gravels) admixed with a minor mud fraction in certain places, blankets the seabed. Extensive areas of bedrock devoid of sediment cover are found across the region, particularly in the central area. A conceptual model of sediment sources, inputs, pathways and sinks has been advanced in this study.

The region is classified as mesotidal (local Spring tidal range at Cemaes Bay is 4.95 m) and influenced by the astronomical variation of the tides. Peak (Spring) tidal currents vary in magnitude spatially, exceeding 2 ms^{-1} in an offshore zone delimited approximately by an arc running across the principal promontories (Trwyn Cemlyn in the west, Wylfa Head and across to Llanlleiliana Head in the east); there is a pronounced tidal asymmetry in this zone with a net drift to the west during each tide. Flow velocities decrease with distance inshore. Within the major embayments tidal currents are typically low (velocities $< 0.4 \text{ ms}^{-1}$ and commonly $< 0.2 \text{ ms}^{-1}$). The region is dominated by the formation of headland-associated recirculating gyres on both the flood and ebb phases of the tide.

The area is exposed to waves from all cardinal directions except the south and southeast. Evidence derived from an oceanographic monitoring campaign and numerical modelling exercises indicate that the offshore wave climate is dominated by a low wave (typically $H_{m0} < 1 \text{ m}$), short period ($T_z < \sim 2\text{-}5 \text{ s}$) wind sea environment. The highest incidence of offshore waves is from the southwest, but with distance inshore the modal direction changes to westerly / northwesterly due to interaction of the waves with the coastline. Wave heights commonly reduce to half the offshore height within the embayments. At intervals during winter months the site experiences more energetic conditions, with offshore wave conditions in excess of 4m and with



associated periods of ~4 – 8 s experienced. The 1:100 return period offshore wave height, which comes from the north, is 5.9 m.

Under tidal forcing, both sand and gravels are judged to be mobile within the high flow offshore region (which is largely rectilinear in form) on a regular (tidal) basis, and this is supported by limited morphological evidence of bedforms situated to the northwest of the site. The prevalence of exposed bedrock beneath the high flow offshore region suggests (under tidal forcing) there is powerful erosion potential; however, consistently low concentrations of suspended sediments recorded through the oceanographic monitoring campaign suggest that generally the sedimentary system is supply limited. Within the coastal embayments (Cemlyn Bay, Cemaes Bay, Porth y Pistyll) bottom sands and gravels are stable under tidal action. These lines of evidence suggest there is not a large volume of sediments being transported in suspension by regular tidal action. Average tidally generated suspended sediment concentrations are centred on approximately $\sim 30 \text{ mg l}^{-1} \pm 10 \text{ mg l}^{-1}$ at the offshore monitoring stations, reduced by $\sim 50\%$ at the inshore monitoring stations. These data indicate that tidal resuspension elevates background near-bed suspended sediment concentrations by a factor of 5 – 10. Suspended sediment concentrations across the site are influenced by the fluvial input from five catchment areas, though this is not considered to be a significant contributor to coastal sediment concentrations. Concentrations are, from time to time, enhanced by the presence of algal blooms.

Superposition of wave action on tides, as found during winter months, can commonly enhance sediment transport. However, this investigation indicates that surface wave action only rarely penetrates to the seabed. Consideration of a 2.0m H_{mo} wave (a typical winter condition) onto a Spring tide produces measurable enhancement of excess bed stress across the offshore high velocity region, much of the interior of Cemaes Bay, the outer part of the sand lens within Cemlyn Bay and some areas within Porth y Pistyll. The worst storm (nearly a 1 in 10 year magnitude event) recorded within the monitoring period occurred during 13 – 15th November, 2010. This was recorded at both of the deep water monitoring stations (s2 and s4). The peak suspended sediment concentrations observed during this event were 37 mg l^{-1} and 289 mg l^{-1} at monitoring station s2 and s4, respectively, which indicates the loadings generated by such storms and the influence of depth on resuspension (more sediment is suspended at the shallower monitoring station, s4). Bigger wave events progressively expand the area across which bed stresses become high. Within the embayments, currents are low and the sediment relatively coarse; since waves act only to bring sediments into suspension storm events are not anticipated to change the pattern of surficial cover greatly, nor are they anticipated to promote onshore-offshore transport of sands. Thus, the embayments generally act as closed sediment compartments, even under storms, with little or no exchange of sediment from one bay to the next. Within the high flow offshore zone wave amplification of sediment transport is likely under big storms, with perhaps an order of magnitude increase in suspended sediment concentrations, with any resuspended material likely to be re-distributed in the alongshore direction by the tidal currents.

It is widely expected that climate change will result in global scale effects which will be manifested at regional scales by increased storminess and rising mean sea level. An increase in the frequency and magnitude of storm events will increase the potential for resuspension of sediment across the site due to the likelihood of wave conditions occurring which are sufficient to penetrate to the seabed. However, despite resuspension frequencies and magnitudes being enhanced, as the tidal currents are comparatively weak in many of the inshore areas the sediment response, and corresponding advection distances and distribution patterns, would remain similar. The recirculating gyres around Wylfa headland would still act to retain sediments resuspended by wave action locally. Sea level rise may impact the coastline (i.e. via coastal flooding and coastal erosion), in particular sensitive geomorphological features such as Esgair Gemlyn, but the anticipated magnitude of change is small in relation to storm surges which occur at the site.

ABBREVIATIONS

POL	Proudman Oceanographic Laboratory
NTSLF	National Tidal Sea Level Facility
AWAC	Automated Wave and Current Meter
ADCP	Acoustic Doppler Current Profiler
MV	Moving Vessel
VM	Vessel Mounted
UKCP	United Kingdom Climate Projections
MOLF	Material Off Loading Facility
H_{m0}	Significant Wave Height
T_z	Mean Zero Crossing Period
T_{m02}	Spectral estimate of the mean zero crossing period
SMP	Shoreline Management Plan
PDZ	Policy Development Zone
BGS	British Geological Survey
OD	Ordnance Datum
CD	Chart Datum
τ_0	Bed Shear Stress
τ_{ocrit}	Critical Bed Shear Stress
WS	Water Sample
S	Station (monitoring)
FTU	Formazin Turbidity Unit
HD	Hydrodynamic
H_{max}	Maximum Wave Height
SSC	Suspended Sediment Concentration
SPA	Special Protected Area
SSSI	Site of Special Scientific Interest

SAC	Special Area of Conservation
NRW	National Resources Wales
EIA	Environmental Impact Assessment
DCO	Development Consent Order
ES	Environmental Statement
HAT	Highest Astronomical Tide
SPM	Suspended Particulate Material



CONTENTS

1. INTRODUCTION	13
1.1 Project Overview	13
2. OUTLINE METHODOLOGY	14
2.1 Area of Investigation	14
2.2 Method of Investigation	14
3. BATHYMETRY	18
3.1 Survey Datasets	18
3.2 Generalised Distribution of Water Depths	18
3.3 Cemlyn Bay and Porth-y-Pistyll	18
3.4 North and Northwest of Wylfa Head	19
3.5 East of Wylfa Head towards Cemaes Bay	19
4. HYDRODYNAMIC REGIME	20
4.1 Oceanographic Survey Datasets	20
4.2 Water Elevations	20
4.3 Non-Tidal Currents	21
4.4 Tidal Flows	22
4.5 Tidal Asymmetry and Tidal Excursion Distances	24
5. WAVE REGIME	26
5.1 Existing (Observational) Wave Data	26
5.2 Wave Modelling	31
5.3 Bed Stress due to Combined Waves and Currents	34
6. SEDIMENT REGIME	35
6.1 Regional Setting	35
6.2 Seabed sediments	47
6.3 Offshore Sediment Transport by Tides and Waves	50
6.4 Extreme Events, Evolving Baseline and the Importance of Climate Change	57
6.5 Summary of Sediment Transport Regime	59
6.6 Conceptual Understanding of the Sediment Transport Regime	63
6.7 Esgair Gemlyn	65
7. REFERENCES	68
APPENDIX 1 – FIGURES	70

FIGURES

Figure 1. A schematic diagram detailing the various components which underpin the assessment of the sediment regime.....	70
Figure 2. Map showing the extent of coastal cell – sub cell 10b. Source: Motyka & Brampton (1993).	71
Figure 3. The approximate 'near field' and 'far field' boundary.....	72
Figure 4. The study area and the SWAN model grid (over all 500m & nested 200m and 50m grids).....	73
Figure 5. Model grid and bathymetry for the Delft3D HD model. Source: RWE (2017).....	74
Figure 6. General distribution of water depths across the investigation site. Note depths relative to OD. Source: Horizon (2011).....	75
Figure 7. Seabed bathymetry in Cemlyn Bay and Porth-y-Pistyll. Areas of exposed bedrock are marked. Source: Titan (2009).....	76
Figure 8. Seabed bathymetry to the north and northwest of Wylfa Head. Source: Titan (2009).	77
Figure 9. Bathymetry to the east of Wylfa Head. Source: Titan (2009).	78
Figure 10. Wylfa oceanographic monitoring stations. The location of the four fixed point monitoring systems are marked (S2, S4, S9 and S11). Source: Horizon (2012).	79
Figure 11. Example of water level variation through time for each of the four oceanographic monitoring stations. Data source: Horizon (2012).....	80
Figure 12. Depth-averaged current magnitude by deployment (i.e. each colour represents a separate instrument deployment) at the four oceanographic monitoring stations. Data Source: Horizon (2012).....	81
Figure 13. Current roses for the four oceanographic monitoring stations. Data source: Horizon (2012). ...	82
Figure 14. The vessel mounted ADCP survey. The plots show the data from the Spring tide currents. Source: Jacobs UK Ltd, 2016	83
Figure 15. Depth averaged velocity vector plot (upper panel) showing the current velocity magnitude (and direction) at neap tide, mid ebb; the corresponding tidal bed stresses are shown in the lower panel.	84
Figure 16. Depth averaged velocity vector plot (upper panel) showing the predicted current velocity magnitude (and direction) at neap tide, mid flood; the corresponding tidal bed stresses are showing in the lower panel.	85
Figure 17. Depth averaged velocity vector plot (upper panel) showing the current velocity magnitude (and direction) at spring tide, mid flood; the corresponding tidal bed stresses are shown in the lower panel.	86
Figure 18. Depth averaged velocity vector plot (upper panel) showing the current velocity magnitude (and direction) at spring tide, mid ebb; the corresponding tidal bed stresses are shown in the lower panel.	87



Figure 19. Illustration of tidal asymmetry at station s4 (offshore). This analysis reveal a longer (by approximately 2 hrs), and slightly stronger (by approximately 11%) ebb current phase. Data source: Horizon (2012)	88
Figure 20. Lagrangian (continuous in time) trajectories of drogue releases made during the oceanographic survey. Data Source: Horizon (2012)	89
Figure 21. Time series showing the significant wave height (H_{m0}) observed at the four monitoring sites. Data Source: Horizon (2012)	90
Figure 22. Wave roses for the four monitoring stations (July 2010 – November 2011) showing significant wave height (H_{m0}) (left column) and wave period (T_z) (right column) and the associated direction. Data Source: Horizon (2012)	91
Figure 23. Frequency of predicted significant wave heights (H_{m0}) at model point 3 for the entire dataset ('all') and for the North sector only ('north'). Data Source: RWE (2017)	92
Figure 24. Frequency of predicted associated wave period at model point 3 for the entire dataset ('all') and for the North sector only ('north'). Data Source: RWE (2017)	93
Figure 25. Wave roses showing significant wave height (H_{m0}) (left) and wave period (T_{m02}) (right) and the associated direction predicted at model point 3. Data Source: RWE (2017)	94
Figure 26. The position of the nearshore prediction points (1 -10) and 'offshore' model point 3 in relation to the Anglesey coastline. Prediction points 3, 4 and 6 (marked 0) and points 7, 8 and 9 (marked 1) provide two shore-normal gradients useful for examining wave modification at the site. Source: HR Wallingford (2017)	95
Figure 27. The predicted wave height across the site for a typical wave scenario (H_{m0} 0.9 m, 228°) on a Spring tide.	96
Figure 28. The predicted wave height across the site for a winter wave scenario (H_{m0} 2.0 m, 228°) on a Spring tide.	97
Figure 29. The predicted significant wave height across the site for a high (98%ile) wave from the north scenario (H_{m0} 2.85 m, 346°) on a Spring tide.	98
Figure 30. Geospatial distribution of maximum bed shear stress acting upon the bed during a Spring tide, mid-Ebb condition (the strongest currents) with a typical winter wave scenario (H_{m0} 2.0m, 343°).	99
Figure 31. Geospatial distribution of maximum bed shear stress acting upon the bed during a Spring tide, mid-ebb condition (the strongest currents) with an high wave (98%ile) from the north scenario (H_{m0} 2.85m, 358°).	100
Figure 32. Boomer record showing typical conditions in Cemaes Bay. The sediment lenses within Cemaes bay are clearly visible (Source: Titan, 2009).	101
Figure 33. The locations of the samples collected in 2010 (grab, borehole, water). Source: Jacobs UK Ltd (2011)	102
Figure 34. Particle size data from samples collected at various locations across the site during the benthic sampling campaign in 2011. Data source: Jacobs UK Ltd (2011).	103
Figure 35. Seabed features plot with grain size data presented in the form of gravel: sand: mud [> 2 mm; 2 mm – 0.063 mm: < 0.063 mm] ratio data, superimposed on the sediment type determined from geophysical survey (AGDS). Source: Jacobs (2015).....	104



Figure 36. The 'anonymous' sediment map which distinguishes between the two principal seabed components (sediment and bedrock).	105
Figure 37. Tidal stress exceedance plots, by station, for various size fractions in Table 27	106
Figure 38. Time series overlay showing the fraction-specific critical stress values for sand in relation to stress amplitude at station s9. Data Source: Horizon (2012).	107
Figure 39. Geospatial excess bed stress plots for the sand fraction for a Spring tide, mid-ebb condition. 108	
Figure 40. Geospatial excess bed stress plot for the fine gravel fraction for a Spring tide, mid-ebb condition (the strongest currents).	109
Figure 41. Time series of SPM concentration, significant wave height (H_{m0}) (orange), maximum wave height (H_{max}) (orange), and current velocity for all deployments at monitoring station, s2. Data Source: Horizon (2012).	110
Figure 42. Time series of SPM concentration, significant wave height (H_{m0}), maximum wave height (H_{max}) (orange), and current velocity for all deployments at monitoring station, s4. Data Source: Horizon (2012).	111
Figure 43. Time series of SPM concentration, significant wave height (H_{m0}), maximum wave height (H_{max}) (orange), and current velocity for all deployments at monitoring station, s9. Data Source: Horizon (2012).	112
Figure 44. Time series of SPM concentration, significant wave height (H_{m0}), maximum wave height (H_{max}) (orange), and current velocity for all deployments at monitoring station, s11. Data Source: Horizon (2012).	113
Figure 45. SSC exceedance plots, by station. The background suspended sediment concentration values for offshore sites (30 mg l ⁻¹) and inshore sites (20 mg l ⁻¹) are marked. Data source: Horizon (2012).	114
Figure 46. Geospatial excess bed stress plot for the sand fraction for a Spring tide, mid-ebb condition (the strongest currents) with a typical wave scenario (H_{m0} 0.9 m, 228°).	115
Figure 47. Geospatial excess bed stress plot for the sand fraction for a Spring tide, mid-ebb condition (the strongest currents) with a winter wave scenario (H_{m0} 2.0 m, 228°).	116
Figure 48. Geospatial excess bed stress plot for the sand fraction for a Spring tide, mid-ebb condition (the strongest currents) with an high wave from the north (98%ile) (H_{m0} 2.85 m, 358°).	117
Figure 49. Geospatial excess bed stress plot for the fine gravel fraction for a Spring tide, mid-Ebb condition (the strongest currents) with a typical wave scenario (H_{m0} 0.9 m, 228°).	118
Figure 50. Geospatial excess bed stress plot for the fine gravel fraction for a Spring tide, mid-ebb condition (the strongest currents) with a winter wave scenario (H_{m0} 2.0 m, 228°).	119
Figure 51. Geospatial excess bed stress plot for the fine gravel fraction for a Spring tide, mid-ebb condition (the strongest currents) with an high wave from the north scenario (H_{m0} 2.85m, 358°).	120
Figure 52. The conceptual understanding of the local sediment regime in proximity to Wylfa head. It has been collated from a variety of sources and informed by expert judgement. The transport pathways are indicative and the arrows represent inferred magnitudes of transport.	121
Figure 53. Comparison of 2010 and 2017 aerial LiDAR data. Data source: Jacobs UK Ltd (2017)	122



Figure 54. Wave roses of significant wave height (H_m0) and the associated direction for the 30 year hind-cast modelled wave data at model points 6 (a) and 4 (b) 123

Figure 55. Frequency of occurrence of significant wave heights (H_m0) for the 30 year hind-cast modelled wave data at points 6 (a) and 4 (b). 124

TABLES

Table 1. Data and information sources used within this commission.	14
Table 2. Modelled data and information sources used within this commission.	15
Table 3. Summary of the model runs performed for this study together with the rationale their selection. The model outputs for bed stress and velocity are also detailed. Source: RWE (2017) and HR Wallingford (2017).	17
Table 4. Field surveys conducted as part of the oceanographic monitoring programme relevant to this report. Source: Horizon (2012).....	20
Table 5. Water elevation statistics at the Holyhead Tide Gauge from 2008 -2016. Data Source: NTSLF (2017).	21
Table 6. The ten highest recorded levels for the Holyhead tide gauge in the lead up to November 2017. Data Source: National Tidal Sea Level Facility (NTSLF) (2017).	22
Table 7. Extreme tide levels, including tidal surge. Please note the data does not account for future sea level rise. Data source: Halcrow (2012).	22
Table 8. Statistical information related to measured currents at the oceanographic monitoring stations. Data Source: Horizon (2012).....	23
Table 9. Joint probability distribution of significant wave heights (H_{m0}) and peak spectral wave approach measured over the deployment period at monitoring station, s2. Data Source: Horizon (2012).	26
Table 10. Joint probability distribution of significant wave heights (H_{m0}) and peak spectral wave periods (T_z) measured over the deployment period at monitoring station, s2. Data Source: Horizon (2012).	27
Table 11. Joint probability distribution of significant wave heights (H_{m0}) and peak spectral wave approach measured over the deployment period at monitoring station, s4. Data Source: Horizon (2012).	27
Table 12. Joint probability distribution of significant wave heights (H_{m0}) and peak spectral wave periods (T_z) measured over the deployment period at monitoring station, s4. Data Source: Horizon (2012).	28
Table 13. Joint probability distribution of significant wave heights (H_{m0}) and peak spectral wave approach measured over the deployment period at monitoring station, s9. Data Source: Horizon (2012).	28
Table 14. Joint probability distribution of significant wave heights (H_{m0}) and peak spectral wave periods (T_z) measured over the deployment period at monitoring station, s9. Data Source: Horizon (2012).	29
Table 15. Joint probability distribution of significant wave heights (H_{m0}) and peak spectral wave approach measured over the deployment period at monitoring station, s11. Data Source: Horizon (2012).	29
Table 16. Joint probability distribution of significant wave heights (H_{m0}) and peak spectral wave periods (T_z) measured over the deployment period at monitoring station, s11. Data Source: Horizon (2012).	30

Table 17. Key statistics associated with the wave regime at the site derived from the oceanographic data collected at the four monitoring stations. Data Source: Horizon (2012).....	30
Table 18. Joint probability distribution of significant wave heights (H_{m0}) and associated direction (compass quadrants) predicted at model point 3. Data Source: RWE (2017).....	31
Table 19. Joint probability distribution of significant wave heights (H_{m0}) and peak spectral wave periods (Tm02) predicted at model point 3. Data Source: RWE (2017)	32
Table 20. Key statistics associated with the wave regime at the site derived from the modelled data collected at model point 3. Data Source: RWE (2017).....	32
Table 21. Wave height (H_{m0}) and direction along two shore-normal gradients (data garnered from nearshore prediction point 3, 4 and 6 and nearshore prediction point 7, 8 and 9, respectively). Data source: HR Wallingford (2017)	33
Table 22. The description of the coastal regime at sub-cell 10b (Isle of Anglesey) as described in Motyka & Brampton (1993).	36
Table 23. Wylfa area shallow sub-seabed stratigraphy (Titan, 2009).	44
Table 24. Down-core sediment description of the Wylfa Newydd site boreholes to a depth of 5 m. Source: Fugro (2010, 2010b).....	48
Table 25. Suspended sediment monitoring data. Data source: Horizon (2017).	49
Table 26. Suspended sediment monitoring data (Total Suspended Solids mg l ⁻¹). Data source: Jacobs UK Ltd (2017).....	50
Table 27. Summary of critical stress % exceedance for various bottom sediment size fractions. Following the method of Soulsby (1997), based upon the entire available flow velocity records, and using a C100 value of 0.0024. Data source: Horizon (2012)	52
Table 28. The limiting significant wave height required for waves to feel the seabed at the locations of the four monitoring stations. The percentage of time waves which exceed these limiting thresholds are observed are detailed and the modal wave direction noted. Data Source: Horizon (2012).....	54
Table 29. The associated nearbed suspended sediment concentrations (SSC) during a ~1:10 storm event detailed in Horizon (2012). The corresponding nearbed suspended sediment concentrations recorded at monitoring stations, s9 and s11, were not reported. Source: Horizon (2012).....	55
Table 30. Extreme significant wave height and direction estimated for offshore model points 1-5 for 1, 10, 20, 50, 100 and 200 year return periods. HR Wallingford (2015). These values are generated from a 3 hourly record and are 3 hourly averaged values. The most likely associated mean wave direction is 285 - 15° N (HR Wallingford, 2015). The position of the model points is detailed in Figure 2.....	58
Table 31. Estimates of relative sea level rise relative to levels observed in 1990 under three differing scenarios. Data Source: UKCP09 (2017)	58
Table 32. Summary statistics for significant wave height extracted from the 30 year hindcast wave model Wave Height H_{m0} (m) percentile. Data source: (HR Wallingford, 2017)	67

1. INTRODUCTION

1.1 Project Overview

Jacobs UK Limited commissioned Partrac Limited to undertake a baseline assessment of the offshore sedimentary regime at the Wylfa Newydd Development Area, on the coast of North Anglesey, Wales. The assessment provides the developer, consultants and other stakeholders with the regional and site-specific characterisation of the sediment regime in proximity to the site. This will enable baseline environmental conditions to be determined, against which the effects of the proposed development, and the in-combination and cumulative effects of other local developments can be assessed.

The construction, operation and decommissioning of the Power Station Site have the potential to bring about changes to near (e.g. within ~ 500m from the proposed location) and far field (e.g. the coastline, sites of scientific and conservation interest outside the direct survey area where remote effects may occur) hydrodynamic and sedimentary processes. To assess the impacts of the proposed development on hydrodynamic and sedimentary processes (termed the sediment regime) it is considered prudent to thoroughly investigate and assess the baseline (i.e. currently occurring pre-development) sediment regime at the Wylfa Newydd Development Area. This Report does not cover the sediment regime at the Holyhead North Disposal Site. Rather information/ data related to this specific site for disposal of dredgings is detailed in Chapter D13 and in the associated appendix to the chapter entitled “IS040 Holyhead North Dredge Disposal – 3D Sediment Transport Modelling” (Jacobs, 2017a).

The approach adopted for the work has been to complete a combination of qualitative and quantitative assessments of site data; empirical evaluation; detailed site modelling; and the application of professional judgement. Assessments have been performed over a range of spatial scales according to the marine processes involved. This report provides a description of the following relating to the site of the proposed Wylfa Newydd Development Area:

- The area of investigation;
- The general nature and form of the coastal physiography;
- The distribution of water depths and associated sediment cover;
- The nature of the tidal and wave regimes, including extremes thereof; and
- A synthesis of the sediment regime, including transport pathways and a conceptual understanding.

Figure 1 details the components which underpin the assessment of the sediment regime.



2. OUTLINE METHODOLOGY

2.1 Area of Investigation

The proposed Wylfa Newydd Development Area is located within Sub Cell 10b of the national classification for identifying major regional littoral drift cells advanced by Motyka & Brampton (1993) (Figure 2). For the purposes of this study the area of investigation reflects boundaries implemented within the hydrodynamic (HD) and wave models used to support the Development Consent Order (DCO) Environmental Statement (ES) assessment (Section 2.2.2 provides further details). In the context of this assessment the 'near' and 'far' field have been defined as follows:

Near field: A detailed inner boundary area encompassing the development site and coincident with the marine area between Trwyn Cemlyn in the west to Llanlleiana Head in the east, and extending ~2 km offshore.

Far field: The shelf sea boundary, and the majority length of the northern coastline of Anglesey, extending ~3 km offshore.

The adoption of these spatial scales facilitates a robust assessment of the sediment regime at, and in the vicinity of, the proposed Power Station Site. These spatial scales are also plotted on a map of the area (Figure 3).

2.2 Method of Investigation

2.2.1 Data and Information Sources

A wide variety of sources have been consulted during the compilation of this assessment. Site specific geophysical, geotechnical and metocean data sets have been extensively used, and these have been supported through inclusion of regional and site-specific data from elsewhere. Table 1 summarises the data sources consulted.

Table 1. Data and information sources used within this commission.

Data Source	Study/Data Name	Date	Data Theme(s)	Data Location
Horizon Nuclear Power	Wylfa Newydd DCO Environmental Statement	2017	Coastal Processes, Coastal Geomorphology, Seabed features, habitats/landscapes	At Power Station Site
Halcrow	Wylfa Marine Off Loading Facility Feasibility Study	2012	Numerical Wave Modelling, Wave Transformation	At Power Station Site
Titan Environmental Surveys Ltd	Wylfa Power Station Preliminary Nearshore Geophysical Investigation	2009	Seabed features	At Power Station Site
Horizon, Titan Environmental Surveys Ltd	CSO286 Wylfa Oceanography Interpretative report	2009/ 2012	Oceanographic regime	At Power Station Site
Fugro	Wylfa New Build Intermediate Offshore Ground Investigation	2010/ 2016	Geotechnical factual report, Borehole logs	At Power Station Site
HR Wallingford	Wylfa Newydd Further wave modelling, Phase 2	2016	Wave regime, historic wave data	At Power Station Site
Jacobs	Wylfa Newydd Project	2015	Subtidal Benthic Assessment	At Power Station Site
Jacobs	Sediment Mobility Potential Note	2016	Sediment mobility potential	At Power Station Site



Data Source	Study/Data Name	Date	Data Theme(s)	Data Location
Jacobs	Wylfa Newydd Project Benthic Ecology Surveys Report	2015	Benthic ecology, Sediment characterisation, particle size data	At Power Station Site
K Pye Associates	Cemlyn Bay and Adjoining Areas, Anglesey: Geomorphological Assessment	2010/2016	Coastal geomorphology, geological character, coastal processes	North Anglesey
Royal Haskoning /Pembrokeshire Unitary Authority	West of Wales Shoreline Management Plan 2 – Section 4. Coastal Area G	2012	Shoreline processes	Isle of Anglesey
Natural Resources Wales	Marine Character Areas, MCA O6 North Anglesey Coastal Waters	2015	Background, broader site description	North Anglesey Coastal Waters
National Oceanography Centre	National Tidal and Sea Level Facility (NTSLF)	2017	Tide Gauge and historic statistics	Holyhead North Disposal Area
Various stakeholder engagement	-	various	Various	At Power Station Site
British Geological Survey	1:50,000 scale geological map for Anglesey (sheets 92.93, 94, 105 and 106)	2017	Geology	At Power Station Site

2.2.2 Modelling Tools and Applications

Development of the knowledge base in relation to the sediment regime has been assisted through the utilisation of several numerical modelling approaches at a range of spatial and temporal scales. For the present study the combination of modelling tools listed in Table 2 has been selected to enable a thorough and complete consideration of the relevant coastal sedimentary issues.

Table 2. Modelled data and information sources used within this commission.

Process	Regional Scale (Far Field)	Local Scale (Near Field)
Waves (refraction, shoaling & breaking)	AMEC - HR Wallingford (Simulating Waves Nearshore [SWAN] wave model). Driven by MetOffice WaveWatchIII model.	AMEC- HR Wallingford (Simulating Waves Nearshore [SWAN] wave model). Driven by MetOffice WaveWatchIII model.
Hydrodynamics	Deltires Delft3d framework	Deltires Delft3d framework
Coupled currents and waves	Coupling of SWAN model with Delft3d	Coupling of SWAN model with Delft3d

The AMEC-Wallingford SWAN Wave Model

Numerical modelling of waves in coastal areas is a useful means of understanding wave climatology and wave processes over broad areas and over longer periods. Wave models typically use long-term historical wind datasets to simulate to force the formation of waves over a water body. They generate a spectrum of historic wave conditions, which are validated at certain times and points in space using measured wave data. As the period of time over which in situ data are available is limited and the wave climate can display a high degree of intra-annual variability, modelling studies enable short-term monitoring campaigns to be extended

to the long term in order to derive wider data for sediment transport description and estimation of extreme metocean conditions.

Wave modelling studies conducted for various purposes have provided information on the regional – local wave regime at the proposed Wylfa Newydd Development Area. Of principal interest are the two numerical modelling exercises (principally utilising the SWAN program) conducted for the site, by Halcrow, (2012), and more recently HR Wallingford/AMEC FW (HR Wallingford, 2015 and HR Wallingford/Amec FW, 2016). The modelling conducted by Halcrow was undertaken to support the design of a proposed Material Off-Loading Facility (MOLF) for the site. Comparatively, the wave modelling undertaken by AMEC/HR Wallingford formed part of a flood hazard assessment for the Wylfa Newydd Project and thus contained associated extremes analysis, including joint probability with sea levels, climate change assessment and estimation of overtopping rates.

The AMEC-HR Wallingford SWAN model was driven at the outer boundary using wave and wind data (a 3-hourly record) from the MetOffice WaveWatchIII model calibrated to collected metocean data (HR Wallingford, 2015), to generate results over a 35 year period from January 1980 to June 2015. The SWAN model domain includes all of the north coast of Anglesey. The model grid size was nested, and varied from 500m offshore, through 200m, to a 50m and 20m grid nearshore (Figure 4). Results from the model were generated for five offshore model points which were located at equally spaced locations southward of the northern boundary of the 50m grid. A full description of the setup of the model and subsequent calibration/validation of the model is provided in (HR Wallingford, 2015 and HR Wallingford/Amec FW, 2016).

The Deltires Delft3d Hydrodynamic Model

An appreciation of the wider distribution and geospatial variation of tidal currents across the site is available through development of a site specific hydrodynamic model developed using the Delft3d modelling software. A depth-averaged hydrodynamic model has been developed within the Deltires Delft3d framework. The model has three nested grids of increasing resolution: an outer 2D grid and two 3D inner grids. The resolution of the grids (mesh size) increases from 350m in the outer grid to 70m in the mid grid and to 23m in the innermost grid (Figure 5). The grid configuration used increases in nodal density around the immediate proposed development area, decreasing in density in both the alongshore and offshore directions. The model returns a single value for current magnitude and direction at any given nodal point in time. Bathymetry data sources for the model include survey datasets collected on behalf of Horizon Nuclear Power (inshore), and various survey and digital charts for offshore region from SeaZone. The development and validation of the hydrodynamic model has been described (in a series of published reports (detailed in RWE, 2017), and the model has been subject to external independent auditing (ABPmer, 2016).

Water movement associated with tides (and waves) creates a frictional drag on seabed sediments termed bed stress. The frictional drag per unit area denoted by τ_0 , is measured in units of Newtons per square metre (Nm^{-2}). The Delft3d model computes bed stresses from the velocity field and bed roughness information and data are presented in the form of bed stress maps. The bed stress acting on sediments is the principal driver of sediment entrainment (mobilisation and transport).

Coupled Wave and Hydrodynamic Modelling

In shallow continental shelf environments waves are also capable of sediment suspension and transport if the energy associated with the wave is able to penetrate to the seabed. Except during brief periods of high/low tide standstill (when currents are close to zero), the presence of waves will mean that bottom sediments will experience a combined stress (i.e. one due to wave action plus tidal currents). This superposition is complex and non-linear. Various, often very complex, methods exist to describe the bottom boundary layer under combined current and wave action and the resulting virtual roughness.



The setup and calibration of the coupled wave and hydrodynamic model is described in RWE (2017). For the assessment of wave plus current interactions (and definition of associated bed stresses) the Amec-HRWallingford SWAN wave model was adapted to conform to the Delft3d implementation of SWAN in online mode; thus, at each coupling interval the influence of the hydrodynamics on the wave climate was computed. The coupled flow and wave model was then used to determine the maximum bed shear stress impacting upon the seabed due to the combinations of tidal flow and waves. The coupled flow and wave model calculated bed shear stress from the depth averaged current at mid ebb and mid flood over a spring and neap tide cycle and then superimposed waves to compute wave-current bed shear stresses. Waves chosen were typical summer wave, winter wave and an extreme wave from north direction.

2.2.3 Model Application

For the investigation of the baseline sediment regime the following series of model runs were developed and implemented (see Table 3).

Table 3. Summary of the model runs performed for this study together with the rationale their selection. The model outputs for bed stress and velocity are also detailed. Source: RWE (2017) and HR Wallingford (2017).

Model Type	Process	Scenario	Output	Rationale
HD Model	Tides alone	Spring tide	Mid-flood velocity / stress vector map Mid-ebb velocity / stress vector map	Tidal velocity and associated stress during the maximum tidal phase (Spring tides) (i.e. to investigate the strongest tidal currents).
		Neap tide	Mid-flood velocity / stress vector map Mid-ebb velocity / stress vector map	Tidal velocity and associated stress during the minimum tidal phase (Neap tides) (i.e. to investigate the weakest tidal currents).
Coupled	Tides plus Waves	Spring tide + typical wave (H_{m0} 0.9 m, 228°)	Mid-ebb velocity / w/c stress vector map	Tidal velocity and associated stress during the maximum tidal phase (Spring tides) during a period of 'typical waves' (i.e. to simulate 'typical' summertime conditions).
		Spring tide + winter wave (H_{m0} 2.0 m, 343°)	Mid-ebb velocity / w/c stress vector map	Tidal velocity and associated stress during the maximum tidal phase (Spring tides) during a period of 'typical winter waves' (i.e. to simulate 'typical' wintertime conditions).
		Spring tide + high wave from N (H_{m0} 2.85 m, 358°); 98% wave condition.	Mid-ebb velocity / w/c stress vector map	This condition is also referred to as the 98% wave condition, as it was derived from statistical analysis of the 35.5 yr SWAN model output for the offshore boundary Point 3 (see Figure 4). Selected to represent tidal velocity and associated stress during the maximum tidal phase (Spring tides) during a period of high waves from the north (i.e. to simulate a powerful storm event).

3. BATHYMETRY

3.1 Survey Datasets

High resolution swath bathymetry data was collected during a series of surveys conducted by Titan in 2009/2010¹. These data are presented as seabed bathymetry plots, with a colour-banded bathymetry merged with a shaded relief image chart. All charts are presented at 1:2500 scale contoured at a vertical interval of 1 m, relative to Ordnance Datum (OD) (Titan, 2009). The bathymetry data is presented in four plots covering the following survey areas:

- General distribution of water depths across the site (Figure 6);
- Cemlyn Bay and Porth-y-Pistyll (Figure 7);
- North and Northwest of Wylfa Head (Figure 8); and,
- East of Wylfa Head towards Cemaes Bay (Figure 9).

3.2 Generalised Distribution of Water Depths

Within the boundaries of the survey the bathymetry data shows seabed levels range from -3.0m OD at the south-easterly limit within the small cove inside Cemaes Bay, to -42.0m OD at the north-westerly extent of the survey area (Figure 6). Between the -22.0m OD and -30.0m OD contour the seabed has a very slight gradient with a slightly more complex bathymetric structure to the north of the site. In the outer survey area the seabed consists of relatively smooth, tidally swept sediments. Bedform features such as ripples and megaripples are evident on the seabed, though these features are generally poorly defined. At a number of locations across the survey area various rock outcrops, irregularly located, rise up to around 4 to 5 metres above the general seabed level. Offshore from Wylfa Head, the seabed level quickly reduces from ~ -24.0m OD to ~ -36.0m OD with a series of depressions within the seabed reducing the seabed level in places -42.0m OD.

3.3 Cemlyn Bay and Porth-y-Pistyll

In Cemlyn Bay and Porth-y-Pistyll seabed levels range from -2.0m OD to -30.0m OD (Figure 7). Bathymetry in this area ranges from -5.0m OD in the small cove at Porth-y-Pistyll down to -19.0m OD within the sandy centre of the bay and -26.0m OD offshore. The data reveals the inshore coastal zone in this area is dominated by exposed bedrock, with various areas of exposed bedrock appearing further offshore towards the centre of the survey area. The entrances to Cemlyn Bay and Porth-y-Pistyll are separated by a rocky headland. The entrance to each bay is characterised by shallow (<14.0m OD) gently sloping gradients extending out to the centre of the survey area.

¹ The data presented are the most up-to-date data available. Despite the [limited] potential for geomorphological change in the elapsed time between survey and assessment, based upon the authors' professional judgment and understanding of nearshore coastal dynamics in the vicinity of the development site, these data are considered to be appropriate for the assessment.



3.4 North and Northwest of Wylfa Head

To the north (and northwest) of Wylfa Head seabed levels range from -10.0m OD to -30.0m OD. Around the immediate vicinity of Wylfa Head, large rocky outcrops dominate and shelve off quickly into deeper water (Figure 8). The area consists of a gently undulating seafloor at depths of -32m OD to -34m OD, with a series of complex depressions up to 7m deeper than the local seabed. In the north-western corner of the survey the seabed exhibits an area of low relief, due to the presence of poorly defined megaripples lying on a gently undulating seabed. Depths in the NW corner of the survey area range from -31m OD down to -42m OD. In these deeper areas complex seabed topography is visible within the data. The generally gently sloping seabed becomes gouged and multiple seabed depressions are visible. Two large rocky outcrops (pinnacles) rise between 3m and 8m above the general seabed level. A significant gully feature is also evident within which the seabed level reduces to -41.0m OD.

3.5 East of Wylfa Head towards Cemaes Bay

Eastward from Wylfa Head the large rocky outcrop shelves off quickly and a large shallow area is present, stretching from Wylfa Head towards Cemaes Bay with seabed levels ranging from -4.0m OD to -12.0m OD (Figure 9). The seabed east of Wylfa Head appears to be distinctly different from the seabed to the west. The north-eastern part of the survey area is characterised by a wide gently sloping expanse towards a deeper basin-like feature parallel with Wylfa Head. South of the break of slope at -30m OD, the seabed shelves to the crest of a sand bank occupying the centre of Cemaes Bay. The bank has a 260-080° trending crest with minimum depth at the crest of -13m OD. Well-developed megaripples are present on the bank's northern face. Moving inshore a shallow seabed depression is present, where depths increase gently to -15m OD then rise sharply to the shoreline above a pronounced break of slope at -9m OD.



4. HYDRODYNAMIC REGIME

The hydrodynamic regime is defined herein as the behaviour of bulk water movements driven by the action of tides and non-tidal influences such as river flows and meteorological conditions (winds, atmospheric events and storm surges).

4.1 Oceanographic Survey Datasets

A range of available datasets have been utilised in these analyses (see Table 4). A metocean survey (data acquisition) programme was conducted by the survey company Titan collecting wave and current data at the Wylfa Newydd Development Area (Horizon, 2012). Table 4 summarises the surveys conducted of relevance to this report and that have been consulted to inform the sediment regime across the region. The metocean data acquisition programme employed a range of approaches and techniques to measure the hydrodynamic regime including fixed point measurement stations (4), moving vessel surveys, and tidal excursion drogues. The survey programme also collected data on near-bed sediment concentrations. Figure 10 displays the location of the fixed point monitoring stations at the site.

Table 4. Field surveys conducted as part of the oceanographic monitoring programme relevant to this report.
Source: Horizon (2012).

Programme	Location	Length of monitoring
Fixed point monitoring system consisting of, variously:- <ul style="list-style-type: none">- Bottom mounted Acoustic Doppler Current Profiler (ADCP) with directional wave capability.- Tide gauges (one offshore location and one shoreline location)- Conductivity, Temperature, Depth (CTD) sensor- Near bed Optical Backscatter Sensor	Four stations. Two monitoring systems deployed at locations offshore of Wylfa Head (S2, S4) and one system deployed in the Western (S9) and Eastern Bays (S11), respectively.	~1 year Jun 2010 – Nov 2011
Vessel mounted ADCP surveys	Pre – defined transect paths:- <ul style="list-style-type: none">- Either side of Wylfa head (termed chevron)- The western and eastern bays- Western boundary line	Duration of transect
Tidal excursion drogues (streamline and satellite drogues)	Releases from existing and potential cooling water outfall locations at different tidal states	Tidal cycle

4.2 Water Elevations

Tidal variation of water levels is driven by the passage of a tidal wave propagating northward (during flood tide) up St George's Channel (a region of seabed located between the Irish and Welsh coast's) and entering the southern Irish Sea. At a regional level the standard reference station for tides in the area is Holyhead. At this location ($53^{\circ} 18' 50.04 \text{ N } 004^{\circ} 37' 13.44 \text{ W}$) the Proudman Oceanographic Laboratory (POL) operates a Class A tide gauge. This is also the nearest "standard port" to the proposed developments at the Wylfa Newydd Development Area (approximately 15 km away). Elevations are relative to Admiralty Chart Datum. Table 5 summarises water elevation statistics for the Holyhead gauge. The coastal location may be classified as mesotidal with a mean Spring tidal range of 4.95 m.

Table 5. Water elevation statistics at the Holyhead Tide Gauge from 2008 -2016. Data Source: NTSLF (2017).

Tidal Levels	Height (m) relative to Chart Datum
Highest Astronomical Tide (HAT)	6.33
Lowest Astronomical Tide (LAT)	0.00
Mean High Water Springs (MHWS)	5.66
Mean High Water Neaps (MHNS)	4.51
Mean Low Water Neaps (MLWN)	2.02
Mean Low Water Springs (MLWS)	0.71
Highest for year (2017)	6.10
Lowest for year (2017)	0.19
Mean Spring Range (MSR)	4.95
Mean Neap Range (MNR)	2.49

Tidal height measurements were also collected (via a temporary tidal gauge) every 15 minutes over a 12-month period (March 2010 to February 2011) installed at the jetty of the Existing Wylfa Power Station Site. These data also demonstrate a semi-diurnal tidal signal with a maximum measured range of 7.5m. The maximum and minimum recorded tidal heights were +3.9m OD to -3.6m OD. Figure 11 provides an example of the temporal variation in water level measured by a pressure sensor at each of the four oceanographic monitoring stations, which shows clearly changes in water elevation are largely similar across the site, and consistent in magnitude with the measured tide gauge data.

4.3 Non-Tidal Currents

Superimposed on the regular tidal behaviour, various random non-tidal effects may be present. Many of these non-tidal effects originate from meteorological influences. Persistent winds can generate wind-driven currents, elevate water levels and develop sea states that lead to wind-wave generation. Table 6 lists the top ten highest recorded tidal levels due to surges obtained from existing tidal records at Holyhead. The maximum surge was recorded in the winter of 2002 and measured 1.2m above MHWS and 0.53m above HAT i.e. local water levels were this amount above mean and maximum tidally expected values, respectively. Records from the Holyhead tide gauge exist from 1964 to November 2017, resulting in a dataset covering the 53 year period between 1964 and 2017. The record indicates the majority of surge heights are within 0.5m of the astronomic (tidal) component (Highest Astronomical Tide [HAT]) and 1.2m of the MHWS. Extreme tide levels at the Wylfa headland are presented in Table 7.



Table 6. The ten highest recorded levels for the Holyhead tide gauge in the lead up to November 2017. Data Source: National Tidal Sea Level Facility (NTSLF) (2017).

Tidal Levels (m)	Date Recorded	Height 'm' above HAT relative to Chart Datum	Percentage Increase	Height 'm' above MHWS relative to Chart Datum	Percentage Increase
6.86	1 st Feb 2002	0.53	8	1.2	19
6.74	3 rd Jan 2014	0.41	6	1.08	19
6.68	10 th Feb 1997	0.35	5	1.02	17
6.64	12 th Dec 2000	0.31	5	0.98	16
6.61	3 rd Feb 2014	0.28	4	0.95	17
6.60	23 rd Dec 1999	0.27	4	0.94	15
6.59	30 th Mar 2006	0.26	4	0.93	15
6.58	10 th Mar 2008	0.25	4	0.92	15
6.55	8 th Oct 2006	0.22	3	0.89	15
6.55	5 th Dec 2013	0.22	3	0.89	15

Table 7. Extreme tide levels, including tidal surge. Please note the data does not account for future sea level rise. Data source: Halcrow (2012).

Return Period (years)	Annual probability of occurrence (%)	Cemaes Bay	Wylfa
		(metres OD Newlyn)	(metres OD Newlyn)
1	63	+ 3.9	+ 3.7
5	20	+4.1	+ 3.9
10	10	+4.1	+ 4.0
100	1	+4.4	+ 4.2
200	0.5	+4.4	+ 4.3
1,000	0.1	+4.6	+ 4.4
10,000	0.01	+4.7	+ 4.6

4.4 Tidal Flows

4.4.1 Observational Data

The definition of the tidal regime adopted for the present study is based on describing water movements and water elevations that are derived from astronomical influences and variations to these effects brought about by atmospheric pressure and winds.



Figure 12 shows time series of (depth-averaged) tidal current magnitudes at the four monitoring stations. The Spring to Neap transition is clear with lower current magnitudes observed during the Neap tide and higher current magnitudes observed during spring tides (Figure 12). Statistical information for these time series is presented in Table 8. From this information the following is evident:

- Offshore from Wylfa head (stations s2 and s4) current magnitudes are notably greater, with peak velocities in excess of 2 m s^{-1} , and mean velocities over twice that at the inner Stations;
- At the more inshore sites (stations s9 and s11), current magnitudes rarely exceed 1 m s^{-1} and mean velocities are typically 0.3 m s^{-1} to 0.4 m s^{-1} .

Table 8. Statistical information related to measured currents at the oceanographic monitoring stations. Data Source: Horizon (2012).

Monitoring Station	Minimum velocity observed (ms^{-1})	Mean velocity observed (ms^{-1})	Maximum velocity observed (ms^{-1})	Associated standard deviation (ms^{-1})
S2	0.047	0.848	2.014	0.428
S4	0.043	0.778	2.301	0.397
S9	0.043	0.367	1.034	0.162
S11	0.038	0.325	1.149	0.154

Figure 13 displays current direction vs magnitude at the four monitoring stations in the form of current roses which provides for a visually simple appreciation of the predominant tidal axis. Offshore from Wylfa Head, the tidal currents are strongly rectilinear in form with a principal tidal axis oriented E to W (i.e. the flood currents flow eastward and the ebb currents flow westward). Farther inshore (s9, s11) the currents are responding to the shoreline orientation and the rectilinearity is less pronounced, particularly at s11.

4.4.2 Mobile Vessel Survey Data

An alternative means of collecting flow velocity data is to mount the flow sensor (an ADCP instrument) onto a moving vessel. Sophisticated software is used in the post-processing phase to decouple the vessel motion (pitch, roll etc.) and transit from the ambient current velocities leaving the only the net current. This type of survey is termed a 'moving vessel [MV]' or 'vessel mounted [VM]' ADCP survey. Although tides change continually and spatially through time, these types of survey afford a synoptic view of the velocity field in space at intervals through time, and therefore provide a wider perspective on the hydrodynamic regime.

A number of VMADCP investigations were undertaken during the oceanographic campaign (Titan, 2009), and an example of the outputs from a Spring tide survey are presented in Figure 14. The chief findings of these surveys in relation to the tidal regime can be summarised as follows:

- There are recurrent circulatory gyres formed in the embayment's to the east and west of Wylfa Head;
- two clockwise rotating eddies form, one in each embayment, in the lee of Wylfa Head and Trywyn Cemlyn Head during flood Neap and Spring tides between HW-5 to HW-3 hours;
- on ebb tides, two counter-clockwise rotating eddies are formed due to the interaction of the tidal currents with Wylfa head and Llanlleiana head;
- current velocities within these eddy formations were generally lower, being on average $\sim 0.3 \text{ m s}^{-1}$;

- Flow patterns generated during Spring tides were more pronounced in comparison to the feature formed during ebb tides;
- these nearshore circulation patterns did not show significant seasonal variation;
- Inspection of the VMADCP data also reveals that current velocities generally increase as they flow around the tip of Wylfa Head.

The interaction of the tidal currents and the numerous coastal headlands of Anglesey are a key driver in near shore current circulation patterns. It is postulated that these observed gyre formations are the result of separation of the tidal flow as the tidal currents flow past these headlands and across the entrance to the embayment's resulting in transient but recurring eddies forming in the lee of the headland. These phenomenon have been observed in a variety of coastal environments e.g. Pingree (1978), Wolanski et al. (1984), Black and Gay (1987), Pattiarchi et al. (1987), Geyer and Signell (1990) and are extensively described in Signell and Geyer (1991).

4.4.3 Modelled Tidal Currents and Bed Stress

Figure 15 - Figure 18 present geospatial outputs from the Delft3D hydrodynamic model for the Wylfa Newydd Development Area showing a) tidal current velocity and direction and b) associated bed stress, for Spring and Neap tidal cycles, during mid-ebb and mid-flood, respectively. Note, since bed stress is intrinsically related to tidal current velocity, the two outputs are highly similar in their graphical presentation. These data reveal a distinct and broadly stationary pattern in regional scale flow velocities / bed stress:

- A high flow / bed stress offshore region (velocities $>0.8 \text{ ms}^{-1}$; bed stress $>2.0 \text{ N m}^{-2}$, $>6 \text{ N m}^{-2}$ on Spring tides) delineated approximately by an arc running across the principal promontories (Trwyn Cemlyn in the west, Wylfa Head and across to Llanlleliliana Head in the east);
- A lower flow regime (velocities $<0.8 \text{ m s}^{-1}$ and commonly far lower; bed stress $<0.4-0.5 \text{ Nm}^{-2}$) within the coastal bays (Cemlyn, Cemaes) and southward of this arc (i.e. inshore); and
- Very low flow velocities (velocities $<0.4 \text{ m s}^{-1}$ and commonly $<0.2 \text{ m s}^{-1}$; bed stress $<0.2 \text{ N m}^{-2}$ in many areas) in the inner regions of Cemlyn and Cemaes Bays.

The distribution of current velocities corresponds well quantitatively with velocities recorded at the (four) fixed monitoring stations (Table 8). The broad scale spatial velocity (and bed stress) distribution is most pronounced on ebb Spring tides (the strongest tidal flows), but is observed (albeit more patchily) at other tidal states. Strong flows are evident also around headlands, namely Trwyn Cemlyn and Wylfa Head, but during ebb Neap tides only. Recirculating circulations are evident in both Cemaes and Cemlyn Bay during peak flows, consistent with the flow observations made during moving vessel surveys (see Section 4.2.2). There is a region of high flow / stress just to the east of Wylfa Head (Figure 18) but this is observed to occur only during Spring ebb tides. These data indicate that the more severe tidally-related sediment transport is most likely to occur offshore, rather than within the embayments.

4.5 Tidal Asymmetry and Tidal Excursion Distances

4.5.1 Asymmetry

The data from the numerical hydrodynamic model (Figures 15-18) and the observed data from the current roses (Figure 13) indicate that the ebb tidal phase currents are always (i.e. on both Neaps and Springs) stronger than corresponding flood currents. Such tidal asymmetry can drive a residual (i.e. net) sediment (sand) transport in the ebb (i.e. westerly) direction for both bedload and suspended load sediments, particularly during Spring tides which are of greater magnitude.

An analysis has been undertaken using time series data from the fixed point oceanographic monitoring station and an example given in Figure 19 for station s4 (farther inshore the ebb dominance is evident but the flood tide curves are distorted, probably as a result of proximity to the coast). This analysis indicates that not only are the ebb tidal currents stronger but they exist for longer durations than the corresponding flood currents. This phenomenon is consistent with flow magnitude asymmetries within the Delft3D model, and is a persistent feature across all the oceanographic monitoring datasets.

4.5.2 Tidal Excursion Distances

The tidal excursion distance is a function of tidal curve asymmetry and represents the net horizontal distance a water particle moves during a half-tidal cycle (i.e. the distance over which a water particle travels during the flooding and ebbing tide; Savenije, 1989). Knowledge of these distances is central to several areas. It provides an understanding of the maximum distances resuspended sediments could be transported away from their source e.g. during scour and release around structures. The tidal excursion distance computed from oceanographic time series data from station s2 from Figure 19 is 14.7 km for Spring flood tides and 19.8 km for the associated ebb indicating net sediment transport in the ebb (westerly) direction in the offshore region from Wylfa Head.

Supporting data also exist from Horizon (2012) who released excursion drogues from existing and proposed outfall locations at the site. Whilst a direct quantitative comparison with excursion distances computed from current data at station s4 (Figure 19) should be cautioned, as drogues can be influenced by coastal physiography and other factors such as wind and areas of shoaling, these data provide generally corroborating evidence regarding tidal flows and the tidal excursion distances at the site. On each occasion two drogues were released and subsequently tracked for a 6.5 hour period following release. The Lagrangian paths of the drogues are plotted in Figure 20 and generally drogue releases conducted from various existing or proposed outfall locations showed similar results. The drogues released on a flooding spring tide generally tracked around Wylfa head, continuing east along the coastline finally being retrieved from around Dulas bay, comparatively the drogues released on an ebbing tide were transported west around the peninsula before being retrieved offshore from Rhyd-wyn. The distances travelled by the drogues ranged between approximately 15km and 18 km on a flooding tide and approximately 10km and 16 km on an ebbing tide excepting where drogues were recirculated within the embayments by the prevailing gyre formations.

5. WAVE REGIME

Waves result from the transfer of wind energy to create sea states and the propagation of such energy across the water surface by wave motion. The amount of wind energy transfer and wind-wave development is a function of the available fetch distance across which the wind blows, wind speed, wind duration and the original sea state. The longer the fetch distance, the greater the potential there is for the wind to interact with the water surface and generate waves. Since wind generated waves originate from meteorological forcing the wave regime is highly episodic and exhibits strong seasonal variation.

5.1 Existing (Observational) Wave Data

Bottom mounted Automated Wave and Current meters (AWACs), each with directional wave capability, were deployed at four monitoring stations (Figure 10) from ~ July 2010 – November 2011. Time series plots showing the wave height observed at each monitoring station across the deployment period are presented in Figure 21.

Figure 22 presents' wave roses showing the significant wave height (H_{m0}) (defined as the mean wave height, trough to crest, of the highest third of the waves observed), and wave period (T_z), and the associated direction recorded at each of the monitoring stations. Unfortunately, each figure plots data from various dates / seasons throughout the monitoring campaign (see Figure 21 for data gaps), and thus direct comparison between the data sets should be made with caution.

A more accurate assessment of the frequency – magnitude of the wave climate around Wylfa headland is accessible via Table 11 - Table 18 which present joint probability distributions with respect to significant wave height (H_{m0}) and wave approach (compass quadrants), and significant wave height and wave period (T_z) for each monitoring station.

The key statistics in regards to the wave climate and the most frequently observed wave conditions during the monitoring period are detailed in Table 17.

Table 9. Joint probability distribution of significant wave heights (H_{m0}) and peak spectral wave approach measured over the deployment period at monitoring station, s2. Data Source: Horizon (2012).

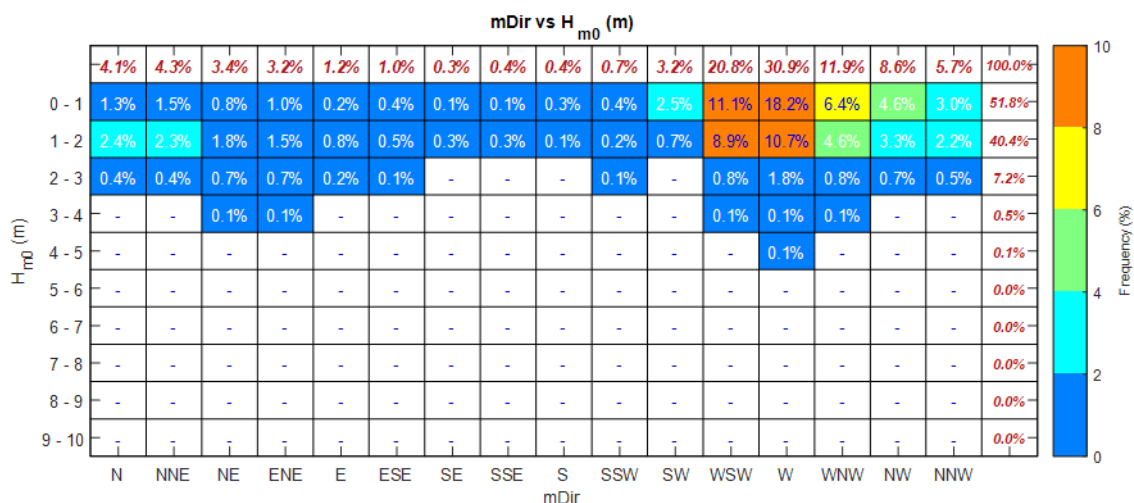




Table 10. Joint probability distribution of significant wave heights (H_{m0}) and peak spectral wave periods (T_z) measured over the deployment period at monitoring station, s2. Data Source: Horizon (2012).

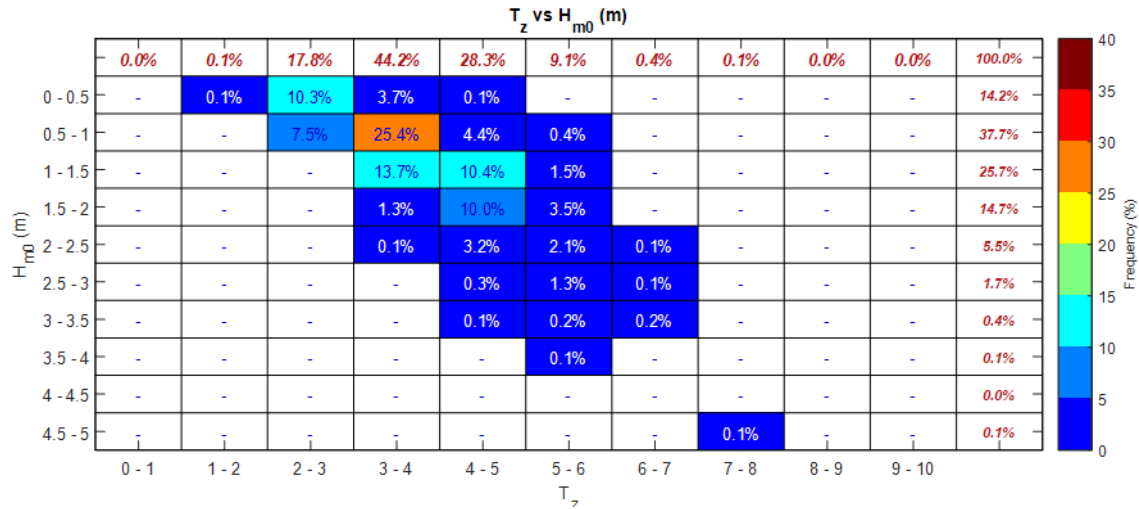


Table 11. Joint probability distribution of significant wave heights (H_{m0}) and peak spectral wave approach measured over the deployment period at monitoring station, s4. Data Source: Horizon (2012).

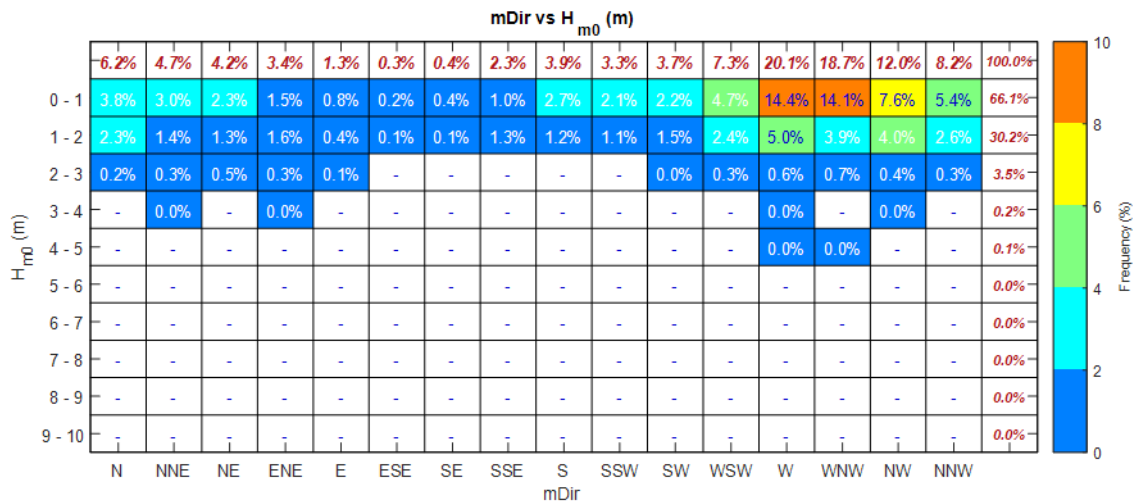




Table 12. Joint probability distribution of significant wave heights (H_{m0}) and peak spectral wave periods (T_z) measured over the deployment period at monitoring station, s4. Data Source: Horizon (2012).

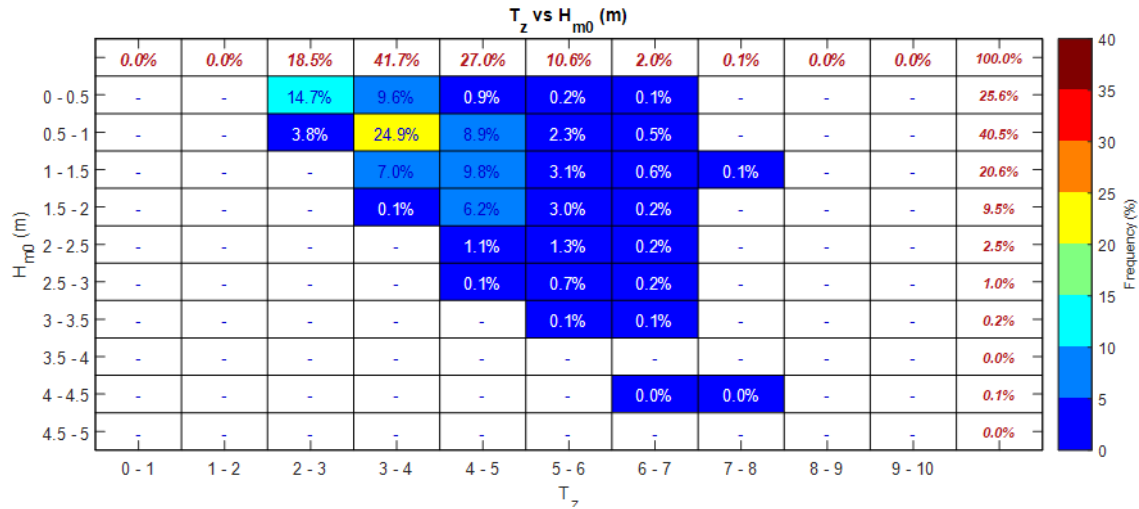


Table 13. Joint probability distribution of significant wave heights (H_{m0}) and peak spectral wave approach measured over the deployment period at monitoring station, s9. Data Source: Horizon (2012).

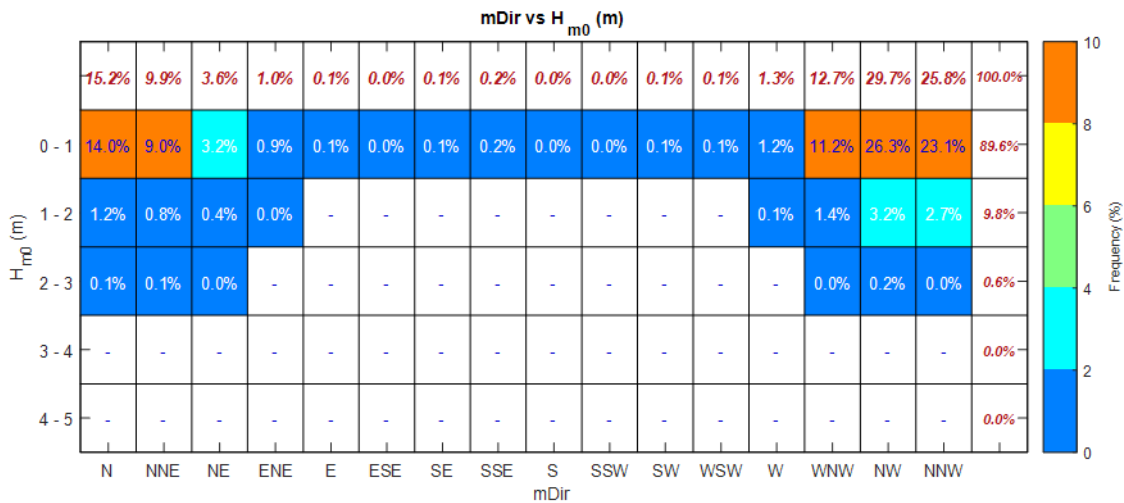




Table 14. Joint probability distribution of significant wave heights (H_{m0}) and peak spectral wave periods (T_z) measured over the deployment period at monitoring station, s9. Data Source: Horizon (2012).

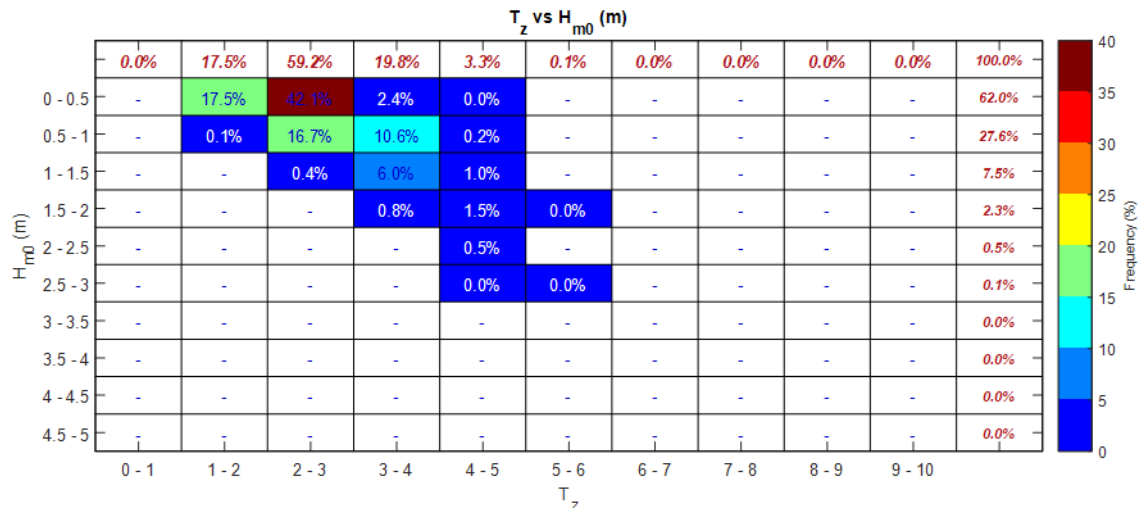


Table 15. Joint probability distribution of significant wave heights (H_{m0}) and peak spectral wave approach measured over the deployment period at monitoring station, s11. Data Source: Horizon (2012).

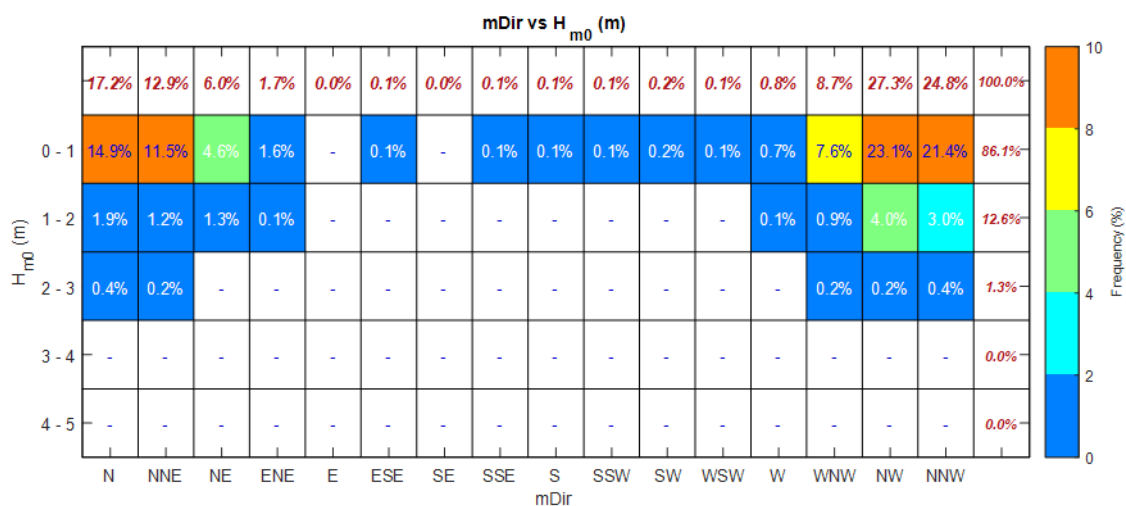




Table 16. Joint probability distribution of significant wave heights (H_{m0}) and peak spectral wave periods (T_z) measured over the deployment period at monitoring station, s11. Data Source: Horizon (2012).

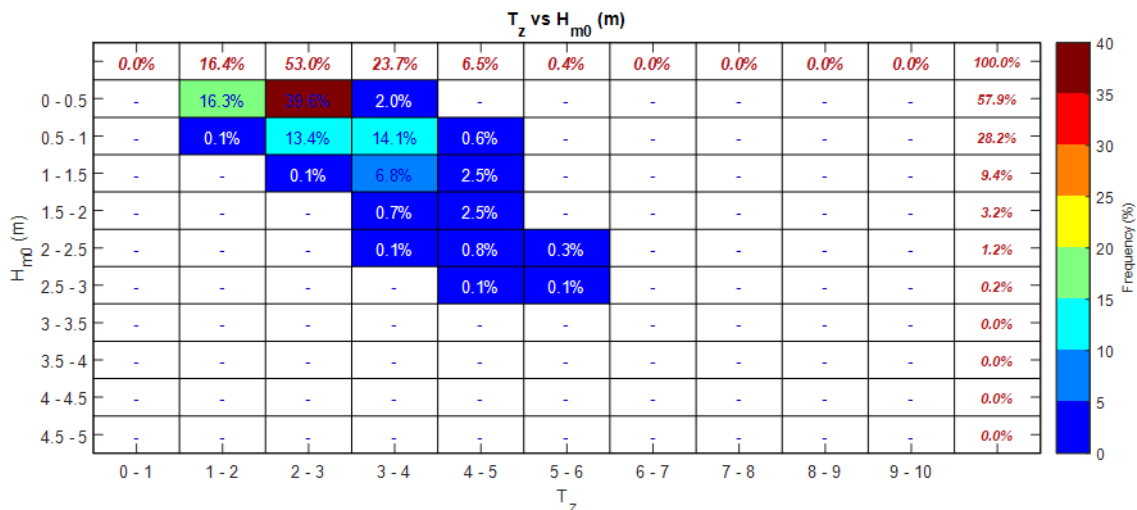


Table 17. Key statistics associated with the wave regime at the site derived from the oceanographic data collected at the four monitoring stations. Data Source: Horizon (2012).

Station	Smallest wave observed H_{m0} (m)	Largest wave observed H_{m0} (m)	Median wave height (m)	Mean wave height (m)	Components most frequently observed		Frequency observed (%)	Components most frequently observed H_{m0} (m)	Components most frequently observed T_z (s)	Frequency observed (%)	Maximum T_z (s)
					H_{m0} (m)	Dir (compass quadrants)					
S2	0.15	4.57	0.97	1.09	0.5 - 1	W	9.2	0.5 - 1	2 - 4	32.9	8
S4	0.11	4.18	0.78	0.89	0.5 - 1	W	9.5	0.5 - 1	2 - 4	28.7	8
S9	0.07	2.63	0.40	0.51	0 - 0.5	NW	13.4	0 - 0.5	2 - 4	44.5	6
S11	0.09	2.90	0.43	0.57	0 - 0.5	NW	13.5	0 - 0.5	2 - 4	41.6	6

The following summarise the key features of the observed wave regime at the site:

- The data reveals there is a greater frequency of storms during winter months (i.e. winter storms generate frequent higher energy episodes).
- At monitoring station s2 (the farthest offshore) higher energy episodes are observed (e.g. where maximum wave heights of > 5m are observed). However, generally waves are observed of <2m in the summer months, increasing to <3m in the winter months.
- The most common wave period is between 2 and 4 seconds, indicative of local (wind generated) sea; higher period events (to maxima of 6s inshore and 8s offshore) occur very infrequently.

- At monitoring station s2 the wave direction spectrum shows a greater incidence of waves from the W (as they are unaffected by the coastline).
- At monitoring stations farther inshore, the data reflects the process of wave shoaling where due to the shallower water observed significant wave heights are lower due to the frictional dissipation of wave energy at the seabed and a slowing of the waves as they enter shallow water.
- At monitoring station s9 and s11 the modal direction shifts and is centred on NW, and there is a greater incidence of waves between this direction and due N. This is due in part as a result of the protection provided from waves arising from the west by the orientation of the coastline and, to wave refraction in which the angle of the wave crests to the shoreline is modified by the shallowing water, and the wave crests become increasingly parallel to the shoreline.
- The wave direction spectrum at monitoring station s9 and s11 are highly similar.
- The frequency and magnitude data show a relatively dynamic wave regime at the site.
- At monitoring station s2 the wave height (H_{m0}) is > 1m with an associated wave period of >4 seconds 33.6 % of the time.
- Farther inshore, these conditions occur 26.8%, 10.3% and 13.2% of the time at monitoring station s4, s9 and s11, respectively.

5.2 Wave Modelling

The long term wave climate was assessed from inspection of the data from the coupled hydrodynamic model offshore (RWE, 2017 described in section 2.2.2) model point, model point 3 (-39.18 m CD, 235700 E, 396480 N) (RWE, 2017). The frequency-magnitude of the long-term wave climate around Wylfa headland is accessible via Figure 23 and Figure 24 which present frequency of occurrence plots with respect to significant wave height (H_{m0}) and the associated period (T_{m02}). 'All' relates to the entire dataset, whereas 'north' specifically relates to data within the directional sector 345 – 15°. Further joint probability distribution tables detailing significant wave height (H_{m0}) and wave approach (compass quadrants), and significant wave height and wave period (T_{m02}) predicted at model point 3 are presented in Table 18 and Table 19. In addition, the key statistics derived from the annually-averaged predicted wave climate (wave height, period and direction) at Point 3 are presented in Table 20 supporting direct comparison of the modelled and measured data. At point 3 the wave direction spectrum shows a greater incidence of waves from the WSW (Figure 25). The predicted modal wave height was between 0.5 to 1.0 m.

Table 18. Joint probability distribution of significant wave heights (H_{m0}) and associated direction (compass quadrants) predicted at model point 3. Data Source: RWE (2017).

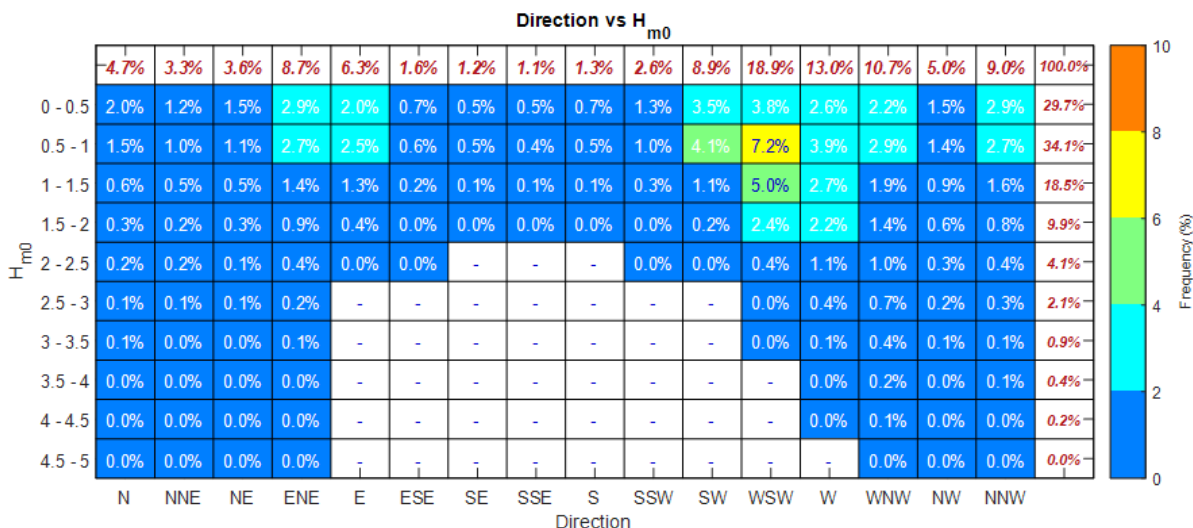




Table 19. Joint probability distribution of significant wave heights (H_{m0}) and peak spectral wave periods (T_{m02}) predicted at model point 3. Data Source: RWE (2017).

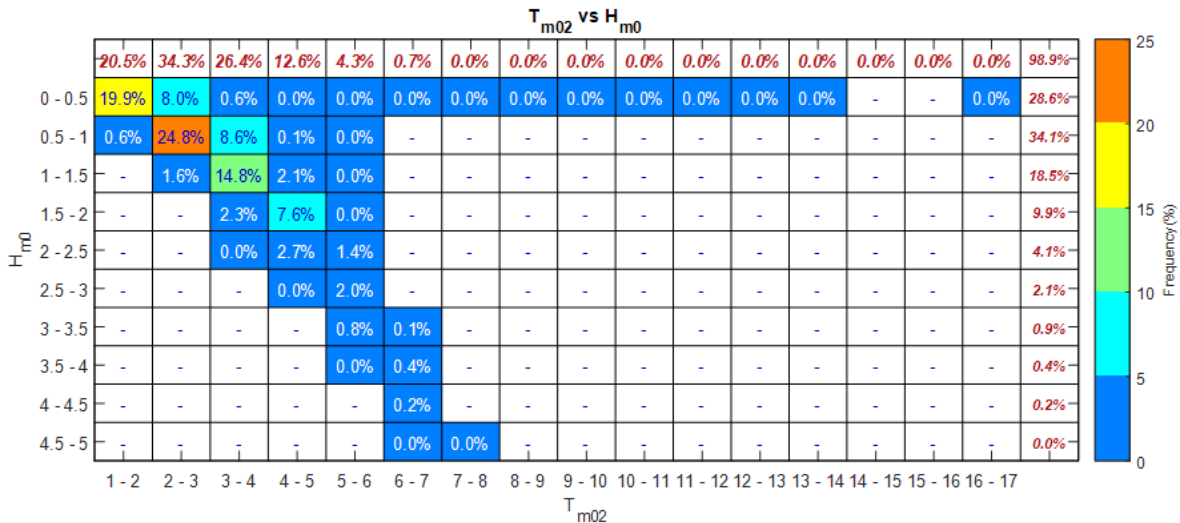


Table 20. Key statistics associated with the wave regime at the site derived from the modelled data collected at model point 3. Data Source: RWE (2017).

Model point	Smallest observed H_{m0} (m)	Largest wave observed H_{m0} (m)	Median wave height (m)	Mean wave height (m)	Components most frequently observed		Frequency observed (%)	Components most frequently observed		Frequency observed (%)
					H_{m0} (m)	Dir (compass quadrant)		H_{m0} (m)	T_{m02} (s)	
Point 3 All	0	5.61	0.76	0.93	0.5-1	WSW	7.2	0.5-1	2-3	24.8
Point 3 North Sector	0.03	5.2	0.59	0.81	0-0.5	n/a	2 (all waves 41.9 (this sector))	0.5-1.0	2-4	31.0

The following summarise the key features of the modelled wave regime at the site:

- The summary statistics for the modelled and measured data show a good level of agreement, indicating that the observational data is not 'atypical' of the general longer term wave climate in any sense, although peak wave periods are about 20% higher than observed values.
- The most frequent conditions were significant wave heights of 0.5-1m, from the WSW, with an associated period of 2-4 s.
- At model point 3 the wave direction spectrum shows a greater incidence of waves from the WSW and this is simply a reflection of its greater offshore distance; when comparing this data to the measured data it is clear that shoaling and refraction of waves as they approach the coastline changes the wave direction spectrum.

5.2.1 Wave Modification

In deep water, waves will move across the sea surface without major modification but as they move into shallower water the orbital motion of the wave through the water column eventually reaches the seabed where upon frictional drag changes the shape of the wave. Refraction, shoaling (wave steepening) and



eventually wave breaking will occur as the waves move progressively into shallower water and towards the shore. A number of important modifications occur as waves begin to interact with the seabed. These are:

- Shoaling and refraction (depth and current);
- Energy loss due to breaking;
- Energy loss due to bottom friction; and
- Momentum and mass transport effects

There is evidence for these processes at the site, and waves affected in this way are normally termed shallow water waves. In addition to the couple hydrodynamic model (RWE, 2017), wave modification was assessed from inspection of data generated from a nearshore wave transformation model commissioned to support the EIA (HR Wallingford, 2017). The wave transformation model generates a thirty year hindcast data set for ten nearshore wave prediction points. Of these ten points, 6 points (nominally prediction point 3, 4 and 6, and prediction points 7, 8 and 9, respectively) comprise two shore-normal gradients; particularly useful for assessing wave modification. Figure 26 shows the locations of the nearshore prediction points and offshore model point 3 in relation to the Anglesey coastline; the two shore-normal gradients are marked. Table 21 provides the key statistics from the two shore-normal gradients defined in the nearshore wave transformation modelling (HR Wallingford, 2017). Figure 27, Figure 28 and Figure 29 show the spatial distribution of predicted wave height across the site for the following scenarios:

- Typical wave scenario (H_{m0} 0.9 m, 228°) on a flooding, Spring tide;
- Winter wave scenario (H_{m0} 2.0 m, 228°) on a flooding, Spring tide; and,
- Large wave from the north scenario (H_{m0} 2.85 m, 346°) on a flooding, Spring tide.

Table 21. Wave height (H_{m0}) and direction along two shore-normal gradients (data garnered from nearshore prediction point 3, 4 and 6 and nearshore prediction point 7, 8 and 9, respectively). Data source: HR Wallingford (2017).

	Wave Scenario (Model point 3)					
	Typical wave scenario (H_{m0} 0.9 m, 228°)		Winter wave scenario (H_{m0} 2.0 m, 228°)		High (98%ile) wave from the north scenario (H_{m0} 2.85 m, 346°)	
Nearshore prediction point	H_{m0}	Dir (degrees)	H_{m0}	Dir (degrees)	H_{m0}	Dir (degrees)
Point 3	0.34	312	0.78	324	2.39	001
Point 4	0.28	008	0.75	008	1.70	015
Point 6	0.20	065	0.56	068	1.20	035
Point 7	0.40	287	0.96	293	2.64	352
Point 8	0.34	314	1.09	322	2.48	359
Point 9	0.26	354	0.80	007	1.81	012

The model outputs (Figure 27 – 29) reveal the impact of seabed bathymetry and coastline topography on the significant wave height, and show how waves approaching the coastline from various directions are modified (dissipated). Offshore waves will reduce in height somewhere in the order of 50% by the time they reach inshore areas. Typical waves and typical winter waves are predicted to reduce to ~ 0.5m and ~ 1.0m at inshore sites, respectively. Inspection of the hindcast time series data generated by HR Wallingford (2017)



corroborates these findings indicating wave heights during a typical wave scenario and winter wave scenario reduces by > 50 % at nearshore prediction point 3 and point 7 (the two farthest offshore points of the two shore normal gradients), reducing by > 60 % at nearshore prediction point 6 and 9 (the two farthest inshore points of the two shore normal gradients). In addition, the hindcast data indicates that the direction of wave approach could change by up to 149° from offshore (model point 3) to inshore areas (nearshore prediction point 6) and that these transformation effects would be slightly more pronounced in higher wave conditions.

Areas of shelter (i.e. where wave heights are significantly reduced due to the coastline topography) differ according to incident wave direction. Further, it is evident that when waves approach from the NW (i.e. the typical direction of wave approach at inshore sites), wave heights persist into areas to the west of Wylfa head and into easterly areas of Cemaes Bay. An additional area of shelter is observed in the westerly corner of Cemaes Bay, in the lee of Wylfa head.

When extreme winter waves approach from the north (i.e. the worst case / largest energy scenario) wave heights at inshore sites are predicted to reduce to ~ 1.5m – 2.5m, however significant wave heights > 2m persist into inshore areas across the full extent of the area of investigation. It is clearly evident that when waves approach from a northerly aspect there are fewer areas sheltered from wave action and significant wave heights penetrate farther inshore in both Cemlyn Bay and Cemaes Bay. An area of shelter remains in the most westerly corner of Cemaes Bay, in the lee of Wylfa head, but during the worst case scenario, even in this most sheltered location, greater wave heights persist. These findings are corroborated by the hindcast model data which reveals wave heights during a high wave event from the north only reduce by 16 % and 7% at nearshore prediction point 3 and point 7, respectively (the two farthest offshore points of the shore normal gradients), finally reducing by up to 58 % and 36 % at nearshore prediction point 6 and 9 (the two farthest inshore points of the two shore normal gradients).

5.3 Bed Stress due to Combined Waves and Currents

The coupled HD and wave model set up within Delft3D has been used to provide information on the geospatial distribution of bed shear stress acting upon the bed where tidal currents and waves are coincident (RWE, 2017). The maximum bed shear stress (i.e. the bed shear stress acting upon the bed due to the forcing exerted by a combination of peak Spring tides and waves) was modelled for two of the three metocean scenarios in Table 3, specifically:

- Spring tide, mid ebb (strongest currents) with a winter wave (H_{m0} 2.0 m, 343°)
- Spring tide, mid ebb (strongest currents) with an high wave from the north (H_{m0} 2.85m, 346°).

The coupled model outputs are presented in Figure 30 and Figure 31. Under tidal forcings the predicted bed shear stress during a mid-ebb tide (the strongest tidal currents) can effectively be divided into a 'high' (>2 N m⁻²) and a 'low' (<2 N m⁻²) stress zone by the line connecting the headlands either side of Wylfa Head. The data reveal that when wave events are coincident with spring ebb tides the bed shear stress acting upon the bed is enhanced and thus waves must be considered an important influence on bed shear stresses, particularly within inshore areas (i.e. the coastal embayments).

During the winter wave scenario bed shear stress is more pronounced inshore, with areas of significant stress (> 2 N m⁻²) predicted to occur in the west of Cemaes Bay and off the headland between Porth y Pistyll and Cemlyn Bay (Figure 30). The maximum bed shear stress exerted upon the bed is more pronounced during a high wave event from the north, which is a function of both wave height and direction. During this scenario significant stress is predicted to be exerted upon the bed at all inshore areas including Cemaes Bay, Porth y Pistyll and Cemlyn Bay. Isolated pockets of stress >3.5 N m⁻² are predicted to occur along the rocky headlands off Wylfa Head and between Porth y Pistyll and Cemlyn Bay, and in the west of Cemaes Bay towards the village of Cemaes (Figure 31).



6. SEDIMENT REGIME

6.1 Regional Setting

The northern coastline of Anglesey is characterized by a series of rocky cliffs interrupted by numerous embayments. The geology of Anglesey is notably complex and ancient, comprising rocks of the Neoproterozoic to Cambrian New Harbour Group to the South of Wylfa Head and the Gwna Group to the north. The rock formations to the south comprise a sequence of phyllites, psammites, fissile green mica schist, gritty green mica schist, with bedded jasper, jasperphyllite and peltic lava, and the formations to the north comprise quartzites, phyllites, psammites, granites, basalts, limestones, schists, graphitic phyllites and spilitic pillow lavas (Fugro, 2010b). This geology extends offshore as a series of broad, shallowly dipping to flat platforms and deeply incised channels and troughs (Mallet et al. 2015). The Welsh Platform lies directly offshore from Anglesey. This solid geology is overlaid by discontinuous layers of Devensian Till and various coastal and fluvially derived deposits (Mallet et al. op. cit.; Strategic Environmental Assessment of the Irish Sea (SEA 6) report for the Department of Trade and Industry; Holmes and Tappin, 2005).

Multiple regional glaciations during the Quaternary period have acted to shape the seabed physiography and distribution of seabed sediments. Following the last (Devensian) glaciation, sediments were significantly reworked and redeposited. Fluvio-glacial outwash was deposited into the Irish Sea basin and as the ice retreated it left behind significant deposits of unsorted gravelly, sandy and muddy deposits. These diamicton deposits form the primary sediment type underpinning the surficial seabed sediments. Due to the dynamic nature of the subglacial changes and submarine processes of erosion and deposition the superficial strata below the seabed sediments have significantly different properties to those of the seabed sediments. In the Wylfa Newydd Development Area seabed sediments are a combination of unconsolidated sediment (<5m thick), mud and undifferentiated mud, sand and gravel (Holmes and Tappin, 2005). These sub-marine sediments typically consist of reworked (by coastal and / or marine processes) glacigenic and fluvial sediments with additionally up to 20% (by weight) biogenic carbonate component derived from fossil biota. Much of this material forms 'lag' deposits overlying the Holocene/Devensian sediment and are exposed at the seabed where the 'mobile' fraction of the sediment has been removed, for example, by scouring. A lag deposit is an accumulation of coarse grained sediment that is left behind as currents winnow and remove finer sediment. Such a deposit is most commonly created during post glacial sea level rise as the continental shelf is flooded and transgressed, but it can also occur where modern day currents scour the seabed. On the Irish Sea seabed the lag deposit can comprise cobbles and boulders (Holmes and Tappin, 2005). It is apparent that in places on the seabed sediment is mobile under certain prevailing currents and waves and that this mobile sediment creates features upon the seabed that range from small ripples to large sediment banks and migrating sediment (sand and gravel) waves.

In areas of particularly high flows, such as immediately (~10 km) offshore of the northern and western coast of Anglesey (Howarth, 2005), the currents have completely scoured the bedrock free of surficial sediments (see Fig. 73 in Jackson et al., 1995). Although the seabed may in places be regarded as highly dynamic, the modern sedimentary environment of offshore areas of the Irish Sea continental shelf is now dominated by very low sediment supply.

6.1.1 Local Setting

The proposed Wylfa Newydd Development Area is located on the northern coastline of the Isle of Anglesey within coastal Sub Cell 10b of Motyka & Brampton (1993). A detailed overview of the coastal geomorphology and shoreline processes in the area is given as a series of coastal sub-cell/management unit descriptions within Motyka & Brampton (op. cit.) and the West Wales Shoreline Management Plan 2 (SMP2; Haskoning UK Ltd., 2012). Figure 2 shows the coastal cell within which the proposed Wylfa Newydd Project falls. Table 22 presents the description of Sub Cell 10b from Motyka & Brampton (1993).



Table 22. The description of the coastal regime at sub-cell 10b (Isle of Anglesey) as described in Motyka & Brampton (1993).

Process	Information
General	Rocky coastline of Anglesey has little interaction with the mainland coast with the possible exception of sand banks at the west and east ends of Menai Strait.
Beaches	Predominantly sandy
Backshore	Hard pre-Cambrian rocks form an indented coastline which is resistant to erosion. The southern part of Anglesey is carboniferous, limestones mostly where exposed on the coast. Where there is a cover of glacial boulder clay it is rapidly eroded. In many areas small dune systems back the bays.
Erosion	Local coast protection works in areas of clay cliff erosion. There do not appear extensive areas of erosion. Erosion tends to occur more on the west coast than the north or east. Erosion in Cymyran Bay, for example, is probably related to the exposure to predominant south westerly storms. The shoreline of Menai Strait is generally stable with the exception of low boulder clay cliffs near Beaumaris
Accretion	Newborough Warren, in the southwest corner of the Island
Areas of flood risk	Low lying areas in the south west corner of the Island (e.g., at Maltreath Marsh and in the Menai Strait, near Newborough Warren)
Littoral processes	Littoral drift is very low and variable in direction. Most beaches within embayments or between headlands can probably be treated individually as far as coastal defence works are concerned. Little is known about coastal processes. However, because of the indented nature of the coast, tidal currents probably play a minor role (possibly with the exception of helping siltation take place between Holy Island and 'mainland' Anglesey.) Wave action at high tides causes beach lowering and attack on dunes at heads of indentations, and of low glacial cliffs, particularly on west facing coasts.

The physical processes operating at the shoreline are a function of the geology and geomorphology of the coastline, shoreline orientation, tidal regime and exposure to wave action. Whereas hard areas such as cliffs and headlands are considered highly resistant to marine erosion, much of the unconsolidated material along the coastline, deposited during the glacial period and subsequent deglaciation, has since been moved and sorted by waves and tidal currents. Sand and gravel lag deposits on the seabed have been swept into these areas by rising sea levels and form the sediments within the Cemlyn and Cemaes Bays. Pye and Blott (2010) state "...embayments along the north Anglesey coast generally act as closed sediment compartments, with little or no exchange of sediment from one bay to the next, and only limited supply of new sediment at the present day from eroding sections of open coast between the bays.....". For example, Porth-y-Pistyll can be described, from a geomorphological perspective, as a bay-head or pocket beach contained within an embayment bounded by headlands (between Cerrig Brith and Trwyn y Galen ddu). This has been described as a 're-entrant trap' by Haslett (2000). Normally sediments captured in such bays may undergo some alongshore transport or recirculation within the bay itself, but the sediment is generally unable to escape from the enclosed system due to shape of the coastline and the relatively high wave energy conditions affecting the headlands.

The area of the proposed development has been considered within the West of Wales Shoreline Management Plan (SMP2: Haskoning UK Ltd, 2012) and this document contains some useful information of relevance to the regional – local sediment regime.

Wylfa Head and the neighbouring stretches of coastline that have the potential to be impacted, and are examined within the present assessment, are located in Policy Development Zone (PDZ) 18 (Holy Island and



West Anglesey: Twyn y Parc to Twyn Cliperau Isle of Anglesey Chainage: 49km to 101km) within Coastal Area G (Isle of Anglesey) of the SMP2.

The SMP2 states that for this zone the principal coastal processes significant to the SMP process work at the local scale. The western section of the coast is exposed to the dominant wave direction (southwest), with the northern coastline section (more relevant to the Wyfla Newydd development) is affected far more by waves approaching from the west and northwest (Horizon, 2012; Halcrow, 2012). The eastern section is more sheltered from the main wave directions but is vulnerable to waves diffracting around the north east headland of Ynys Mon and to direct attack from waves approaching from the north east. Waves approaching from the north-west, rather than those from the predominant south-westerly wave direction, along this coastline can cause a net movement of material from west to east, whereas exposure to waves from the northeast can drive material westwards; there is commonly a null point at the centre of some bays where little or no transport occurs. However, even though the coast is exposed to high wave energies the rate of longshore transport of sediment is relatively low due to limited sediment supply. Sediment movement is essentially limited to individual bays as rock platforms and headlands provide barriers (natural groynes) thus preventing the easterly movement of sediment.

Aeolian transport is also responsible for transport of sand within large exposed bays such as Cemaes Bay and Porthllechog/Bull Bay.

Within PDZ 18 a number of Policy Units have been defined. For the purposes of the current assessment the following units are considered:

- 18.6: Cemlyn Bay and Headland
- 18.7: Wyfla Power Station
- 18.8: Cemaes Bay West

The SMP2 provides a localised appraisal of coastal processes outlining the sediment sources, transport pathways and sinks, and the controls and sensitivities within local coastal process units. The following tables provide a brief description of the significant features and characteristics of the coastline in each of the above units (modified from the SMP2). Also stated is the currently recommended shoreline management policy for the plan over of the Short (to 2025), Medium (to 2055) and Long Term (to 2105).

**Policy Unit 18.6: Cemlyn Bay and Headland**

Description								
General:	This unit comprises Cemlyn Bay including the hard rock headland of Trywn Cemlyn.							
Physical:	Cemlyn Bay is backed by a large shingle bank in the lee of the hard rock headland of Trywn Cemlyn. Behind the shingle ridge is a broad brackish lagoon extending within a narrower valley to the west. The lagoon is partially divided by a ridge of high ground running down to the back of the lagoon. The water level in the lagoon is managed via a weir located at the main inlet to the lagoon in the western end of the bay. At the western shoreline of the bay there is a narrow shingle sand ridge feature.							
Defences and Man Made Features:	The sluice and weir control water levels within the lagoon and additional defence around the car park and behind the weir to protect the properties in the area and the car park.							
Tide and Water Levels (mCD):	Holyhead	MLWS 0.71	MLWN 2.02	MHWS 5.66	MHWN 4.51	HAT 6.33	Spring Range 4.95	
Extreme water levels (mOD):	Source (Halcrow, 2012)	1:1	1:5	1:10	1:100	1:200	1:1000	1:10000
Cemaes Bay	Wylfa	+ 3.9	+ 4.1	+ 4.1	+ 4.4	+ 4.4	+ 4.6	+ 4.7
		+ 3.7	+ 3.9	+ 4.0	+ 4.2	+ 4.3	+ 4.4	+ 4.6
Currents:	On the flood the tidal stream flows from west to east, while on the ebb this is reversed and it flows east to west.							
Wave Climate:	The dominant wave direction is from the south west although there is substantial energy from the west, north west and north east sectors. The 1:100 year significant offshore extreme wave height is 5.9 m (HR Wallingford, 2015).							
Sediment:	Overview:	There is limited sediment feed into the bay from offshore. Sediment supply is limited to the long term erosion of the adjacent cliff line. The sediment in the bay is trapped.						
	Material Type:	Predominantly Shingle						
	Sources:	External	No significant inputs	Internal	No significant inputs			
	Movement:	Transport within the bay occurs due to the forcing of waves which can enter the bay creating some variation in movement of the shingle along the shoreline. Generally, due to the predominant wave direction the main energy (i.e. forcing) acting on the shoreline is due to waves diffracting around the headland. This process acts to create a relatively uniform wave approach ultimately allowing for the development of the shingle ridge.						



Geomorphology

Process description: Overall description of coastal processes: sediment sources, transport and sinks	Within the main Cemlyn Bay, the shingle ridge (Esgair Gemlyn) has been developed within a very constrained inlet, opening to the north east. While waves can enter the bay directly from this direction causing some variation in movement of the shingle along the frontage, the main energy acting on the natural feature is, and has been, waves diffracting around the headland. This very dominant aspect of the inshore wave climate, effectively filtering the variation in offshore wave approach and creating a uniform and tightly banded wave approach direction at the shoreline has allowed development of the long shingle ridge. It seems probable that there is limited sediment feed into the bay from the offshore and that the only [limited] supply is from the very slow erosion of the adjacent cliff line. The most vulnerable section of the ridge is at the northern end which is coincident with a small island feature in the lagoon which may have an associated underwater outcrop which may influence flows in the bay. It is noted that the influence of the feature on flow may have been sufficient to have prevented the natural backface development of the shingle ridge.			
Future evolution (unconstrained):	Within Cemlyn Bay there would be roll back of the shingle ridge resulting in the existing channel being infilled and a shingle beach being formed within the area.			
Dependency:	Controls and sensitivities	Control features	Significance	Dependence
Factors affecting the evolution of the frontage both internally and externally	Cemlyn Bay and the hard rock headland of Trywn Cemlyn will become more exposed to erosion with sea level rise as their foreshore rock platforms are submerged exposing the cliffs to greater wave energy. Defence structures at the eastern end of Cemlyn Bay would act to reduce the impact.	Trywn Cemlyn and rock platform	Secondary	Variable with sea level rise
		Defence structures at the power station	Secondary	Variable with sea level rise
Influence: Factors which may influence evolution of other areas:	The intent is to let the shingle ridge evolve naturally but undertake and maintain local defences. This is not considered to significantly influence the evolution of other areas.			
SMP2 Policy	2025	2055	2105	Comment
	Managed Realignment	No Active Intervention	No Active Intervention	Requires development of a detailed management plan.

Policy Unit 18.7: Wylfa Power Station

<u>Description</u>	
General:	This unit comprises the existing Wylfa Power Station constructed on Mynnydd y Wylfa headland.
Physical:	The Mynnydd y Wylfa headland is located at the western headland to Cemaes Bay.
Defences and Man Made Features:	The (now closed) existing Wylfa Power Station is constructed on the Mynnydd y Wylfa Headland at the western headland to Cemaes Bay. There is a pier and water inlet to the western side of the headland and the cooling water outlet within a small cove to the main head of the headland. Defences have been constructed to the western frontage. These are founded to the rock.

Baseline Information

Tide and Water Levels (mCD):		MLWS	MLWN	MHWS	MHWN	HAT	Spring Range
Holyhead		0.71	2.02	5.66	4.51	6.33	4.95
Source (Halcrow, 2012)				1:1	1:5	1:10	1:100
Extreme water levels (mOD):	Cemaes Bay			+ 3.9	+ 4.1	+ 4.1	+ 4.4
	Wylfa			+ 3.7	+ 3.9	+ 4.0	+ 4.2
Currents:	On the flood the tidal stream flows from west to east, while on the ebb this is reversed and it flows east to west.						
Wave Climate:	The dominant wave direction is from the south west although there is substantial energy from the west, north west and north east sectors. The 1:100 year significant extreme wave height is 5.9 m (HR Wallingford, 2015).						
Sediment:	Overview:	No sediment available.					
	Material Type:	Rock.					
	Sources:	External		No significant inputs	Internal		No significant inputs
	Movement:	N/A					

Geomorphology

Process description: Overall description of coastal processes; sediment sources, transport and sinks	The coastal defences in the unit have little impact on coastal processes. The headland is exposed to deep water waves from all main directions and the defended area is exposed to the dominant southwest to northwest wave climate.				
Future evolution (unconstrained):	The coast would slowly erode.				
Dependency:	Controls and sensitivities	Control features	Significance	Dependence	
Factors affecting the evolution of the frontage both internally and externally	Wylfa will become more exposed to erosion with sea level rise as their foreshore rock platforms, and defence structures are submerged exposing the cliffs to greater wave energy.	Defence structures at the power station	Secondary	Variable with sea level rise	
Influence: Factors which may influence evolution of other areas:	The defences deteriorate over time. This is not considered to significantly influence the evolution of other areas.				
SMP2 Policy	2025 Hold the Line	2055 Hold the Line	2105 Hold the Line	Comment	

Policy Unit 18.8: Cemaes Bay West

<u>Description</u>	
General:	Cemaes Bay is formed between the headlands of Wylfa Head to the west and Trwyn Buarth to the east.
Physical:	Along the main sea front, south of Trwyn y Penrhyn, a seawall protects the road (Ffordd y Traeth) that runs along the shoreline to the properties on the headland at Penrhyn. To the western end of this promenade a small stream runs down to the shoreline. There is a small pocket beach in this area and areas of sand and shingle to several local sections of the sea wall. However, much of the foreshore through to the harbour is rock outcrop. The harbour is protected by a large masonry breakwater and providing shelter. A relatively new promenade protects the coastal slope to the east of the harbour which also incorporates a small car park. The main beach sits in front of this promenade, with a coastal slope behind. The Afon Wygyr (stream) runs in a steeply sided valley in the lee of the harbour breakwater
Defences and Man Made Features:	The principal defences in the area are the sea wall along Ffordd y Traeth, the main breakwater and defences within the harbour area and the promenade wall to the east of the harbour. This last structure is relatively new and follows around the crest of much of the sandy/shingly beach to the eastern part of the village. The sea wall along Ffordd y Traeth has a relatively high crest wall above the height of the road.

Baseline Information

Tide and Water Levels (mCD):	MLWS	MLWN	MHWS	MHWN	HAT	Spring Range
Holyhead	0.71	2.02	5.66	4.51	6.33	4.95
Extreme water levels (mOD):	Source (Halcrow, 2012)		1:1	1:5	1:10	1:100
Cemaes Bay			+ 3.9	+ 4.1	+ 4.1	+ 4.4
Currents:	On the flood the tidal stream flows from west to east, while on the ebb this is reversed and it flows east to west.					
Wave Climate:	The dominant wave direction is from the south west although there is substantial energy from the west, north west and north east sectors. The 1:100 year significant extreme wave height is 5.9 m (HR Wallingford, 2015).					
Sediment:	Overview:	No sediment available.				
	Material Type:	Rock.				
	Sources:	External	No significant inputs		Internal	No significant inputs
Movement:		N/A				

Geomorphology



Process description: Overall description of coastal processes; sediment: sources, transport and sinks	The main offshore wave energy is from the south west through to north and this spread of direction is highlighted by the shape of the several small sub-bays within the larger Cemaes Bay, so that without the constraint of the significant hard rock sections within Cemaes Bay one might expect the bay to form quite a uniform curving backshore facing out to the north. The hard rock coast within the main bay holds this shoreline forward, with the several sub-bays being set back around this uniform curve. This would suggest that the waves entering the sub-bay of within which the village sits is limited by direction, tending to be channelled down the narrow entrance before spreading out within the softer wider head of the bay. The area would also be subject to relatively long period waves generated over the significant offshore fetch. Quite probably, there is significant reflection off the steep hard cliffs on the northern side, giving rise to an interaction of incident and reflected waves hitting the southern shoreline, particularly in the area just seaward of the harbour. There is evidence of wave overtopping along Ffordd y Traeth. With this type of behaviour, there is significant and long term pressure for the coast to realign. Despite the increased wave energy, the coast is held well forward of this suggested line by the structures at the harbour and the ridge running down through the village in the area of the harbour. The development of a sandy beach both in this area and within the various bays with Cemaes Bay would suggest that there is some nearshore supply of sediment and that where there is sufficient width in the shoreline system there is the capacity for some natural development and retention of a beach.				
Future evolution (unconstrained):	In the absence of defences the coastal slope to the western side of the village would suffer significant toe erosion and encouraging slope instability in the area. The harbour breakwater helps form the shape of the shoreline at the head of the bay and this would realign with significant erosion at its southern end. The new wall along the main beach follows the crest of the beach; however, without the defence the beach would roll back exposing the toe of the coastal slope behind.				
Dependency: Factors affecting the evolution of the frontage both internally and externally	Controls and sensitivities Wylfa will become more exposed to erosion with sea level rise as their foreshore rock platforms, and defence structures are submerged exposing the cliffs to greater wave energy.	Control features Defence structures at the power station.	Significance Secondary	Dependence Variable with sea level rise	
Influence: Factors which may influence evolution of other areas:	The defences deteriorate over time. This is not considered to significantly influence the evolution of other areas.				
SMP2 Policy	2025 No Active Intervention	2055 No Active Intervention	2105 No Active Intervention	Comment	



6.1.2 Seabed Geology

Between 2009-2016 Titan Surveys and Fugro Ltd conducted geophysical surveys and [geotechnical] borehole investigations (respectively) into the seabed adjacent to the existing Wylfa Newydd Power Station Site (Cemlyn Bay and Cemaes Bays) in advance of the proposed development. The results of these studies have been utilised to provide greater insight into the nature of the seabed and sub-seabed in proximity to the proposed development. The particle size analyses completed upon borehole samples provided insight into the local shallow geological stratigraphy a summary of which is presented in Table 23.

Table 23. Wylfa area shallow sub-seabed stratigraphy (Titan, 2009).

Unit	Description
Veneer	Thin sands and gravels forming complete cover in all areas other than where rock outcrops at the seabed. Forms gravelly sand beaches at head of coves and larger bays. Sand component forms bank in Cemaes Bay. Bedforms rare. Thickness 0m – 10m.
Sandy Channel Fill	Infills former drainage system channels incised into underlying boulder clay in Cemaes Bay (thickness 0 - 6m). Forms thin patchy late-stage fill in 'palaeochannels' in Cemlyn Bay (thickness 0-2m).
Boulder Clay	Heterogeneous till draped over buried landscape. Largely filling depressions entirely in western half of survey area and extensive areas of exposure at the seabed. Thickness 0-20m
Bedrock	Forms cliffs and wave cut terraces along shoreline and isolated irregular outcrops at the seabed offshore separated by areas of thinly covered subcrop. Rockhead erosion surface very difficult to identify at depth as surface lies below irregular in-situ weathered material. Lithology; Weathered to fresh (hard) Pre-Cambrian and Lower Palaeozoic schists and gneisses, with intrusions of unknown age (BGS sources)

Veneer

The shallowest geological unit encountered in the survey area was a thin incomplete gravel and sand veneer / lag deposit. Other than on the tops of bedrock outcrops and on the steeper rock slopes, the unit is found essentially everywhere. The unit was encountered in grab samples that have been collected from the seabed in the local area, and is swept up into the few bedforms identified on the sonar and swathe data collected but was rarely thick enough to be visible on the sub-bottom profiler data (i.e. less than approximately 0.3-0.5m thick) acquired. It is considered that this lag deposit is under predominant prevailing conditions stable, and that only under the more extreme oceanographic conditions are these deposits potentially moved.

Interpretation of the geophysical survey undertaken in 2009 by Titan Surveys at the site (Titan, 2009 indicates that the "seabed gravel and sand" clearly form the sediment wedges lying against the shoreline in Cemaes Bay (see Figure 32 for an example of the boomer record from Cemaes Bay, the only large area in which it was possible to get boomer coverage close inshore) and the much more limited sand bodies swept into the coves along the remainder of the shoreline. Probably consisting of the similar but possibly sandier materials but clearly separated from the inshore coastal wedges by a strip of gravel seabed, most of the seabed in Cemaes Bay consists of the outcrop of a major sand body. This "Eastern Sand" forms a distinct shoal to the south east. The feature forms a sediment accumulation averaging approximately 6m thick lying on a gently undulating erosion surface cut across the underlying bedrock and boulder clay terrain. Internally the unit demonstrates closely spaced, moderate sub-horizontal parallel reflectors probably resulting from the rhythmic alternation of grain size from one layer to another. The sand body forms a dome with the sand diminishing in thickness away from the central maximum development of 10 metres. The sand unit appears to have developed in the lee of the Mynydd y Wylfa peninsula.



A well-developed megaripple field, formed most probably by flood currents accelerated around Wylfa Head, is present on the north western slope of the "Eastern Sand" body with similar but barely discernible features lying on the otherwise featureless gravelly sand seabed to the north of the sand body. The megaripples on the sand deposit have an average crest trend of 165-345°. The base of the "Eastern Sand" is clearly defined by a very clear basal reflector representing an erosional (ravinement) surface cutting across the underlying strata. The reflector on the sub-bottom seismic profile data delineating the base of this unit exhibits areas of abnormally high amplitude probably indicating at least some zones of coarse lag materials. The surface was formed in a high-energy environment, crossing underlying structures with little variation (i.e. most probably the Holocene Transgression).

Sandy Channel Fill

Detected beneath the "Eastern Sand" is an almost (seismically) transparent sub-horizontally bedded unit infilling the most recent of a series of channels cut into the underlying bedrock and boulder clay. Internally, the unit consists of a series of weak reflectors probably representing sand with a minor gravel component. Within the bay the unit is up to 6m thick, typically 300m wide and with its base lying at a maximum depth of approximately 12 m below seabed. The unit also appears to be present forming the last-stage fill in the palaeochannels in the western part of the site. In this situation the unit reaches a maximum development of 2 m.

Boulder Clay

The deepest unconsolidated sediment unit identified on the titan Surveys data is heterogeneous boulder clay forming a blanket deposit draped over bedrock and largely filling depressions in the rockhead erosion surface. The boulder clay demonstrates numerous internal cut and fill channel structures – none traceable for any significant distance laterally. In detail the unit appears as short-lived, weak irregular reflectors suspended in a field of hyperbolic reflectors representing acoustic scattering around point reflectors (cobbles and boulders). The base of the boulder clay unit is not well defined by a single reflector and has not be identified with complete confidence other than at very shallow depth

Bedrock

The topography of the rock head erosion surface is different in the two main bays. In Cemlyn Bay, at least part of the erosion surface forms what appears to be a palaeo-drainage channel system running offshore from Porth-y-Pistyll. The channel system appears to drain to the north but only the deeper parts of the system are present. The system apparently lacks an exit channel out of the survey area. This is interpreted as the result of a planation following the initial channel erosion and subsequent infilling (most of the offshore topography may represent a former landscape, that has been eroded relatively smooth and drowned during post glacial sea level rise. The isolated offshore irregular rock outcrops represent more resistant relict "tor like" features). The Cemlyn Bay system consists of two isolated irregular infilled depressions lying to the west (the channel system) and northwest (a shallow dish like depression) of the existing Wylfa power station. The features have a maximum infill of 8m and the average thickness of material is approximately 5m. The features appear as smooth areas of sand and gravel seabed lying between rocky topographic highs.

The Cemaes Bay rockhead erosion surface is a much broader feature, without the well-defined palaeochannel margins seen to the west. The surface is covered by up to approximately 20m of very heterogeneous till, in turn partly lying below a sandy late stage channel fill, this in turn lying beneath the more "Recent" sands of the "Eastern Sand" unit. The presence of the thick sediment sequence in the centre of Cemaes Bay almost completely buries bedrock. Bedrock exposures are restricted to three small isolated outcrops just protruding above the Eastern Sand. The features are the highest points on a buried rock ridge forming the submarine extension of the cliffs on the north face of Mynydd y Wylfa. Sediments in Cemaes Bay have been interpreted having at least partly of fluvial origin, containing sandy channel fill and appearing to originate at least in part

from the coves on the present shoreline (sub-bottom data shows a shallow channel running north from the cove in the centre of Cemaes Bay, but the cove at Cemaes village lies beyond the survey's coverage).

In Cemlyn Bay, to the northwest of the palaeochannel features, the solid geology appears to mostly comprise weathered bedrock just covered by thin boulder clay and veneer. For all intents and purposes the seabed consists of weathered bedrock separating more resistant bedrock highs (i.e. low lying bedrock is of softer material than harder upstanding areas).

Beyond the detailed survey coverage area the seabed appears to consist of essentially similar sedimentary materials. Bedrock lies at the seabed or sub crops over large areas of the seabed to the limit of survey coverage to the west of the existing Wylfa power station and lies at the periphery of sonar coverage in the southwest of Cemlyn Bay and the east of Cemaes Bay. In both the northwest and northeast of the outer area, the seabed consists of relatively featureless tidally swept modern deposits. Whilst there is too large a distance to extrapolate the sub-bottom data to the northeast corner of survey coverage, it seems likely that the complex rockhead erosion surface encountered in Cemaes Bay falls away at increasing depth to the northeast of sub-bottom profiler coverage.

Geophysical Ground Discrimination

Data collected during the site-wide geophysical survey (Titan, 2009) has been processed to derive a semi-quantitative map of the surficial sediment cover and type. This technique is known as 'acoustic ground discrimination' (AGD); an AGD system makes use of the fact that different seafloor types will scatter and absorb different amounts of acoustic energy. Thus, a measure of the strength of return from the seafloor can be used to class different reflection types through calibration with direct sampling. The strength of the first return echo is typically known as E1, and the strength of the first multiple echo (second return) is known as E2. E1 has been attributed to the "roughness" of the seafloor and E2 with the "hardness". Figure 35² shows the map generated from this approach. AGDS classification of extensive seabed areas must be viewed with caution, especially where they have not been robustly ground-truthed by grab sample or video data (as is the case here). Nonetheless they can provide a useful, general guide.

The general distribution of sediments reveals an underlying rock pavement, patchily covered variously by smooth, featureless sands (e.g. covering most of Cemlyn Bay), sands with intermediate scale bedforms (megaripples) and sands admixed with gravels. Extensive areas of exposed bedrock are prominent in the central region straddling an arc running across the principal promontories (Trwyn Cemlyn in the west, across to Wylfa Head) and in the area around Llanlleiliana Head in the east. A large area of contiguous sediment

² Figure 34 shows the seabed features map derived from the geophysical surveys (AGDS) (Titan, 2009). Grain size data from pertinent sample locations have been superimposed to provide an indicative grain size distribution for the features over which they are positioned. It is of note, the intertidal zone was not included in the AGDS classification, thus benthic samples collected from the intertidal zone have not been included in Figure 34. Further, where bed rock is the dominant AGDS classification, samples collected from these areas were also not included as these samples would only provide information regarding the size distribution of a thin veneer of non contiguous sediment.

covers the bedrock to the east and north of this area, and there is a discrete sediment patch centrally within Cemlyn Bay.

Gravelly deposits, where they occur, are found in the central and offshore zones (around and to the north of this arc) whereas sand only is found in the shallower waters of the major embayments. Notable areas of megarippled seabed are found to the east (major deposit) and west (minor deposit) of Wylfa Head (probably formed by headland associated flow structures), and in a swath to the north and west of the development site. Sand veneers within the major embayments are devoid of any bedforms.

6.2 Seabed sediments

6.2.1 Benthic Environmental Datasets

During the benthic sampling campaign undertaken by Jacobs UK Ltd in 2011 and 2014, 28 discrete seabed sediment samples were collected. Further data is available from the borehole data generated during the ground investigations conducted in 2008 (Soil Mechanics, 2008) and 2016 (Fugro, 2016). These data provide a quantitative dataset on the specific grain sizes that constitute the seabed sediments across the site (see Figure 34 for grain size data, see Figure 33 for sample locations and for broad seabed characterisation data presented in the form of gravel: sand: mud [> 2 mm to $8+$ mm; 2 mm – 0.063 mm: < 0.063 mm, respectively] ratio data) as classified by Blott and Pye (2010). The surficial seabed sediments in the area are predominantly gravelly SAND/sand GRAVEL and/or muddy SAND, which reflects also the classification provided by analysis of borehole surface samples (see Table 24). Figure 34 displays polymodal grain size distributions which are generally very poorly sorted (i.e. a wide variety of grain sizes are found). The sample data generally support well the AGDS view of seabed sediment type, and show that offshore samples are dominated by coarse gravel and medium to coarse sand whereas samples within shallower inshore areas contain less or no gravel; the samples reveal a mud (i.e. silt and clay) fraction, which AGDS cannot resolve; mud (likely formed by erosion of out- or sub-cropping glacial till) is found in variable quantities across a number of the inshore sites, in particular within samples collected in the western areas of Cemaes Bay, in the lee of Wylfa Headland. This is a function of the more sheltered nature of this area.

6.2.2 Borehole Sediment Data

The physical nature (e.g. grain size) of the sediments comprising the unconsolidated sediment formations (described above) beneath the seabed, which form primary input data into any scour potential analysis for example, can only be deduced from the physical analysis of samples from boreholes recovered at the site. A ground investigation was undertaken by Fugro Group (Fugro 2010, 2010b). During this investigation in total 11 over-water boreholes were recovered from across the site, six sited north of Wylfa Head and five located to the west of Wylfa Head. The vertical sequence of sediments, and their varying geological and hydraulic (sediment mobility) properties, is a key factor in the prediction of scour potential across the depth of any proposed structures constructed on or into the seabed.

These data have been assessed and a semi-quantitative sediment description to a depth of 5 m below seabed level is presented in Table 24. The down-hole composition reflects a varying admixture of the principal grain fractions found across the Wylfa Newydd the site (i.e. muds, sand and gravels).



Table 24. Down-core sediment description of the Wylfa Newydd site boreholes to a depth of 5 m. Source: Fugro (2010, 2010b).

Borehole No.	Sample Depth (m below seabed)	% Classification					Soil Description
		Clay	Silt	Sand	Gravels	Cobbles	
BH401	0.50	0	3	88	9	0	Brown slightly silty gravelly SAND
	1.50	0	15	59	26	0	Brown clayey very gravelly SAND
	2.50	0	4	44	52	0	Brown slightly clayey SAND and GRAVEL
BH402	1.50	0	2	56	42	0	Brown slightly silty SAND and GRAVEL
BH403	1.00	0	3	82	15	0	Brown slightly silty gravelly SAND
	3.50	60	34	2	4	0	Brown slightly sandy slightly gravelly CLAY
BH405	0.00	0	1	81	18	0	Brown slightly silty gravelly SAND
	1.40	0	4	21	70	5	Black slightly clayey cobbly very sandy GRAVEL
BH406	1.15	6	11	44	38	1	Brown slightly cobbly clayey very gravelly SAND
	2.15	0	3	4	12	81	Grey slightly clayey slightly sandy gravelly COBBLES
	3.15	0	13	12	74	1	Brown slightly cobbly sandy clayey GRAVEL
	4.15	13	39	34	14	0	Brown slightly gravelly slightly sandy CLAY
BH407	0.50	0	1	31	67	1	Brown slightly cobbly slightly silty very sandy GRAVEL
BH408	0.00	0	0	25	74	1	Brown slightly cobbly very sandy GRAVEL
BH410	0.90	33	30	28	9	0	Grey slightly gravelly slightly sandy CLAY
	2.50	0	7	28	63	2	Brown grey slightly cobbly clayey very sandy GRAVEL
	4.50	0	17	42	34	7	Black cobbly clayey very gravelly SAND
BH412	0.00	0	14	41	45	0	Brown clayey SAND and GRAVEL
BH413	0.00	0	1	10	76	13	Black slightly silty sandy cobbly GRAVEL

6.2.3 Suspended Sediments

Suspended sediment can be an important component of a sediment regime and requires consideration. Sediment in suspension is in general derived from:



- resuspension of bed sediments at the site induced by waves and/or tidal currents;
- fluvial inputs in the vicinity of the site;
- regions external to the site (e.g. advection of turbid waters in the wider Irish Sea; and,
- algal blooms and phytoplankton in the water column (mostly during spring and summer).

A key issue for this study is whether sedimentary material discharging from local rivers impact upon the proposed development site and/or form an important part of the sediment regime at the site. Mineralogical and tracer studies undertaken in the North Sea area by McManus et al. (1993) endorse the view that most offshore sediments do not arise from riverine inputs but are found to be derived from the offshore region itself (e.g. seabed redistribution; erosion of Quaternary sediments). The small quantities of mud found in samples collected during the benthic sampling campaign (Jacobs 2011), are thus likely to have arisen from *in situ* seabed erosion.

Typical concentrations of suspended sediments in the coastal waters around the development have been measured during a dedicated water quality sampling campaign in advance of the development (Horizon, 2017). Typical average suspended sediment concentrations from the 6 sampling stations are presented in Table 25. The samples were collected using a Lund tube which collects an integrated sample of water from the surface to 10m below the surface. The corresponding sample locations are plotted in Figure 33. The data are tightly grouped at 5.6 to 8.2 mg l⁻¹. The data reveals that the fundamental background suspended sediment concentration across the development site is 3 – 4mg l⁻¹

Table 25. Suspended sediment monitoring data. Data source: Horizon (2017).

Monitoring point	Average (mg l ⁻¹)	Maximum (mg l ⁻¹)	Minimum (mg l ⁻¹)	No. of samples
WQ1	5.6	17.1	3	66
WQ2	6.0	22.8	3	68
WQ3	8.2	46.8	3	68
WQ4	6.5	30.4	3	68
WQ5	6.0	23.1	3	68
WQ6	6.3	9.5	3.5	8

Data on near-bed suspended sediment concentration were collected at four monitoring stations (see Figure 10) within the Titan monitoring campaign presented in Titan (2011). Over summer months between July and August SSC was less than 30 mg l⁻¹ overall with the background mean SSC fluctuating with the Spring and Neap tidal cycle, increasing over Springs and decreasing over Neaps. The amount of sediment in suspension over the deployment period was generally low near the seabed and <20 mg l⁻¹ on average. There was an overall increase in background SSC levels between May and June 2011 with values increasing gradually from <20 mg l⁻¹ to reach a peak SSC of 217 mg l⁻¹ at the start of June 2011 before dropping once more to background levels of <60 mg l⁻¹. The increased SSC levels between May and June could have been the result of increased levels of phytoplankton suspended in the water column during the spring / summer algal bloom. Time series data showing the near bed suspended sediment concentration coincident with the prevailing hydrodynamic conditions are presented in Figure 41 - Figure 44 and discussed further in section 6.3.3.



Fluvially derived inputs

A study of the hydrological baseline of the surface water bodies that have the potential to be affected by works associated with the development of the Power Station within the Wylfa Newydd Development Area has been conducted by Jacobs (Jacobs UK Ltd, 2017). The study encompassed five surface water courses that drain through the study area and through and past the Wylfa Newydd Development Area into the sea. They are:

- Tre'r Gof
- Afon Cafnan
- Nant Cemlyn
- Nant Cemaes
- Power Station Catchment

Data have been collected on the typical concentrations of total suspended solids that are recorded from the catchments within the Wylfa Newydd Development Area and are presented in Table 26.

Table 26. Suspended sediment monitoring data (Total Suspended Solids mg l⁻¹). Data source: Jacobs UK Ltd (2017).

Monitoring point	Average (mg l ⁻¹)	Maximum (mg l ⁻¹)	Minimum (mg l ⁻¹)	No. of samples
Tre'r Gof.	624	21000	<2	76
Afon Cafnan	129	2580	2.5	82
Nant Cemlyn	1053	2750	7	6
Nant Cemaes	19.5	106	2	24
Power Station Catchment	14.3	32.6	3.3	8

6.3 Offshore Sediment Transport by Tides and Waves

Seabed sediments are susceptible to resuspension by tidal currents. Resuspension occurs when the frictional drag (the 'bed stress'; τ_0) exerted by currents and waves, separately (e.g. during summer months when waves are negligible) and in combination (e.g. during winter storms), exceeds the submerged weight of particles, which act to retain particles on the bed; the stress at which sediment motion is first produced is called the 'critical bed stress', denoted $\tau_{0\text{crit}}$. When $\tau_0 > \tau_{0\text{crit}}$ sediments are mobilised, and for many coastal environments this is evident by an increase in the concentration of sediments in suspension. The term $[\tau_0 - \tau_{0\text{crit}}]$ is defined as the 'excess bed stress', and smaller values of this metric may be regarded as indicative of relatively low rates of sediment transport, likely evidenced by nearbed sediment concentrations only slightly above background, whereas larger values of this will drive greater rates of sediment transport indicated by significant elevations of suspended sediments. Sediments finer than ~0.2 mm are prone to being mobilized directly into suspension, those > 2 mm are usually transported as bedload and leads to the formation of bedforms, and the intermediate sizes (and for mixed size sediments) the transport mode is commonly a combination of the two.

Whereas tides exert a time varying bed stress on sediments associated with daily tidal and longer term Spring – Neap variability, the superposition of waves on tides, namely during winter-time periods, results in

enhancement of the bed shear-stress by waves. The boundary layers at the bed associated with the waves and the current interact nonlinearly, and this has the effect of enhancing both the mean and oscillatory bed shear-stresses. The bed shear-stress due to the combination of waves and current is enhanced beyond the value which would result from a linear addition of the bed shear-stress due to waves, and the bed shear-stress due to current. When waves occur concurrently with peak tidal currents, the consequent bed stress is a powerful driver of sediment transport.

The chief questions that arise in relation to understanding the baseline sediment transport regime across the site include:

- Are the tidal currents at the site sufficient to generate sediment transport?
 - If so, what is the percentage of time that current conditions exist which are sufficiently powerful to generate transport?;
 - If so, what are the rates of suspension and bedload transport?;
 - Are there asymmetries in transport which create a net transport direction?; and
 - Are there differences in expected transport rate across the site in relation to differing sediment types?
- Is the wave climate sufficient to generate sediment transport?
 - If so, what are the critical height-periods which do so, therefore when seasonally is transport expected to occur?;
 - What is the percentage of time that wave conditions exist which are sufficiently powerful to generate transport?;
 - How variable across the site is transport expected to be ?; and
 - How do wave and tide currents combine to generate sediment transport, and how important is this?

6.3.1 Approach to Understanding the Baseline Sediment Transport Regime

An approach using the stress / excess bed stress concept outlined, majority based upon the use of the various modelling tools, has been adopted here. The Delft3d and Amec-HR Wallingford SWAN models are used to generate, respectively and on a geospatial basis, tide only metrics (velocity data, Spring / Neap, flood-ebb; bed stress) and wave metrics (H_m0 , T_z , dir), and through their combination wave plus current metrics (bed stress). Grab, core and borehole data provided information on grain size and from this the critical bed stress τ_{0crit} was computed following Soulsby (1997). The acoustic (geophysical) ground discrimination map from Horizon (2012) Figure 5.25 was 'anonymised' (sediment type removed) to show only those areas of seabed covered in sediment and bedrock (Figure 36). The anonymous sediment map facilitated an appreciation of the relative mobility for the two major sediment components prevalent across the site. GIS was used to generate excess stress maps for various marine conditions (currents only, waves plus currents; scenarios summarised in Table 3) assuming the sediment cover was a) entirely sand (particles < 2 mm in size) and b) fine gravel (particles < 8 mm in size). These size bins were based upon review of grab, core and borehole data. These geospatial excess stress plots show areas where the entire sand fraction (material up to and including 2 mm) and or gravel fraction (material up to and including 8 mm) would potentially be expected to be mobilised under various oceanographic forcings (tides and waves). The gradation in colour represents differences in the absolute excess stress and is a qualitative indicator of transport severity (the most severe rates represented by the darker colouring). In the following sections there is a focus on the Spring ebb tide condition rather than all of Spring / Neap / flood and ebb, as this represents the 'worst case' in terms of potential seabed mobility (i.e. the offshore regime is ebb dominated).

6.3.2 Tidal Resuspension and Transport

The oceanographic monitoring campaign collected continuous data on the concentration of sediments in suspension (Figure 41 - Figure 44) from which it is possible to judge tidally driven sediment resuspension only (i.e. during periods when there are not numerous waves which also give rise to resuspension and elevated sediment concentrations). If tidally-driven sediment suspension does occur one would expect there to be variability in concentration that reflects (i.e. follows) either individual tides, the Neap-Spring phasing or both.

In areas of the time series where wave resuspension is not occurring, there is a very weak tidal suspension signal, in spite of the offshore high velocity region. The signal indicates a very weak daily tidal suspension signal, and a similarly weak relation (greater resuspension during Springs) to the Spring – Neap phasing. A good quality example of both intra-tidal and lunar period (Spring – Neap) suspension is found in Figure 37 Panel s2(1). Average tidally generated ‘concentrations’ are centred on approximately $\sim 30 \text{ mg l}^{-1} \pm 10 \text{ mg l}^{-1}$ at s2 and s4, and about half this at s9 and s11 (Horizon, 2012). A comparison with data from discrete water samples collected at a variety of locations within the investigation boundary (Table 25) shows that tidal resuspension elevates near-bed suspended sediment concentrations by a factor of 5 – 10 over background.

An indication of the sediment fraction likely to be suspended at each site by the bed stresses, together with an assessment of the percentage of time the critical stress is exceeded (i.e. the expected mobility duration), is afforded through development of ‘exceedence’ plots. Plots have been constructed for each site reflecting the admixed gravel / sand nature of the sediments: fine sand; medium sand; coarse / very coarse sand; and fine gravel (Figure 37). This representation allows for a simple and direct appreciation of the mobility of these grain sizes by tidal currents alone. Table 27 summarises the data from this analysis.

Table 27. Summary of critical stress % exceedance for various bottom sediment size fractions. Following the method of Soulsby (1997), based upon the entire available flow velocity records, and using a C100 value of 0.0024. Data source: Horizon (2012).

Sediment Fraction	Maximum Particle Size (mm)	$\tau_{ocrit.}$ (Nm ⁻²)	Exceedence (%)			
			S2	S4	S9	S11
Fine Sand	0.25	0.19	80.6 %	79.5 %	48.7 %	41.4 %
Medium Sand	0.50	0.26	76.8 %	75.1 %	36.3 %	29.6 %
Very Coarse Sand	2	1.17	40.3 %	34.9 %	0.07 %	0.35 %
Fine Gravel	8	6.93	0 %	0 %	0 %	0 %
Medium	16	14.19	0 %	0 %	0 %	0 %
Very Coarse Gravel	64	56.24	0 %	0 %	0 %	0 %

This approach shows that gravel size material at each of the four monitoring stations is stable under the current regimes. Conversely, sand material is subject to resuspension at all four stations, but there is a

marked difference in both the maximum grain sizes suspended and the relative frequency of suspension³; Figure 38 provides an illustration from s9 which shows frequent tidal mobilisation of fine and medium sand, whereas coarse sand is brought into suspension only during the most energetic portions of the Spring tide. To determine the shear stress acting on the bed (as illustrated in Figure 38) due to tidal flows, the mean depth velocity was converted to the velocity 1m above the bed (u_{100}) using the 1/7th power law velocity profile. The bed shear stress acting on the bed is then derived using the standard quadratic friction law based on an estimated friction coefficient following the method of Soulsby (1997). The overall pattern reflects the fact that stations s2 and s4 are in the region of higher current velocities located offshore where transport rates and frequencies would be expected to be higher.

A spatial extension of this approach is possible through use of the bed stress information generated using the Delft3d HD model (Figure 30 and Figure 31), the critical bed stress data (Table 27) and the 'excess stress' concept. Geospatial excess bed stress plots have been generated for the sand fraction (as a whole) (Figure 39), and the fine gravel fraction specifically (grains between 2 and 8 mm; Figure 40; only the ebb phase is shown since these are the strongest tides). Sediment mobilisation is indicated by positive values for $(\tau_0 - \tau_{0\text{crit}})$, and the absolute difference is an approximate index of the severity of mobilisation.

The observations suggest that sediment entrainment / transport due to tides alone does occur, but the evidence indicates a weak resuspension signal, resuspension magnitudes are low and tidally-related nearbed concentrations are not significantly different from background levels (see Table 25). Farther inshore within the embayments and towards their heads, flow velocities and bed stresses are consistently low and no tidally forced resuspension occurs.

The finding of a weak tidal signal applies equally across the four monitoring stations, in spite of the fact that s4 (definitely) and s2 (probably) are in the pronounced region of high velocity (Figure 15 - Figure 18), and associated excess stress (Figure 39 and Figure 40) offshore from the major headlands. In an otherwise contiguous and homogeneous sandy / gravelly seabed current magnitudes measured at s2 and s4 (Table 8) would be expected to give rise to far greater nearbed sediment concentrations than recorded; some evidence of active sediment transport beneath the high velocity (further) offshore streams is a field of gravel megaripples in the northwest of the site, but the data quality is not high and this cannot be substantiated further. In numerous places, also, the high flow regime has completely scoured the bedrock free of sediments (Figure 36). The lack of evidence for significant sand transport suggests a supply limitation issue across the site; one or more of the following factors may contribute to explaining the low suspended sediment concentrations observed:

- 1) It may be envisioned that in the vicinity of the monitoring stations and laterally along that latitude there is pool of periodically (tidally) re-suspendable sediments (PRS) and it may simply be the case that this pool is finite and not large. Extensive areas of seabed within the offshore region of the site are swept clean of surficial sediments (see Figure 36) which, *de facto*, indicates a very reduced sediment volume available for resuspension (i.e. it is a comparatively impoverished sediment system both in terms of sediment cover and the PRS fraction); this interpretation is consistent with the region having a paucity of contemporary supply of sediments more generally, the lack of any widespread morphological indicators of sediment transport and the presence of areas of smooth sand.

³ This analysis assumes that where sands are brought into suspension then finer constituents (silts, clays), found in some samples, and varying in proportion from minor to dominant, are also brought into suspension.



- 2) Where bottom sediments are exposed to persistent high bed stresses over the long term (e.g. over the last 5000 – 6000 years), and the bed material is heterogeneous, fine material has been removed (creating a source limitation for this sub-fraction) and a coarse surface veneer both protects the bed from further erosion and shelters any finer constituents; gravel rich grab samples (e.g. WS6, WS27), typically found offshore, indicate a particularly low (<~20%) sand content. this “bed armouring” phenomenon is reported for high velocity gravel bed rivers, which bare some similarity to the offshore region (Richards, 1985) albeit under a unidirectional flow regime.
- 3) The four monitoring stations have been deployed onto, or close to, exposed rockhead (certainly a possibility for s4);

6.3.3 Resuspension and transport under combined forcing of tidal currents and waves

The foregoing analysis of tide-only forced sediment transport indicates that bed sediments in the outer embayments at the Wylfa Newydd Development Area, and within a high flow offshore region, are mobilised on tidal time frames but the degree of transport is weak. Farther inshore no tidally-forced resuspension of bottom sands and gravels is evident. This situation exists only during periods when there are no or small waves (e.g. during summer months). In shallow continental shelf environments waves, created by the wind blowing across the ocean surface, can also give rise to sediment entrainment and transport if the energy associated with the wave is able to penetrate to the seabed. Some consideration of the potential for waves to mobilise the seabed sediments is thus necessary. Note that since the sea is nearly always in motion due to tides (except during brief periods of high/low tide standstill [slack water] when currents are close to zero), in reality this consideration is strictly one of waves and currents in combination rather than just solely waves.

From consideration of the characteristics at each of the oceanographic monitoring stations it is possible to determine whether the waves will ‘feel’ the seabed at each location. Waves produce an oscillatory velocity in the water column which is a function of wave properties (namely, height and period) and which decreases in amplitude (magnitude) with depth. Whether the seabed ‘feels’ this flow therefore depends on the ratio of the water depth to wave height and period. As a rule of thumb, wave energy will penetrate to the seabed where:

$$h < 10 H_{m0}$$

1.

Where h is the water depth and H_{m0} =significant wave height (Soulsby, 1997). In the ensuing analyses this criterion has been used to determine the limiting significant wave height above which waves energy is expected to penetrate to the seafloor at each of the four monitoring stations (Table 28).

Table 28. The limiting significant wave height required for waves to feel the seabed at the locations of the four monitoring stations. The percentage of time waves which exceed these limiting thresholds are observed are detailed and the modal wave direction noted. Data Source: Horizon (2012).

Monitoring station	Water depth (m) (mean sea level)	H_{m0} where waves ‘feel’ the seafloor based upon Soulsby criterion (m)	Exceedence (%)	Modal wave direction (compass quadrants)
S2	42	4.2	0.9	W, WNW
S4	35	3.5	0.7	S, SE, SW, W, NW
S9	16	1.6	10.7	NW, NNW
S11	13	1.3	9	NW, NNW

Table 28 presents a semi-theoretical perspective on wave energy and its penetration to the seabed bed. It is useful to compare these expectations with data on the real-world processes from the oceanographic monitoring campaign.

The observed suspended particulate material (SPM), derived from the Optical Backscatter Sensor (OBS) data, are presented in Figure 41 - Figure 44 where the OBS data corresponds with the AWAC record (there is not always coincidence in the time series).

The time series data suggest that very little resuspension of material occurs due to wave action. The plots show generally weak baseline concentrations ($\sim 20-30 \text{ mg l}^{-1}$) attributed to the tidal signal, with slightly elevated concentrations observed during Spring tides and slightly lower concentrations observed during Neap tides. A number of peaks within the time series data occur where SSC is enhanced relative to the 'background' levels. There are occasions of persistent elevated SSC during the summer months and these are attributed to an algal bloom (Horizon, 2012).

At the offshore monitoring station (s2) despite numerous wave events a generally low SSC is observed with occasional isolated incidences of elevated SSC. This is simply a function of the low energy wave climate at the site during the observation period; modal H_{m0} wave heights were 0.5 – 1m, with mean $H_{m0} = 1.09\text{m}$ (Table 8). Much larger waves only ($> 4\text{m}$) are expected to feel the seabed and thus only during the highest energy episodes would waves be capable of re-suspending material.

At site s4 offshore from Wylfa Head a greater SSC is observed most likely as a result of the shallower water depth. Elevated SSC signals generally correspond better with observed wave data (i.e. where higher energy episodes are recorded the SSC is elevated). The theoretical analyses using Soulsby criterion indicated that for waves to feel the seabed they must exceed 3.5m in height (Table 28) and although the significant wave height (H_{m0}) only exceeds this occasionally within the observational period, the maximum wave height (H_{max}) exceeds this threshold more regularly, bringing material into suspension. However, these occurrences of significantly elevated SSC are rare.

The worst storm (nearly a 1 in 10 year magnitude event) recorded within the monitoring period occurred during 13 – 15th November, 2010. This was recorded at both of the deep water monitoring stations (s2 and s4). Table 29 presents the Suspended Sediment Concentration (SSC) associated with this event, which indicates the loadings generated by such storms and the influence of depth on resuspension (more sediment is suspended at the shallower monitoring station, s4).

Table 29. The associated nearbed suspended sediment concentrations (SSC) during a ~1:10 storm event detailed in Horizon (2012). The corresponding nearbed suspended sediment concentrations recorded at monitoring stations, s9 and s11, were not reported. Source: Horizon (2012).

Monitoring station	Date	H_{m0}	Associated SSC (mg l^{-1})
s2	13 TH – 15 TH Nov (2010)	4.58 m ($\cong 7 \text{ m } H_{max}$)	37
s4	13 TH – 15 TH Nov (2010)	2.54 m ($\cong 4 \text{ m } H_{max}$)	289

It is of interest to interrogate a specific storm event to better understand how the combined stress from waves and tidal flows act to suspend sediment at the site and document typical nearbed concentrations associated with such events. The magnitude of naturally occurring suspended sediment concentrations is a key metric in assessing the significance of anthropogenically related changes to coastal sediment concentrations (e.g. that due to construction, dredging etc.).



At the inshore site (s9), a correlation is evident between the SSC and wave data. Despite the inshore location, occurrences of significantly elevated SSC remain rare most likely due to the comparatively quiescent nature of the wave climate during the majority of the monitoring duration (Table 8; Table 17). Again, persistent enhancement of SSC is considered to be algal bloom related and not the result of bottom sediment resuspension. At site (s11) there is a general paucity of data. In addition, the data appears to display more 'sensor noise' which may be due to sensor drift or biofouling, than good quality information.

SSC exceedance plots have been constructed for each monitoring site (Figure 45) to support the assessment of wave related resuspension. Presentation of the SSC information in this manner enables at each of the fixed monitoring stations an assessment of the percentage of time the background SSC (determined from the time series plots as 30 mg l⁻¹ for the monitoring stations positioned offshore [s2, s4] and 20 mg l⁻¹ for the monitoring stations positioned inshore [s9, s11]) is exceeded (i.e. where additional material in relation to that which is suspended by the tidal flows, has been suspended).

The exceedance plots clearly indicate the low SSC that persists across the site for the majority of the time. At the offshore sites the observed SSC signal remains within background levels (i.e. around the values associated with non-wave / tide only periods), for 86.2% and 83.7% of the time, at monitoring station, s2 and s4, respectively. Further the 90th percentile within these plots is achieved at only slightly elevated levels in comparison to tidally generated background values (30 mg l⁻¹), specifically 60 mg l⁻¹ and 39 mg l⁻¹, for monitoring station, s2 and s4 respectively. As expected, wave action acts to suspend sediment more often in the shallower inshore sites. The data shows the observed SSC remains within background levels 76.0% and 44.7% of the time at monitoring station, s9 and s11 respectively. The data from s11 should, however, be treated with caution as the data presented was captured during a significantly shorter deployment period coinciding with winter (where the frequency and magnitude of wave events is naturally greater). Despite this, at both inshore sites exceedance of background levels is generally low evidenced by the 90th percentile value being achieved at 48 mg l⁻¹ and 73 mg l⁻¹, for station, s9 and s11, respectively. Collectively, the foregoing assessment reveals differences between monitoring sites (associated with the variability in depth), but overall the magnitude of exceedance remains low in terms of both magnitude and frequency.

It is noteworthy that although correlation between wave events and increased SSC is observed within the data there are numerous occasions where a correlation does not occur (i.e. where a high energy episode is not reflected with an increase in SSC), or where peaks in SSC were not obviously related to the tidal cycle or enhanced wave action. No reason for these discrepancies is offered in the Horizon report (Horizon, 2012), though they may have occurred due to one, or a combination, of the following reasons:

- Sensor effects (i.e. drift/noise)
- Biological effects (i.e. algal blooms, biofouling)
- Sensor position
- Seabed topography and sediment characteristics

To provide a spatial context, in an approach analogous to Section 6.4, geospatial excess bed stress plots for waves and [Spring tide peak] currents in combination have been generated for the offshore wave scenarios stated in Table 3 (typical wave H_{mo} 0.9 m; winter wave H_{mo} 2.0 m; and high wave from the North H_{mo} 2.85 m) for the sand fraction (as a whole) (Figure 46 - Figure 48), and the fine gravel fraction specifically (grains between 2 and 8 mm; (Figure 49 - Figure 51). For the typical wave condition H_{mo} 0.9 m (nominally representative of the summertime period; Table 17 and 22), there is little difference to the tide-only condition for either sands or gravels. For the typical winter wave condition H_{mo} 2.0 m (selected from the time series data to be representative of winter period waves) and for the high wave from the North H_{mo} 2.85 m, areas of high excess stress essentially migrate inshore and penetrate the embayments, meaning that sediments (both sand and fine gravels) in shallower waters may be susceptible to resuspension.

The wave energy across the site progressively increases from the typical wave condition through to the extreme wave from the north. In the most extreme case, excess stress is greatly elevated in comparison to

the typical wave scenario and areas of excess stress are present further inshore into Cemaes Bay, Cemlyn Bay and Porth y Pistyll (see Figure 46 - Figure 48).

Inspection of the model outputs concerned with the fine gravel fraction reveal that during typical, and typical winter wave scenarios, the area of sediment (fine gravel) where excess stress is present on the bed is highly similar to the tide only condition i.e. the superposition of these specific wave conditions on a Spring tide does not manifestly change the spatial pattern of excess stress. Transport of gravels remains confined to the offshore region to the north and west of the site (Figure 50). However, equivalent superposition of the extreme wave from the north amplifies offshore gravel transport but additionally gives rise to isolated pockets of excess stress within inshore areas in the east of Cemaes Bay, and in areas of Cemlyn Bay and Porth y Pistyll (Figure 49 - Figure 51). The coarse nature of the gravel sediments suggests a localized movement of material as bedload, but any gravel brought into suspension would rapidly fall back to the bed. A major re-adjustment of the sediment distribution on the bed under big storms is not anticipated for the gravel fraction.

In terms of sand transport there remains an offshore region of higher flow delineated approximately by an arc running across the principal promontories (Trwyn Cemlyn in the west, Wylfa Head and across to Llanlleiliana Head in the east) (discussed in Section 6.4) which drives a significant sand transport, but which does not appear to be significantly enhanced by wave action, due to the rarity of waves large enough to feel the seabed in deeper water. Superposition of the winter wave condition H_{m0} 2.0 m exposes sands found farther inshore to positive excess stress and so resuspension will occur; much of the interior of Cemaes Bay, the outer part of the sand lens within Cemlyn Bay and some areas within Porth y Pistyll are exposed to higher stress. As the tidal currents are comparatively weak in many of these zones any sand resuspended is likely to remain in the immediate vicinity and not suffer any long distance transport (the recirculating gyres around Wylfa headland in particular will act to retain sediments locally). Under the 98th percentile wave from the north, resuspension potential is largely in the same areas as per the 2 m wave condition, although there is evidence of the penetration of wave energy deeper (farther) into the heads of both Cemaes Bay and Cemlyn Bay (Figure 48). Larger excess stresses, due to amplification by a substantially bigger wave event, would be expected to elevate resuspension rates, once again, though, whilst there may be some local morphological adjustment at the bed due to especially high bed stresses, any sand resuspended is likely to remain in the immediate locale owing to the comparatively weak currents in the bays.

6.4 Extreme Events, Evolving Baseline and the Importance of Climate Change

Unusually energetic and infrequent metocean events (e.g. storms) give rise to extreme values of significant wave heights and wave periods. Table 30 presents the values for extreme significant wave height (H_{m0}) and the associated wave direction as defined by HR Wallingford (2015). The data reveal the largest wave heights will most likely occur from a northerly aspect. As discussed in Section 5.3, where large waves approach the shore from a northerly aspect significant stress is predicted to be exerted upon the bed in the embayments of Cemaes Bay, Porth y Pistyll and Cemlyn Bay. Isolated pockets of significant stress are also likely to occur along the rocky headlands off Wylfa Head and Cerrig Brith, and in the west of Cemaes Bay. Extreme wave events from the north would significantly increase bed shear stresses across the nearshore and coastline of the development. It is of note, that during the metocean monitoring period, a storm event occurred where H_{m0} exceeded that predicted for a 1:1 return period (Table 30), driving sediment concentrations to above 200 mg l⁻¹ at s4 (Table 29). In areas of sandy sediment cover, concentrations perhaps double this may arise at shallower locations during higher energy storm events, higher in surf zones. Any resuspended material, as presented elsewhere, is anticipated to settle back to the bed rather than suffer any substantial advective transport due to the low inshore currents.



Table 30. Extreme significant wave height and direction estimated for offshore model points 1-5 for 1, 10, 20, 50, 100 and 200 year return periods. HR Wallingford (2015). These values are generated from a 3 hourly record and are 3 hourly averaged values. The most likely associated mean wave direction is 285 - 15° N (HR Wallingford, 2015). The position of the model points is detailed in Figure 26.

Model Point No.	Significant wave height (m) for return period (years)					
	1	10	20	50	100	200
1	4.6	5.6	5.9	6.2	6.5	6.8
2	4.4	5.5	5.8	6.1	6.4	6.7
3	4.3	5.3	5.5	5.7	5.9	6.0
4	4.3	5.3	5.5	5.8	6.0	6.2
5	4.3	5.4	5.5	5.9	6.1	6.3

It is widely expected that climate change will result in global effects which it is anticipated will be manifested at regional scales by increased storminess and rising mean sea level (Lowe et al., 2009). An increase in the frequency and magnitude of storm events will increase the potential for resuspension of sediment across the site due to the increased likelihood of wave conditions that are sufficient to penetrate to the seabed. Waves of greater magnitude would also be likely to increase penetration of wave energy deeper (farther) into the heads of both Cemaes Bay and Cemlyn Bay.

At the location of the proposed development it is anticipated that mean sea level is likely to during over the lifetime of the power station's construction operation and decommissioning. This change is widely accepted to include contributions from global eustatic (water volume) changes in mean sea level and also as a result of regionally varying vertical (isostatic) adjustments of the land. Information on the rate and magnitude of anticipated relative sea level change in during the 21st Century is available from the UKCP09 (United Kingdom Climate Projections, <http://ukclimateprojections.metoffice.gov.uk/21684>) Summary predictions of 21st Century changes in relative sea level are presented in Table 31. These predictions indicate that by 2050, relative sea level at the proposed development location will have risen by 18 cm to 26 cm above 1990 levels. As shown by the rate of increase in values in the table, the majority of predicted sea level rise occurs during the second half of this century when the rate of change is predicted to be greatest. It should be noted that such an increase in mean water level is significantly smaller than the tidal and non-tidal (e.g. barometric pressure) water level variations presently encountered at the site.

Table 31. Estimates of relative sea level rise relative to levels observed in 1990 under three differing scenarios. Data Source: UKCP09 (2017).

Year	Relative Sea-level Rise based on the Low Emissions Scenario (cm)	Relative Sea-level Rise based on the Medium Emissions Scenario (cm)	Relative Sea-level Rise based on the High Emissions Scenario (cm)
2000	2.5	2.9	3.5
2010	5.3	6.2	7.3
2020	8.2	9.7	11.5
2030	11.4	13.4	15.9
2040	14.8	17.5	20.8



Year	Relative Sea-level Rise based on the Low Emissions Scenario (cm)	Relative Sea-level Rise based on the Medium Emissions Scenario (cm)	Relative Sea-level Rise based on the High Emissions Scenario (cm)
2050	18.4	21.8	25.9
2060	22.2	26.3	31.4
2070	26.3	31.1	37.1
2080	30.5	36.2	43.3
2090	35	41.6	49.7
2095	37.3	44.4	53.1

UKCP09 also includes projections of changes to storm surge magnitude in the future as resulting from climate change (Lowe et al., 2009). It is estimated that for the 'medium emissions' scenario, a 1 in 50 - year storm surge event will increase by between 0.08 mm/yr^{-1} and 0.36 mm/yr^{-1} (values apply until 2099). The resultant effect is very small in comparison to the natural variability of storm surge heights (see Table 7) and would not constitute a measurable change.

At Wylfa head the risk from sea level rise (i.e. coastal flooding and erosion) are considered to be low due to the predominantly higher ground comprised of hard bedrock. Within the embayments the rate of erosion is predicted to increase (1.7 to 2.5 times the existing base erosion rate over 100 years) with sea level rise (Haskoning UK Ltd, 2012). Various defences protect the low-lying coastline and key habitation areas, though there are softer cliffs and shorelines which remain unprotected and these are open to enhanced erosion. Of particular note is the SPA, SSSI and SAC designated feature of the Cemlyn Bay lagoon and Trywn Cemlyn Headland. Cemlyn Lagoon owes its origin to the accumulation and formation of a shingle barrier beach. It has been suggested that these gravels and cobbles are a legacy deposit, likely to be supply-limited and therefore potentially vulnerable to change. Pye and Blott (2010) undertook a preliminary geomorphological assessment based largely on previous studies, historical maps and aerial photographs, a site visit and a limited sedimentological analysis. For the Esgair Gemlyn barrier beach the authors stated "...there are no obvious sources of new sediment supply to the barrier and any future acceleration in sea level rise will make it increasingly difficult for the barrier to maintain its relative crest level and an equilibrium cross-sectional profile.....". Their work indicated that the Esgair Gemlyn is in no immediate danger of a major breach and that over-washing is relatively infrequent and small scale. However, the frequency of over-washing appears to have increased along the central part of the barrier since 2000 and a severe event could occur at any time. The authors point out that there are no obvious new supplies of sediment to the beach. As a result, any future acceleration of sea level rise will make it difficult for the barrier to maintain its height and there could be a rapid landward movement of the barrier as it adopts a flatter profile. By 2100, over-washed shingle could cover the area of the lagoon now occupied by the islands and a new tidal inlet could ultimately develop. The West of Wales SMP2 predicts that for more stable features, such as fully developed shingle beaches, there will be a natural roll back of beaches potentially in the range of 10m to 40m over 100 years (Haskoning UK Ltd, 2012).

6.5 Summary of Sediment Transport Regime

1. Site Overview

- a. The Wylfa Newydd development is located within coastal cell, sub cell 10b on the northern Anglesey coast.
- b. The Anglesey coast comprises a range of hard rock and soft sediment regions predominately characterised by a series of low lying sandy or shingly embayments bounded by rocky

headlands. These embayments are frequently fronted by bedrock wave-cut platforms. Examples of these Bays include:

- i. Cemaes Bay
- ii. Cemlyn Bay
- iii. Porth y Pistyll
- c. The area of investigation can be sub-divided into three categories:
 - i. Shelf sea boundary (regional context)
 - ii. The northern coastline of Anglesey, extending ~ 3km offshore (intermediate boundary)
 - iii. The development site coincident with the marine area between Trwyn Cemlyn in the west to Llanlleiliana Head in the east, ~ 2km offshore (detailed inner boundary).
- d. At the local scale, within the area of investigation many key coastal geomorphology features are represented including a number of beach cusps, a small tombolo and remnant sand dunes and short lengths of 'tidal estuary'.
- e. Of particular note is the SPA, SSSI and SAC designated feature of the Cemlyn Bay lagoon and Trywn Cemlyn Headland.
- f. Within the area of investigation five surface water courses drain through the study area into the sea, namely:
 - i. Tre'r Gof.
 - ii. Afon Cafnan.
 - iii. Nant Cemlyn.
 - iv. Nant Cemaes.
 - v. Power Station Catchment.
- g. The general coastline topography and seabed bathymetry was sculpted during the Holocene. Last 10-11,000 years (predominantly the last 5-6000 years)
- h. The solid geology in the area is mainly comprised of very hard Pre-Carboniferous rocks which are Pre-Cambrian in age (Proterozoic). Metamorphic slates and greywackes extend a few kilometres offshore from the Anglesey coastline creating irregular seabed bathymetry.
- i. As the coastline is generally composed of hard rock, erosion rates and thus sediment supply to the subtidal zone is generally limited.

2. Seabed Sediments

- a. Sediment deposited during the most recent glacial period (the Holocene) is typically < 5m thick.
- b. The seabed within the surveyed area is comprised of varying proportions of bedrock exposure and relatively smooth sands and gravels predominantly determined to be gravelly and/or muddy sand. Sediments off Wylfa Head appear to be dominated by coarse gravel and medium to coarse sand. A mud fraction is present in a number of samples within inshore areas probably associated with sub crops of glacial till. The mud fraction is particularly prominent in samples collected from westerly areas of Cemaes Bay, in the lee of Wylfa Head, which is a function of both site geology and seabed topography and sheltering from oceanographic forcing.
- c. Erosion or winnowing of seabed sediment during the Holocene has acted to produce a 'lag' deposit on the seabed characterised by a veneer of coarse grained sediment, in this instance

characterised by a thin incomplete gravel and sand veneer, which “armours” the seabed, but can still be considered a mobile, or periodically mobile under certain extreme events / conditions, .

d. This lag / veneer is found essentially everywhere (other than on the tops of bedrock outcrops and on the steeper rock slopes), and has historically been swept up into the few bedforms found at the site.

e. Though it is likely that there is some {limited) exchange across the littoral zone, with gravel moved offshore during storms. Generally, the movement of sediment into the area from offshore is considered to be minimal.

3. Hydrodynamic Regime – Tidal flows

a. A high flow / bed stress offshore region exists (velocities $> 0.8 \text{ m s}^{-1}$; bed stress $> \sim 2.0 \text{ N m}^{-2}$ on Spring tides, $> 6 \text{ m}^2$ on Spring tides). This area is delineated approximately by an arc running across the principal promontories (Trwyn Cemlyn in the west, Wylfa Head and across to Llanlleiana Head in the east). A lower flow regime exists (velocities $< 0.8 \text{ m s}^{-1}$ and commonly far lower; bed stress $< \sim 0.4-0.5 \text{ N m}^{-2}$) within the coastal bays (Cemlyn, Cemaes) and southward of this arc (i.e. inshore). Very low flow velocities (velocities $< 0.4 \text{ m s}^{-1}$ and commonly $< 0.2 \text{ m s}^{-1}$; bed stress $< \sim 0.2 \text{ N m}^{-2}$ in many areas) are observed in the inner regions of Cemlyn and Cemaes Bays.

b. There are persistent recurrent circulatory gyres formed in the embayments to the east and west of Wylfa Head due to the interaction of the tidal currents with Wylfa head and Llanlleiana head. On the flooding tide two clockwise rotating eddies form, one in each embayment, in the lee of Wylfa Head and Trywyn Cemlyn Head during flood Neap and Spring tides between HW-5 to HW-3 hours, comparatively on ebb tides, two counter-clockwise rotating eddies are formed.

c. Measured current velocities within these eddy formations were generally lower, being on average $\sim 0.3 \text{ m s}^{-1}$ and flow patterns generated during Spring tides were more pronounced in comparison to the feature formed during ebb tides.

d. Current velocities generally increase as they flow around the tip of Wylfa Head.

4. Hydrodynamic Regime - Waves

a. The long term, offshore wave climate (based upon modelling) is dominated by a low wave (typically $H_{m0} < 1 \text{ m}$), short period ($T_z < \sim 2-5 \text{ s}$) wind sea environment, with the highest incidence of waves from the southwest.

b. Data from an approximately 1 year duration oceanographic monitoring campaign generally support the above observations.

c. At intervals during winter months the site experiences more energetic conditions, with offshore wave conditions in excess of 4 m and with associated periods of $\sim 4 - 8 \text{ s}$ experienced.

d. A largely shore-normal gradient in wave heights occurs as waves travel inshore they reduce in height due to shoaling and refraction processes. Typically there is $\sim 50\%$ reduction in offshore wave as they travel towards the coastline.

e. The wave direction spectrum shows a progressive change from the west to northwest with distance inshore, due to the combined sheltering effects of the coastline and wave refraction.

f. The predicted extreme significant wave height offshore for 1, 10, 20, 50, 100 and 200 year return periods are 4.3 m, 5.3 m, 5.5 m, 5.7 m, 5.9 m, and 6.0 m, respectively.

g. The highest frequency of extreme waves is predicted to occur from a Northerly aspect (0°) and due to the angle of approach these waves would maintain greatest height moving into inshore areas. This is thus considered ‘the worst case scenario’ in terms of coastal processes and impacts.

5. Tidally-forced sediment transport

- a. Two distinct sediment transport zones are evident:
 - i. A high flow / excess stress rectilinear offshore region delimited by an arc running across the principal promontories (Trwyn Cemlyn in the west, Wylfa Head and across to Llanlleiliana Head in the east) where both sand and gravels are mobile. The sedimentary system is supply limited and offshore suspended sediment transport is not hypothesised to be pronounced.
 - ii. An inshore zone within the coastal embayments (Cemlyn Bay, Cemaes Bay, Porth y Pistyll) where the bottom sands and gravels are stable under tidal action.
- b. Morphological evidence in support of sediment transport exists in the form of a field of megaripples indicating bedload transport, located in the high flow offshore region to the northwest of the investigation site, and there are widespread areas of exposed bedrock indicative of a high energy erosional environment. Generally, morphological evidence for sediment transport is not widespread.
- c. Pronounced ebb dominance within the offshore tidal regime suggests there may be a residual (net, long-term) westward transport of any material (sand and finer grains) that is resuspended.
- d. Regular formation of recirculating gyre systems within the embayments act to retain any locally resuspended sediments within these areas.
- e. There is an area in the western end of Cemaes Bay subjected to strong currents during Spring ebb tides, where resuspended sediments may be transported out of the embayment.

6. Wave related sediment transport

- a. Resuspension and sediment transport is enhanced when waves occur and the wave bed stress is additive to the current bed stress.
- b. This phenomenon would be at its most pronounced when a high energy episode is coincident with peak ebb, Spring tides (i.e. the worst case scenario).
- c. Frequency analysis of SSC time series indicates that surface wave action only rarely penetrated to the seabed to give rise to resuspension during the observational time period across the site.
- d. Superposition of a 0.9 m H_{m0} wave onto a Spring tide (nominally a typical summertime condition) produces no measurable enhancement of excess bed stress across the investigation site, a situation supported by observations.
- e. Superposition of a 2.0 m H_{m0} wave (a typical winter condition) onto a Spring tide produces measurable enhancement of excess bed stress across the offshore high velocity region, much of the interior of Cemaes Bay, the outer part of the sand lens within Cemlyn Bay and some areas within Porth y Pistyll. This is supported by observations.
- f. As the tidal currents are comparatively weak in many of these zones any sand resuspended is likely to remain in the immediate vicinity and not suffer any long distance transport. Gravel sediments are immobile in the inshore areas under this scenario.
- g. Superposition of a 2.85 m H_{m0} wave (high wave from the north) onto a Spring tide amplifies excess bed stress across the areas above (2 m wave) but there is evidence of the penetration of wave energy deeper (farther) into the heads of both Cemaes Bay and Cemlyn Bay. The sediment response and advection distances would be similar, but resuspension rates would be higher.
- h. A storm with (offshore) significant wave heights of > 4 m occurred which gave rise to nearbed suspended sediment concentrations of 289 mg l⁻¹ at station s4; although no corresponding data exist farther inshore, higher concentrations would be expected in shallower areas for this event.

- i. More extreme, rarer events (e.g. a 1:100 storm) are anticipated to increase the area over which wave driven resuspension occurs (i.e. to occur farther inshore), and for suspended sediment concentrations to be correspondingly higher.
- j. Isolated inshore pockets of gravel mobilisation in Porth y Pistyll and Cemlyn Bay are anticipated under a 2.85 m H_{mo} wave from the north and a Spring tide.
- k. The recirculating gyres around Wylfa headland in particular will act to retain sediments resuspended wave action locally.

6.6 Conceptual Understanding of the Sediment Transport Regime

It is beneficial when considering the sediment regime at a site to develop a conceptual understanding of the sediment transport pathways that are (potentially) present and their relative importance. Such an understanding involves collating all the evidence available of transport pathways to provide as clear an understanding of the regime as possible. This conceptual modelling is complementary to the understanding gained from numerical modelling and from inspection of process datasets, and should form an invaluable asset when assessing potential changes to coastal sedimentary processes arising from the development of the site.

One of the fundamental aspects of developing conceptual models involves defining the key elements of the sediment budget within the investigation area and identifying key controls on sedimentary processes. The approach is often qualitative due to inherent problems associated with quantifying a sediment budget. The degree of confidence that can be placed in the results and outputs of this approach depended on the quality and quantity of information available.

There are a number of different elements of a sediment regime that can broadly be divided into sources, pathways and sinks. Sediment sources can be considered as inputs to the littoral sediment budget and can be provided by a number of mechanisms.

Sediment Sources

Sediment sources are vital to the sustainability of sediment circulation, and can be derived from:

- Eroding cliffs
- Onshore transport of sediments from the offshore seabed
- Marine erosion of beach material;
- Supply of sediment from coastal dune storage
- Fluvial input via estuaries
- Beach replenishment activities
- Longshore transport of sediment into the area from the adjacent coast and seabed

In the area of the proposed development information on the above outlined sediment sources is available as follow:

Eroding Cliffs – the Shoreline Management Plan for the area (SMP2; Haskoning UK, 2015) indicates that the main source of what limited sediment, if any, that is available to Cemlyn Bay and the Esgair Gemlyn barrier beach during its future development will be predominantly derived from the long term slow erosion of the [unprotected] cliff line within the bay. This erosion of the (very) hard rock Precambrian strata from which the cliffs are composed is a very slow process in the order of 0.05-0.1 m per year. Pye and Blott (2010) in their



geomorphological assessment of Cemlyn Bay indicated that there are no obvious sources of new sediment supply to the barrier.

Onshore transport from the offshore seabed – it is apparent for the information available that the bays and headlands in the area of the proposed development are considered to be isolated/ unconnected in relation to littoral sediment transport and that any offshore to onshore transport is extremely limited and only occurs under low frequency high energy storm events

Marine erosion of beach material – as stated above it is unlikely that there is significant supply of material from beaches in the area. It would appear if anything that local beaches are a sink of any sediments that are present within the system. The SMP2 suggests that the presence of sandy beach in Cemaes Bay indicates some nearshore supply (most probably the submerged sand bank in the outer bay as described in Section 6.2.2) that where there is sufficient width in the shoreline system there is capacity for natural development and retention of a beach

Supply of sediment from coastal dune storage – there are no areas of coastal dunes apparent in proximity to the proposed development

Fluvial inputs via estuaries – The fluvial watercourses (streams) in the local catchments that drain into the Irish Sea along the coastline provide potentially significant inputs (over the long term) in terms of sediment to the local sediment regime. The main watercourse in the area is the Afon (River) Wygyr that drains into Cemaes Bay the sediments from which may have been a significant source, over the mid to late Holocene (last 6000 years) to present, of the sediments on the beach and the subtidal sand bank deposits in the wider bay. A similar hypothesis is proposed for the origin of some of the sediment on the beach and intertidal in Porth-y-Pystyll from the Afon (River) Cafnan. However as the watercourse and catchment is much smaller in comparison the Afon Wygyr and the area is exposed to the west no significant deltaic deposits have accumulated at the mouth of the river as these will have been reworked, removed and redistributed by the high energy wave and tidal conditions that operate at the location. There is a small ebb tide delta in Cemlyn Bay from the watercourse that drains into the sea from Cemlyn lagoon however the majority of coarser material that is transported down this catchment is almost certainly trapped and retained within the lagoon.

Beach replenishment activities - there are no known past or present replenishment activities in proximity to the proposed development

Longshore transport of sediment into the area from the adjacent coast and seabed – Motyka and Brampton (1993) stated that Littoral drift of sediment along the Anglesey coast is very low and variable in direction. In addition Pye and Blott (2010) also stated “embayments along the north Anglesey coast generally act as closed sediment compartments, with little or no exchange of sediment from one bay to the next, and only limited supply of new sediment at the present day from eroding sections of open coast between the bays” As such the transport of sediments alongshore from the adjacent coastline is not considered to be of any great significance in the area of the proposed development. Further offshore of Anglesey in the Irish Sea however, as Holmes and Tappin (2005) and Mellet et al. (2015) have indicated high energy conditions operate, and in places on the seabed sediment is mobile under certain prevailing currents and waves and that this mobile sediment creates features upon the seabed that range from small ripples to large sediment banks (up to 40 m high) and migrating sediment (sand and gravel) waves.

Sediment Transport

Sediment transport pathways can be considered as throughputs of sediment within the littoral sediment budget, and are primarily:

- Longshore transport; and
- Onshore / offshore transport

The two mechanisms or transport of coastal sediments:

- Bedload transport; this process refers to all sedimentary material that move, roll or bounce along the seabed as they are transported by currents' this mode of transport is principally related to coarser material (sands and gravels);
- Suspension transport: this process refers to particles of sediment that are carried above the seabed by currents and are supported in the water by flow turbulence.

Sediment Sinks

Sediment sinks and sources can be considered as outputs from the littoral sediment budget and include:

- Offshore banks, spits, bars etc. which temporarily store material that could potentially otherwise feed beaches
- Zones of persistent and significant beach accumulation
- Dune accumulation
- Maintenance dredging and marine aggregate extraction
- Longshore transport of sediment out of the unit to adjacent coasts
- Particle attrition and loss of fines.

These findings have been used to develop a conceptual understanding of the sediment regime at the Wylfa Newydd site presented in Figure 52.

6.7 Esgair Gemlyn

As Cemlyn Bay, the storm/barrier shingle beach of Esgair Gemlyn, and Cemlyn lagoon (or parts thereof) are designated in part as a Sites of Special Scientific Interest (SSSI), a Special Protection Area (SPA), a Special Area of Conservation (SAC) and an Area of Outstanding Natural Beauty (AONB) it is considered worthwhile dedicating special attention to the understanding of the local sediment regime in Cemlyn Bay.

The Cemlyn Estate, including the barrier and lagoon, is owned by the National Trust (NT). NT commissioned two recent studies undertaken by K Pye Associates to perform i) a preliminary geomorphological assessment of the bay (Pye & Blott, 2010) and; ii) a subsequent further geomorphological assessment (Pye & Blott, 2016). In their 2010 study K Pye Associates (Pye & Blott, 2010) concluded that the shingle barrier beach of Esgair Gemlyn currently appears to be in no immediate danger major breaching and that over-washing is relatively infrequent and small-scale. This conclusion is further supported by analyses of aerial LiDAR data collected over the area of the barrier in 2010 and then again in 2017. Figure 53 displays a difference plot of the shape and height of the barrier beach between 2010 and 2017. While some significant differences in beach levels between the two surveys are apparent, which is to be anticipated in a relatively dynamic coastal



environment, the area of the barrier beach that lies above the 0 m (AOD) contour (~mean sea level) has shown an accumulation in the order of circa 4150 m³ of additional material/volume (from 133,394 m³ to 137,547 m³) between the surveys.

The cross-shore transects analysed, and shown in Figure 53, do not appear to indicate any retreat of the barrier beach crest/ shingle ridge between the 2010 and 2017 surveys, if anything there appears to be a somewhat shoreward movement of the beach crest as is seen in transects P7, P7 and P11. K Pye Associates in their 2016 further geomorphological assessment (Pye & Blott, 2016) indicate that to some extent the risk of overtopping of the barrier beach may be countered by vertical growth of ridge in line with rising water/sea levels, but the extent, to which this can occur, without narrowing of the ridges, will be dependent on sediment availability. However as is apparent from the present study (and previous studies) the supply of new sediment to the wider Cemlyn Bay and the barrier beach appears to be somewhat limited at present. Without a continued supply of sediment to the beach any future acceleration in sea level will make it increasingly difficult for the barrier to maintain its relative crest position, level and equilibrium cross-sectional profile.

Historically the longer term rate of retreat of the barrier beach (determined by Pye & Blott, 2010, from historical mapping) has been <0.2 m yr⁻¹ since the late 19th Century. K Pye Associates (*ibid*) projected the positions of the mean High Water (MHW) line along the Esgair Gemlyn barrier shoreline using the average historical rate of movement, which indicated that by 2100 there will be a landward lateral recession of between 3.1 and 8.1 metres. The authors also performed an assessment of the projected positions of the 'MHW' mark under the UKCP09 50th percentile model output value for sea level rise under the medium emissions scenario which was used to calculate percentage increases in sea level rise based on locally observed trends. These elevated sea levels were employed to estimate an erosion 'enhancement percentage' which was then added to the observed historical MHW recession rate. The results of this exercise gave projected MHW recession distances of between 5.2 and 12.6 m by 2100. It also appeared that little change will be observed at the eastern end of the system as a result of low historical rates of recession in this area. The K Pye Associates study indicates that movement at both ends of the Esgair Gemlyn barrier is presently limited/controlled by 'hard points', with the result that in the future as the central part of the barrier retreats landward its' plan form will become increasingly arcuate, and unless additional sediment is supplied, the increased barrier length will most likely result in reduction of the crest height relative to sea level, and there will a consequent increased likelihood of wash over events, especially where the barrier is already at its narrowest and lowest. The risk will become event greater as mean sea level and predicted high water levels increase, and if there is an increase in the frequency or intensity of storm events.

Some insight is gained from inspection of the 30 year hindcast modelled wave climate data from inside Cemlyn Bay (at modelled points 6 and 4; see Figure 26). Cemlyn Bay is exposed to waves originating from the NW, N and NE sectors; Point 4 (Figure 26) is located slightly outside the mouth of the embayment and the directional wave spectrum reflects this general exposure to these wave directions. Deeper within the bay (Point 6) the wave spectrum is modified, reflecting a dominant NE/NNE direction. This is related to the process of wave refraction, where waves from the principal sectors are modified by the local coastal physiography and become aligned normal to the orientation of the embayment. As wave approach the shore they diverge, and wave height decreases to the point where the waves may eventually break. Section 5.2.1 shows that deep-water waves can lose over 50% of their height as then travel towards the head of the embayment.

The distribution of wave heights at Point 4 and Point 6 within the bay indicates a relatively low energy wave climate. Table 32 presents statistical information on wave height for Point 4 and Point 6. This shows that waves do not exceed ~1 m in height for the vast majority of the time; although the importance of wave height increases as water depth shallow towards the shore face, this indicates that the wave climate within the embayment is for the most part of low energy, and consequently unlikely to regularly generate pronounced morphological adjustments to the sediments of the shingle ridge.

Table 32. Summary statistics for significant wave height extracted from the 30 year hindcast wave model Wave Height H_{m0} (m) percentile. Data source: (HR Wallingford, 2017)

Point	Significant Wave Height H_{m0} (m) Percentile				
	10	50	90	99	100
4	0.11	0.32	0.95	1.78	3.70
6	0.05	0.18	0.63	1.26	2.98

For a small fraction of time (less than 1%) more energetic conditions may occur, which have the potential to generate more significant morphological adjustments to the sediments of the shingle ridge. If a 60% loss of wave height as waves moves onshore is assumed (this is supported by model data, Table 21), the 99th and 100th percentile waves at Point 4 correspond approximately to 1:10 and 1:100 offshore (deep-water) wave return periods, respectively (refer to Table 30). This provides some indication as to the frequency of these more extreme conditions, and agrees with the sentiments expressed by Pye and Blott (2010) that 'the Esgair Gemlyn is in no immediate danger of a major breach and that over-washing is relatively infrequent and small scale'. It should be further noted that the peak, worst case combination of events will occur where a high water spring tide, a storm surge (which can raise water levels above MHWS levels by ~0.8-1.2 m, cf. Table 6) is coincident with a rare storm, which has an extremely low joint probability. Certainly, wave formed swash associated with 1:100 and 1:200 year storms may, under such circumstances, be expected to either significantly modify the profile of the shingle ridge and/or over wash it, potentially forming a breach though to the lagoon.

7. REFERENCES

ABPmer (2016). Audit of the Wylfa Hydrodynamic Model, Second Review, ABPmer Report No. R.2583 P2. A report produced by ABPmer for Jacobs UK Ltd, September 2016.

Bide, T. P; Campbell, E; Cave, M; Balson, P. S; Green, S (2013) The Marine Mineral Resources of the UK Continental Shelf: Final Report. British Geological Survey Commissioned Report, CR/13/020.

Black, K.P; Gay, S.L. (1987). Eddy formation in unsteady flows. *Journal of Geophysical Research* . 92, 9514-9522.

Blott, S.J. and Pye, K. (2001) GRADISTAT: a grain size distribution and statistics package for the analysis of unconsolidated sediments. *Earth Surface Processes and Landforms* 26, 1237-1248.

Fugro (2010a) Wylfa New Build Intermediate Offshore Ground Investigation, Borehole Logs.

Fugro (2010b) Wylfa New Build Intermediate Offshore Ground Investigation, Geotechnical Ground Report, C1369/NEA101007

Fugro (2016) Horizon Nuclear Power Wylfa Newydd Detailed Offshore Ground Investigation.

Geyer, W.R; Signell, R.P. (1990). Measurements of tidal flow around a headland with a shipboard acoustic doppler current profiler . *Journal of Geophysical Research*. 95, 3189-3197.

Halcrow (2012) Appendix B, Wylfa Marine Off Loading Facility Feasibility Study, Numerical Wave Modelling, Wave transformation and MOLF down time analysis.

Haskoning UK Ltd (2012) West of Wales Shoreline Management Plan 2. Section 4. Coastal Area G. Ref 9T9001/RSection4CABv1/303908/PBor.

Holmes, R and Tappin, D R (2005). DTI Strategic Environmental Assessment Area 6, Irish Sea, seabed and surficial geology and processes. British Geological Survey Commissioned Report, CR/05/057.

Horizon Nuclear Power Ltd (2011) CSO268 Wylfa Additional Bathymetry Final Report No: 1.

Horizon Nuclear Power Ltd (2012) Wylfa Hydrodynamic and Water Quality Modelling: Phase 2 model build, Calibration and Validation (WYL-PD-PAC-REP-00015)

Horizon Nuclear Power. 2012. Wylfa Oceanographic Interpretative Report. Titan Environmental Surveys Ltd. for Horizon Nuclear Power, WYL-TES-PAC-REP-00024 CS0268/V1/Final.

Horizon Nuclear Power Ltd (2017) Chapter D12 Coastal Processes and Geomorphology (Skeleton). No associated document number.

Howarth, M.J. 2005. Hydrography of the Irish Sea. SEA6 Technical Report, UK, Department of Trade and Industry offshore energy Strategic Assessment programme.

HR Wallingford/Amech FW (2016). Wylfa Newydd – Further wave modelling, Phase 2. DER5524-RT001-R01-00.

HR Wallingford (2015). Further Wave Modelling Phase 1 Study.

HR Wallingford (2017). Wylfa Newydd – 2017 wave transformation modelling. Nearshore time series results for EIA.

Jacobs UK Ltd (2012) Consultancy Report Wylfa Water Quality Surveys (W202.01-S5-PAC-REP-00008)

Jacobs (2015) Wylfa Newydd Project, Benthic Ecology Surveys Report, 60PO8007/AQE/REP/005

Jacobs UK Ltd (2016) Marine Hydrodynamic Modelling, Summary of hydrodynamic modelling undertaken using a cooling water flow of 109 m3s-1, 60PO8032/AQE/REP/006/0.0.

Jacobs UK Ltd (2017a) IS040 Holyhead North Dredge Disposal – 3D Sediment Transport Modelling for Horizon Nuclear Power.

Jacobs UK Ltd (2017b) Wylfa Newydd Development Area Hydrological Baseline Report 60PO8058/HYDR/REP/001. Report ref: WN034-JAC-PAC-REP-00030.

Jacobs UK Ltd (2017c). 2010, 2017 Aerial LiDAR data of Esgair Gemlyn. No associated document reference.

Jackson, D. I; Jackson, A. A, Evans, D; Wingfield, R. T. R, Barnes, R. P; Arthur, M. J (1995). United Kingdom offshore regional report: the geology of the Irish Sea, London: HMSO for the British Geological Survey.

Lowe J, Howard T, Pardaens A, Tinker J, Holt J, Wakelin S, Milne G, Leake J, Wolf J, Horsburgh K, Reeder T, Jenkins G, Ridley J, Dye S, Bradley S. (2009). UK Climate Projections Science Report: Marine and coastal projections. Met Office Hadley Centre: Exeter.

Mellett, C, Long, D, Carter, G, Chiverell, R and Van Landeghem, K (2015). Geology of the seabed and shallow subsurface: The Irish Sea. British Geological Survey Commissioned Report, CR/15/057. 52pp.

Met Office UKCP (UKCP09). (2017). United Kingdom Climate Projections. Available: <http://ukclimateprojections.metoffice.gov.uk/21708>. Last accessed 23/03/2017.

Motyka, J. M & Brampton, A. H (1993) Coastal Management, Mapping of littoral cells. Report SR 328.

National Tidal and Sea Level Facility (NTSLF) . (2017). Holyhead Tide Gauge Site. Available: <http://www.ntslf.org/tgi/portinfo?port=Holyhead>. Last accessed 23/03/2017.

Pattiaratchi, C; James, A; Collins, M. (1987). Island wakes and headland eddies: A comparison between remotely sensed data and laboratory experiments. *Journal of Geophysical Research*. 92, 783-794.

Pingree, R (1978). The formation of The Shambles and other banks by tidal stirring of the seas. *Journal Marine Biological Association UK.*, 58, 211-226.

Pye, K. and Blott, S.J. 2010. Cemlyn Bay and Adjoining Areas, Anglesey: Geomorphological Assessment. Report prepared for the National Trust, Swindon by Kenneth Pye Associates Ltd, External Investigation Report EX1208.

Pye, K. and Blott, S.J. 2016. Cemlyn, Anglesey: Further Geomorphological Assessment: Report prepared for the National Trust, Swindon by Kenneth Pye Associates Ltd, External Investigation Report EX20671.

RWE (2017). Marine Hydrodynamic Modelling. (Appendix D13-8).

Savenije, H.G. (1989). Salt intrusion model for high-water slack, low-water slack, and mean tide on spread sheet. *Journal of Hydrology*. 107 (1-4), 9-18.

Signell, R. P, Geyer, W.R (1991). Transient eddy formation around headlands. *Journal of Geophysical Research*, 96, 2561-2575.

Soil Mechanics (2008) Ground Investigation For Porth Yr Ogof CCGT- Volume 2: Factual Report (Offshore Boreholes) Report no: BL/E/57431

Soulsby, R. L (1997). Dynamics of Marine Sands. London: Thomas Telford. 65-70.

Richards, K (1985). Rivers, form and process in alluvial channels. London: Methuen and Co. Ltd. 245.

Titan Environmental Surveys (2009) Report: Wylfa Power Station Preliminary Nearshore Geophysical Investigation, Volume 2: Results Report CS0257/R2/V2

Wolanski, E; Imberger, J; Heron, M. (1984). Island wakes in shallow coastal waters. *Journal of Geophysical Research*. 89 (10), 10553-10569.

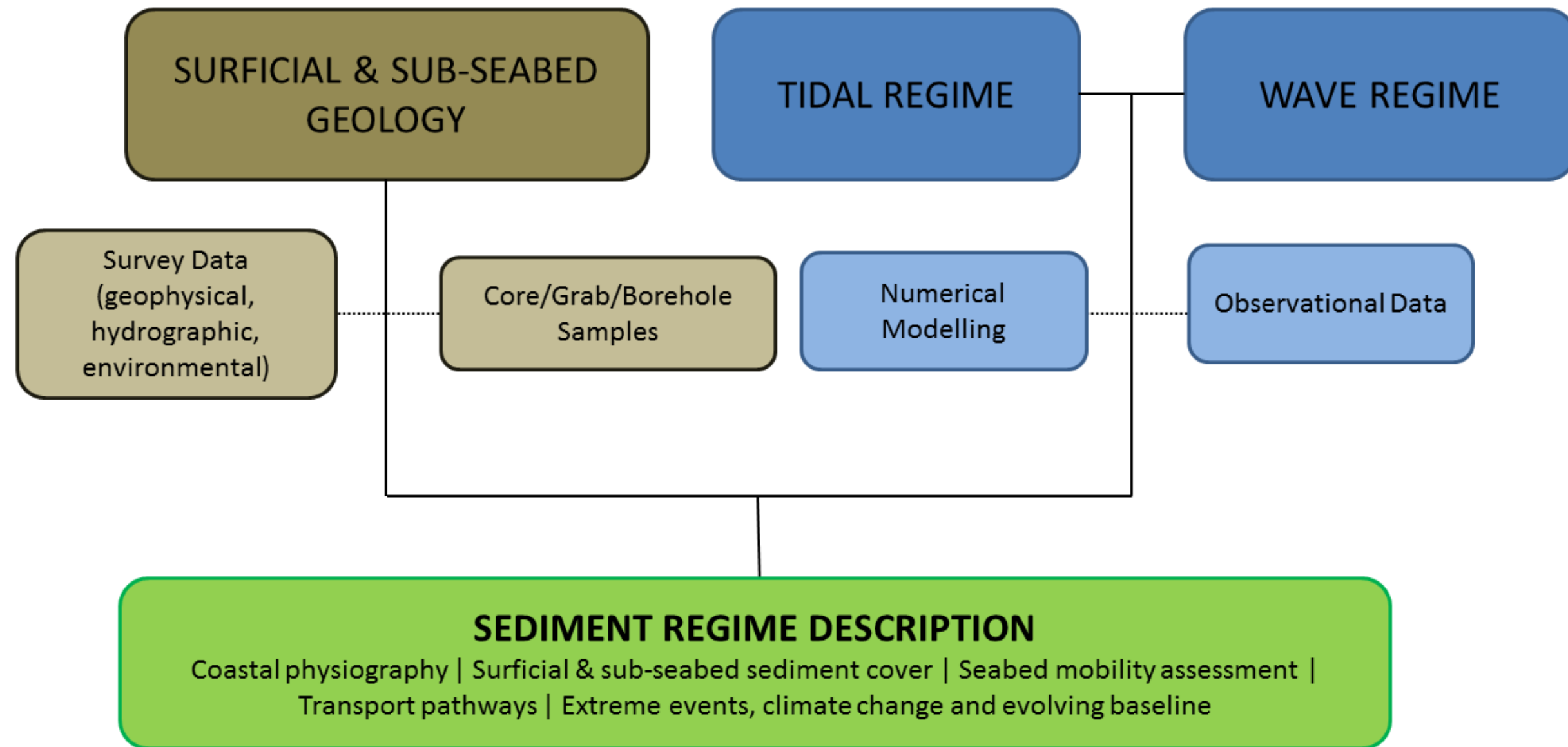


Figure 1. A schematic diagram detailing the various components which underpin the assessment of the sediment regime

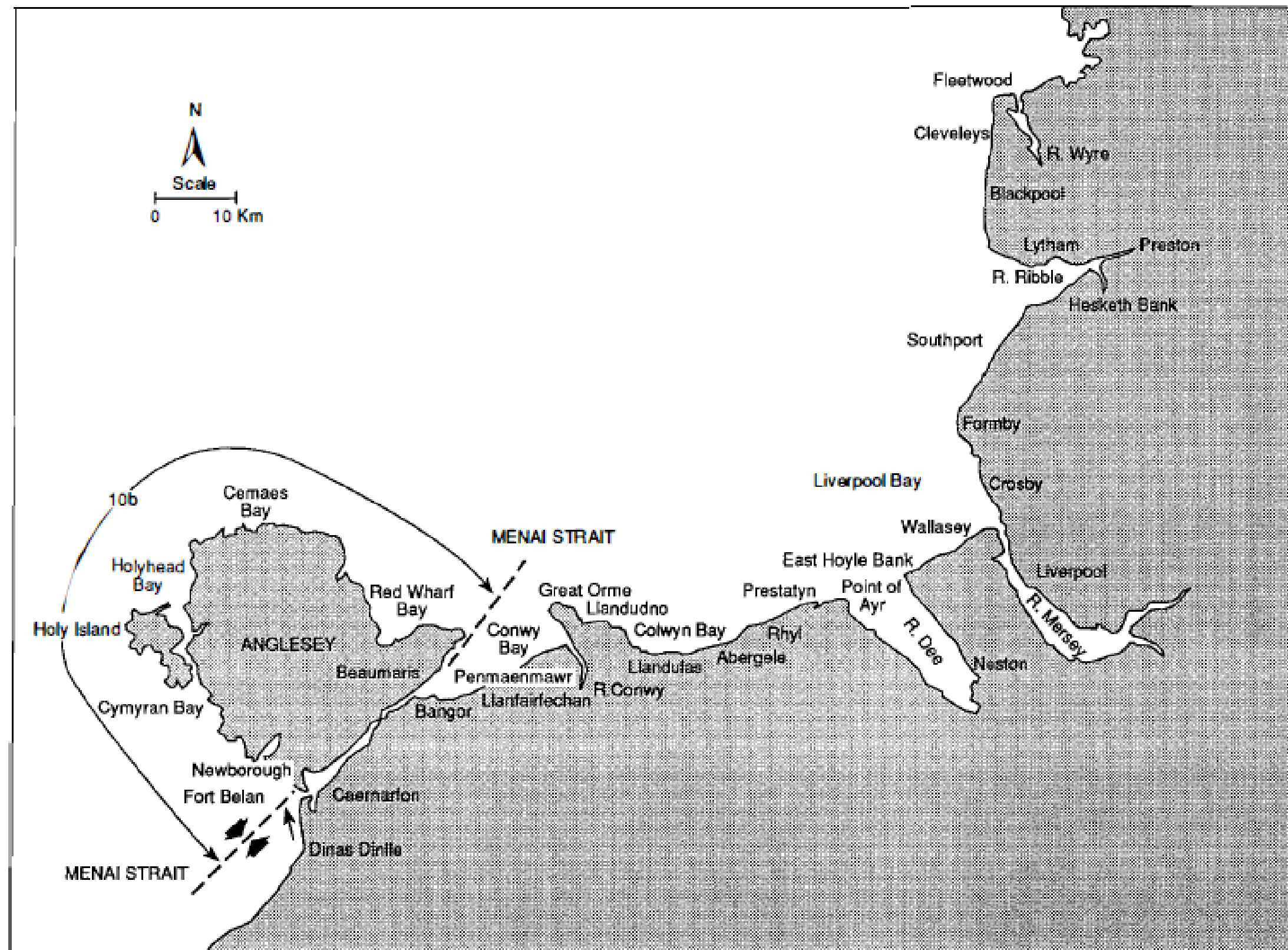


Figure 2. Map showing the extent of coastal cell – sub cell 10b. Source: Motyka & Brampton (1993).

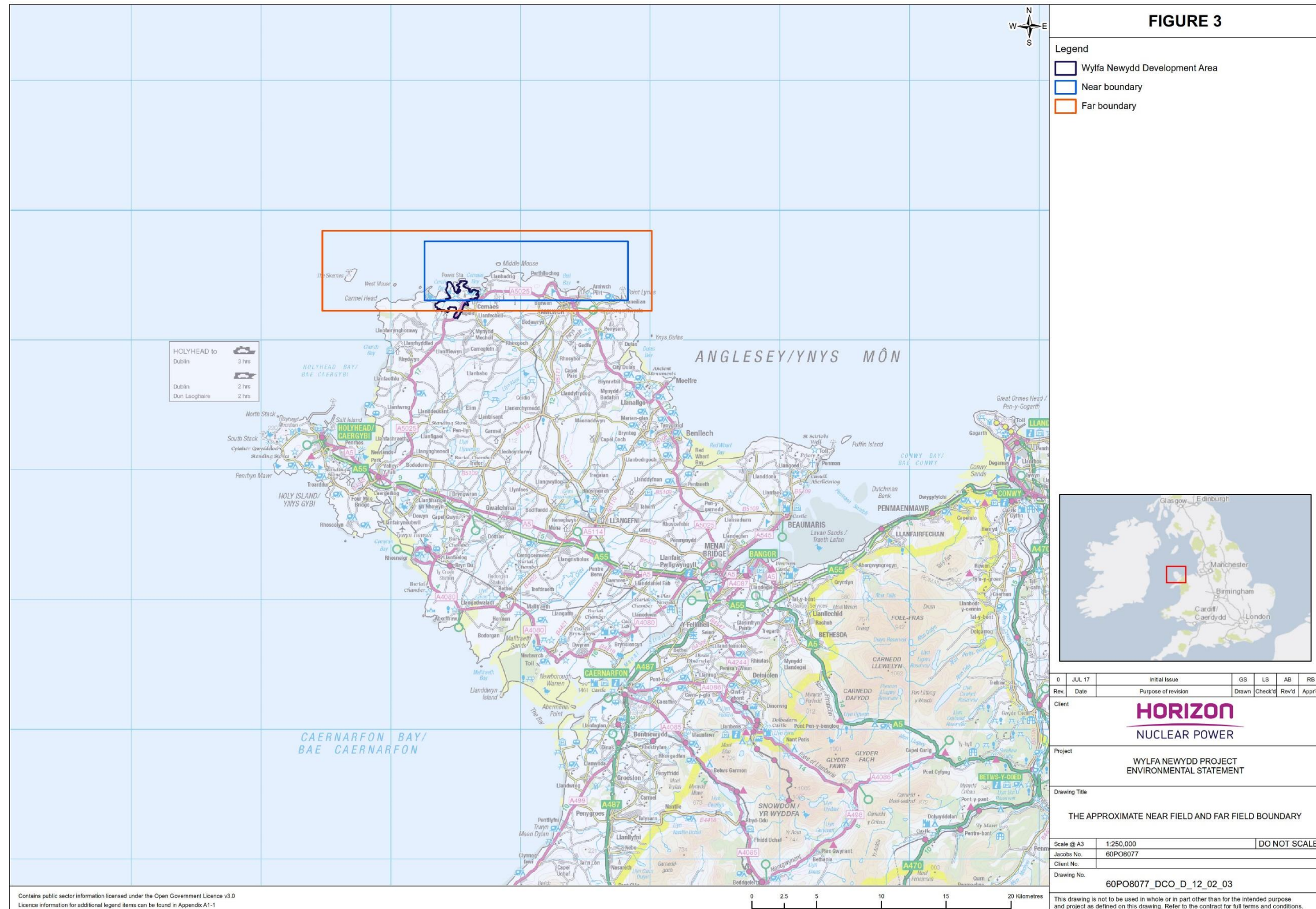
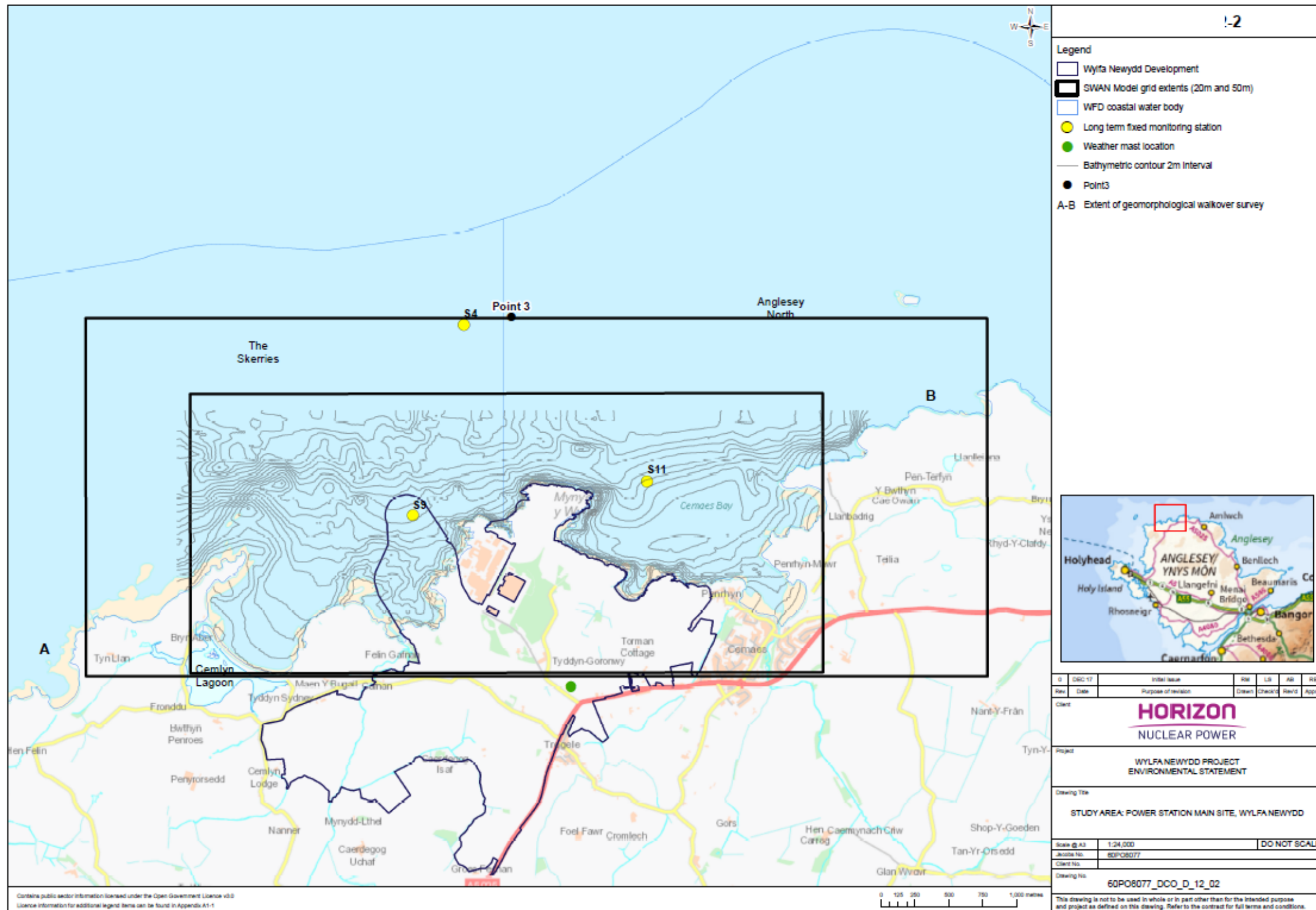


Figure 3. The approximate 'near field' and 'far field' boundary.



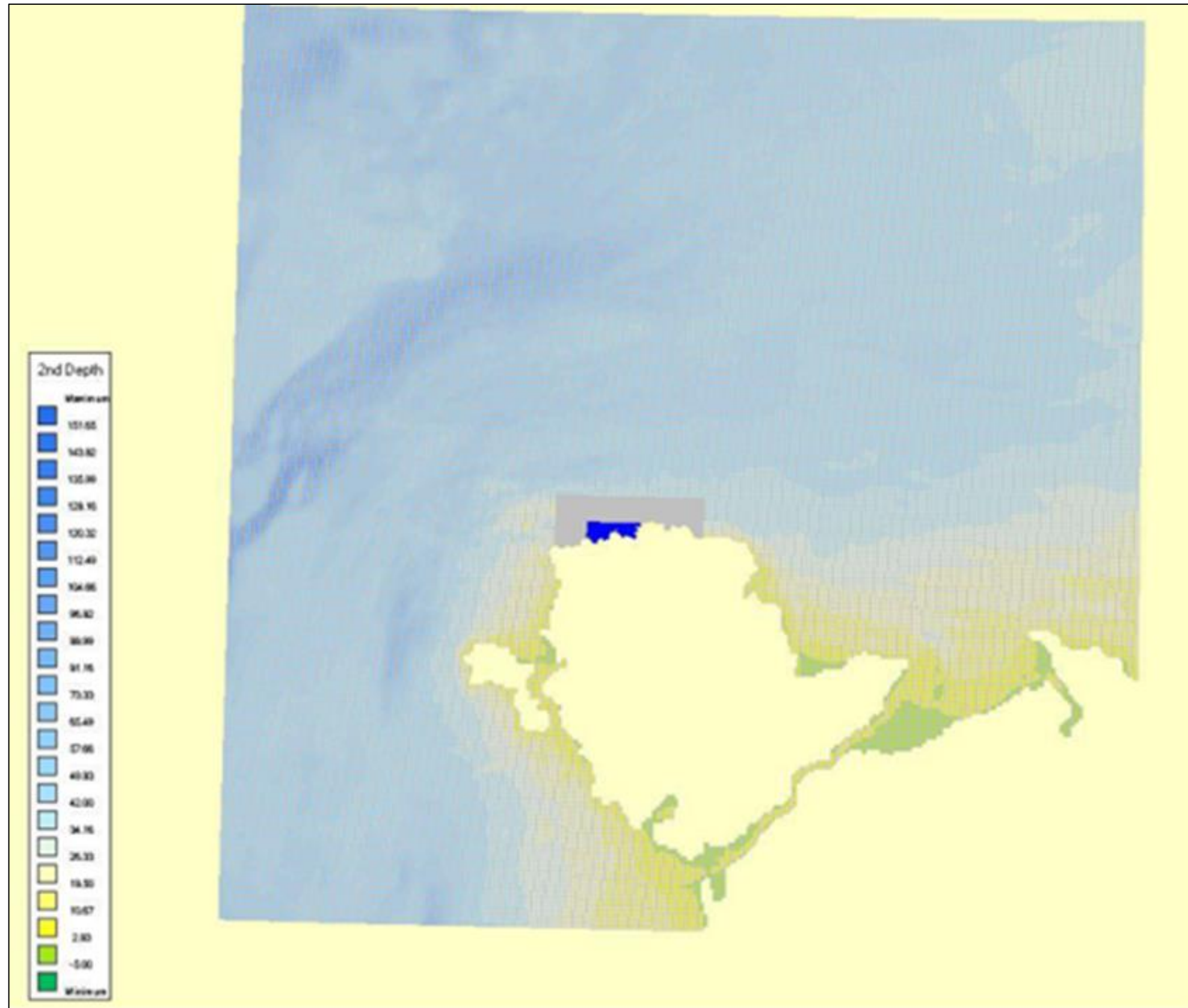


Figure 5. Model grid and bathymetry for the Delft3D HD model. Source: RWE (2017).

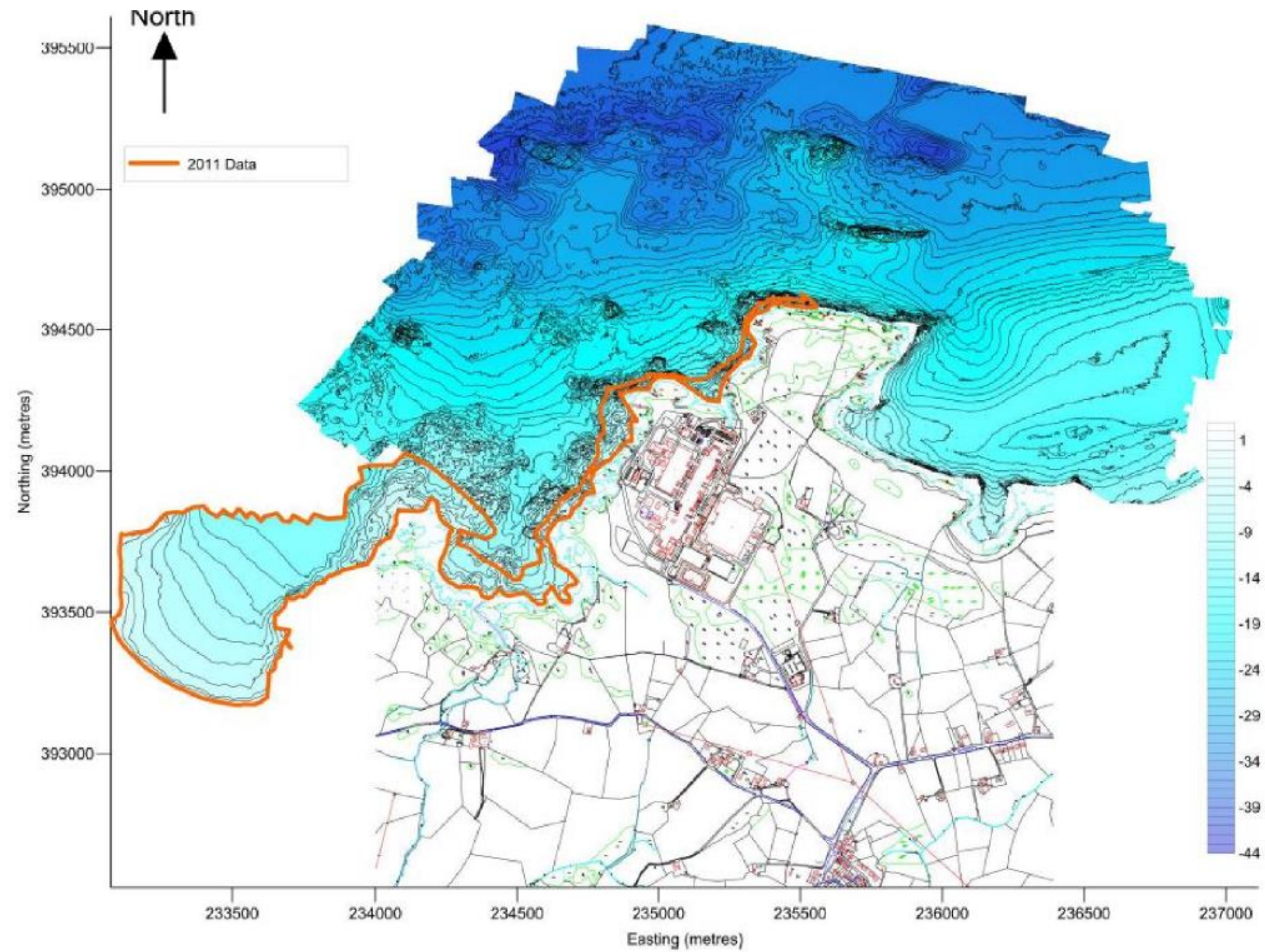


Figure 6. General distribution of water depths across the investigation site. Note depths relative to OD. Source: Horizon (2011).

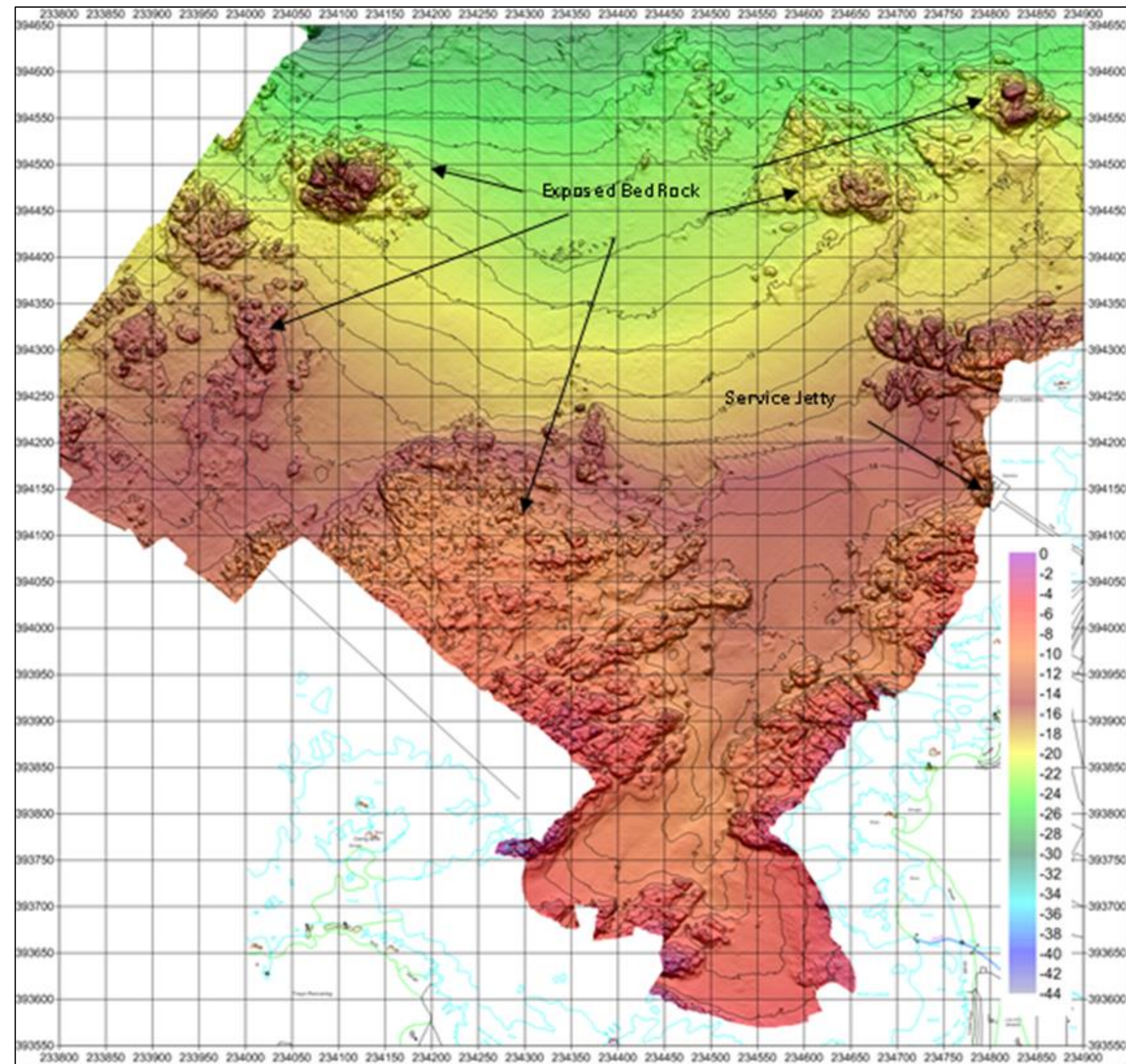


Figure 7. Seabed bathymetry in Cemlyn Bay and Porth-y-Pistyll. Areas of exposed bedrock are marked. Source: Titan (2009).

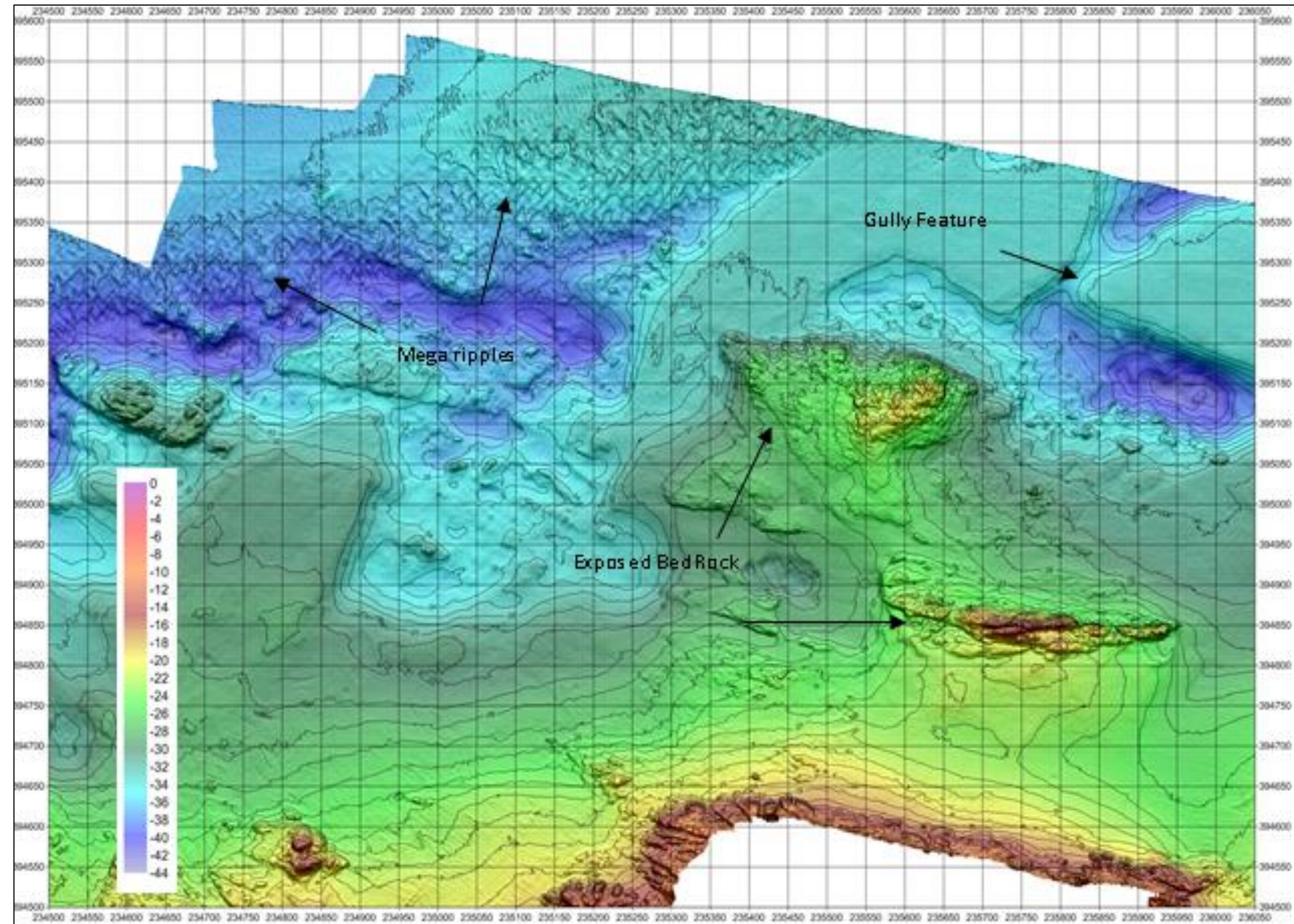


Figure 8. Seabed bathymetry to the north and northwest of Wylfa Head. Source: Titan (2009).

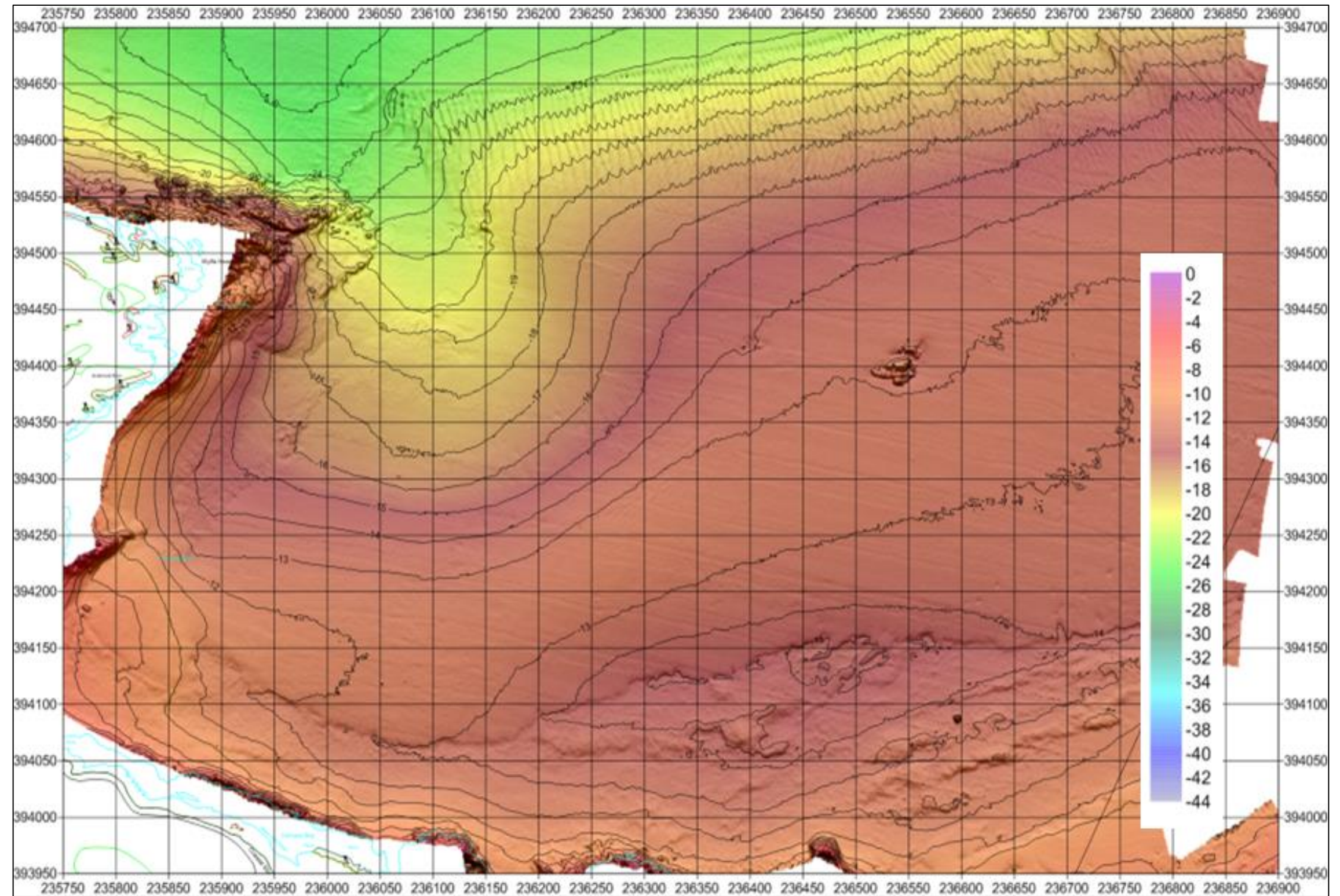


Figure 9. Bathymetry to the east of Wylfa Head. Source: Titan (2009).

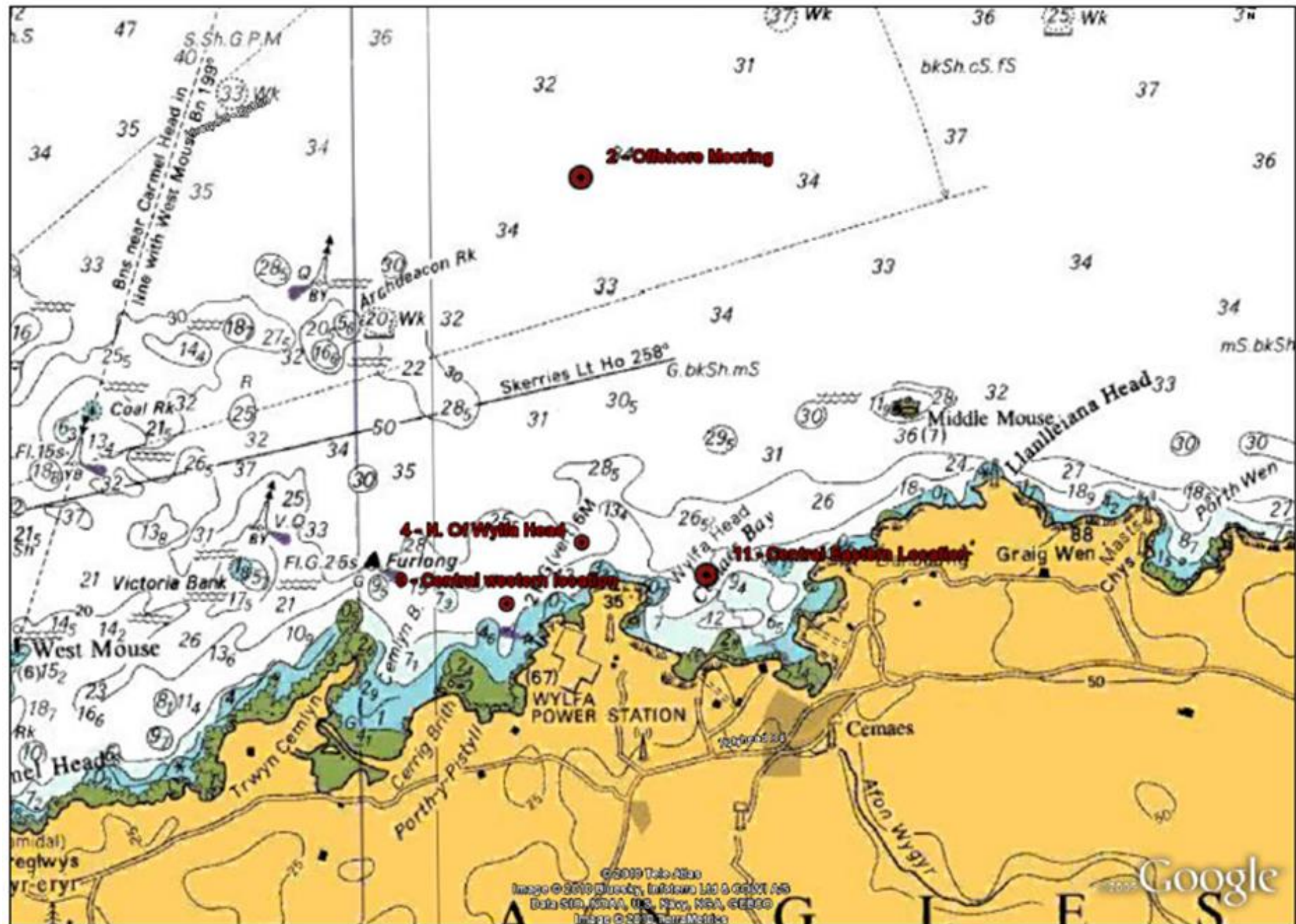


Figure 10. Wylfa oceanographic monitoring stations. The location of the four fixed point monitoring systems are marked (S2, S4, S9 and S11). Source: Horizon (2012).

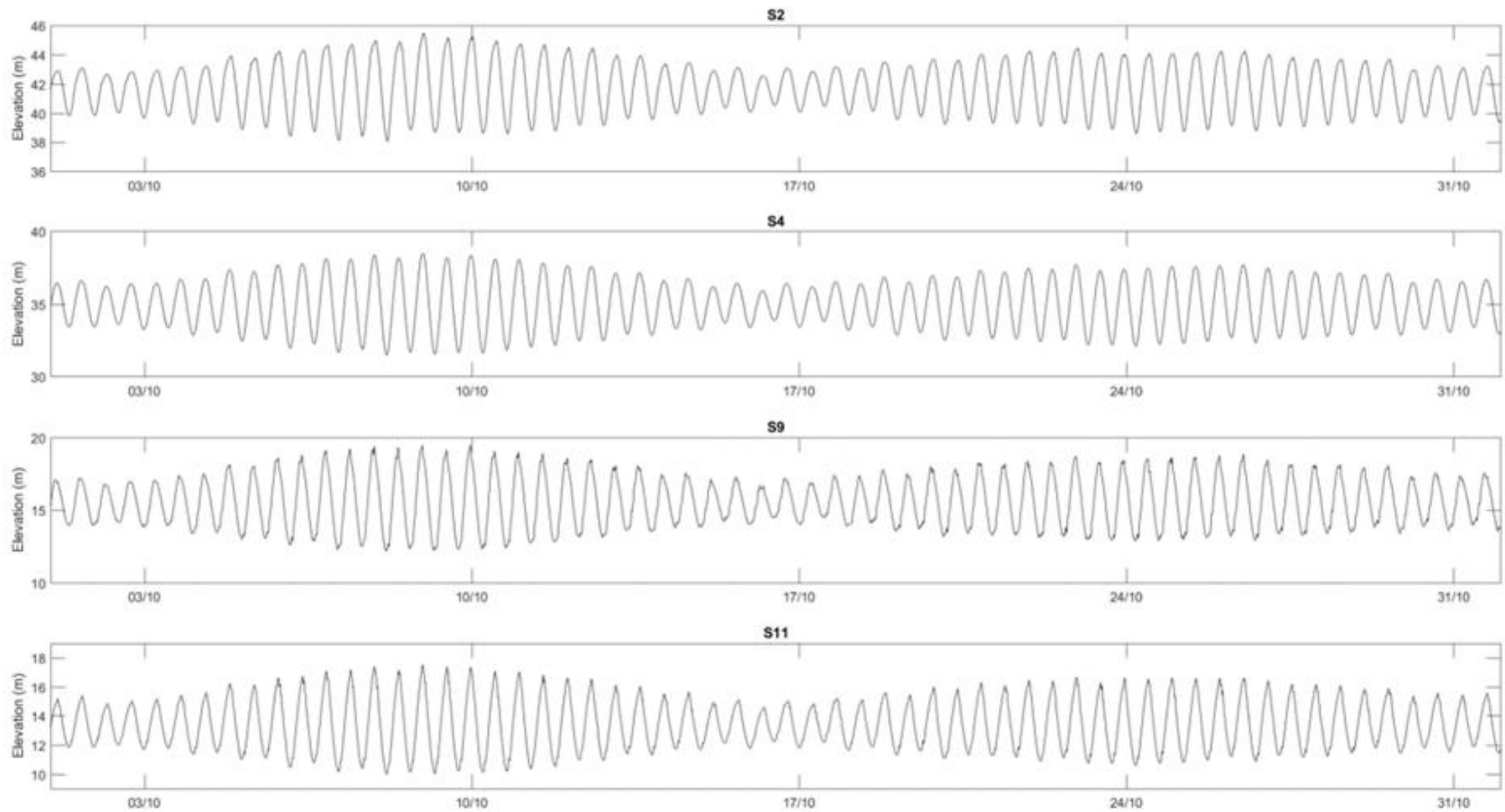


Figure 11. Example of water level variation through time for each of the four oceanographic monitoring stations. Data source: Horizon (2012).

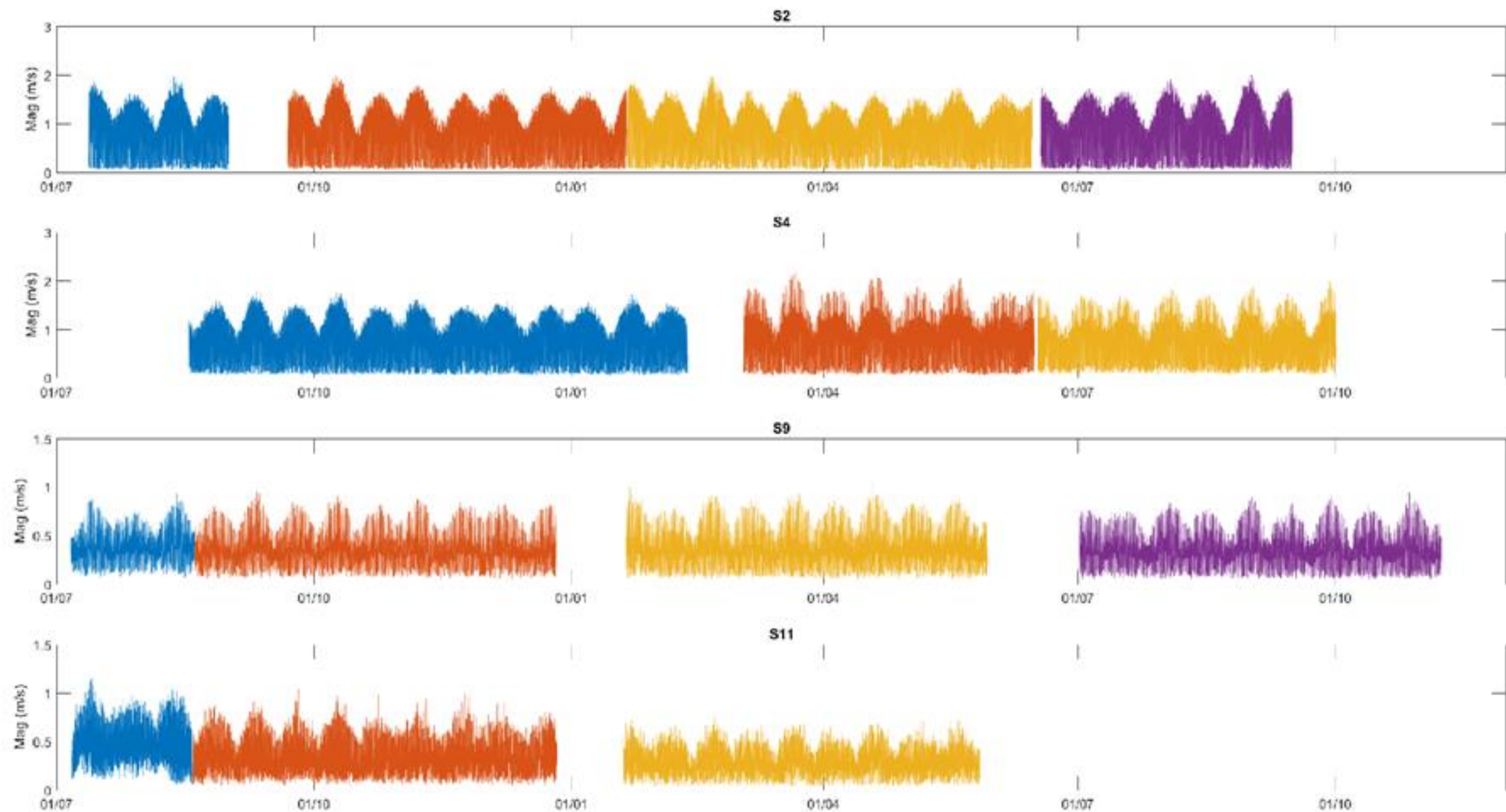


Figure 12. Depth-averaged current magnitude by deployment (i.e. each colour represents a separate instrument deployment) at the four oceanographic monitoring stations. Data Source: Horizon (2012).

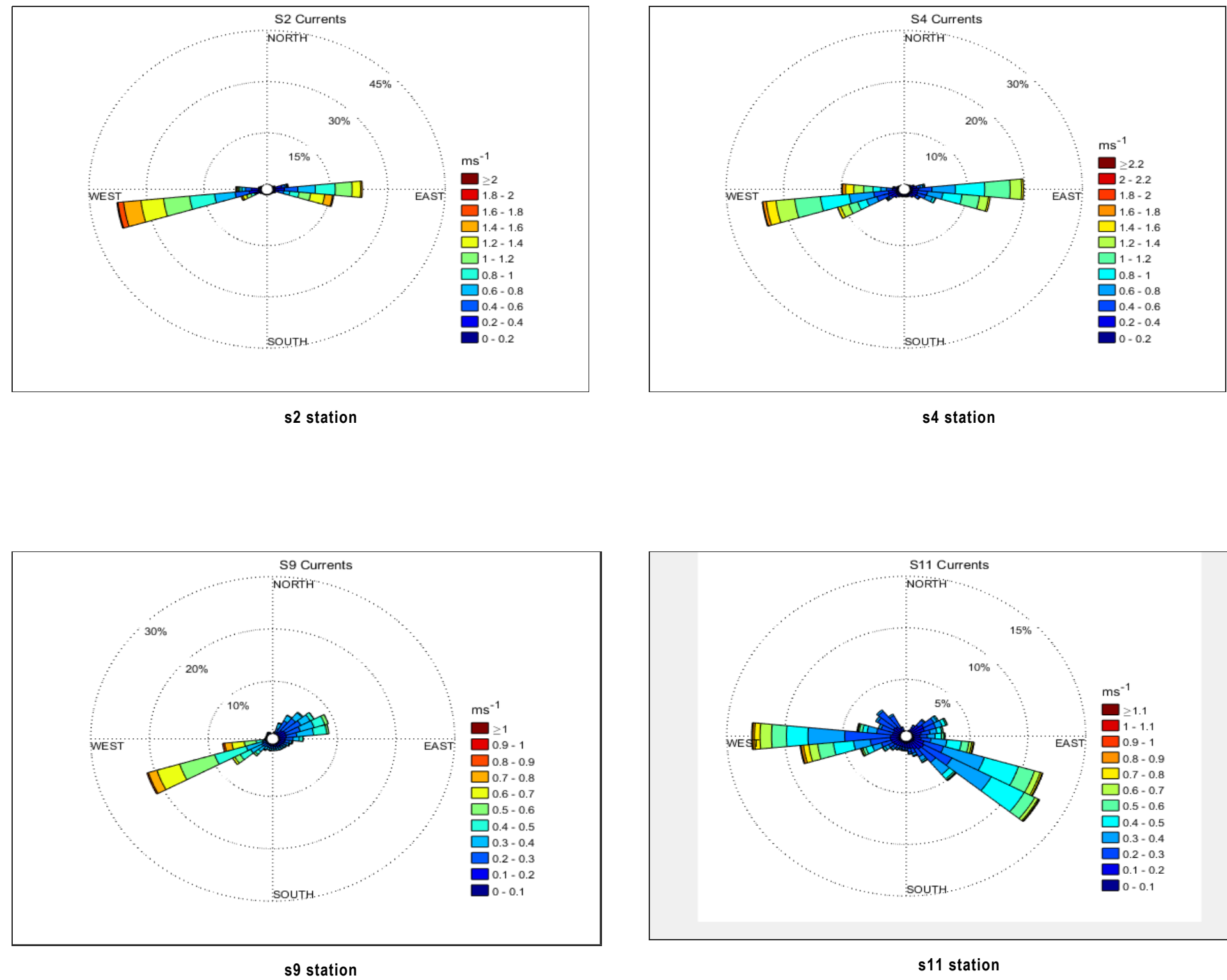
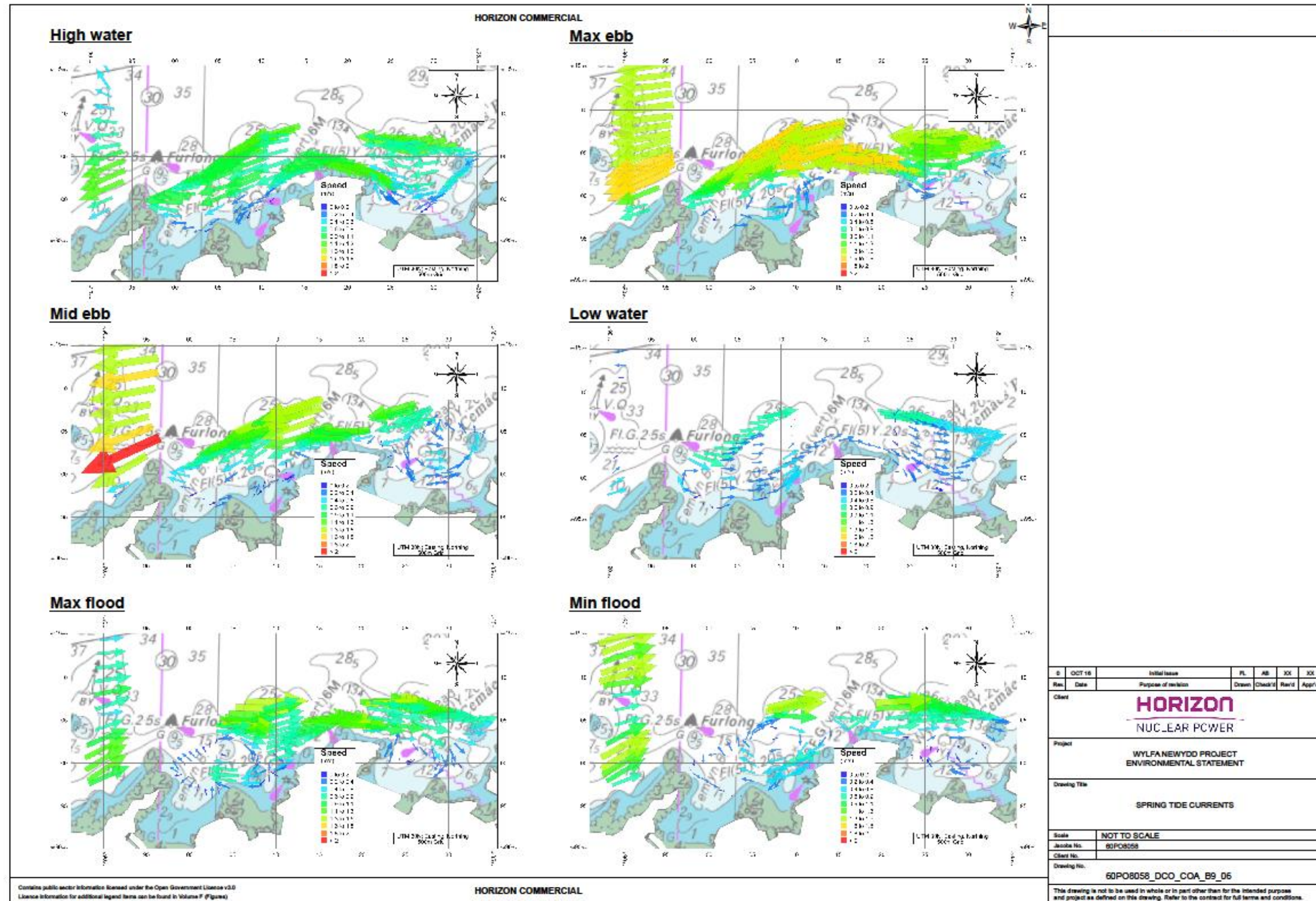


Figure 13. Current roses for the four oceanographic monitoring stations. Data source: Horizon (2012).



PARTRAC



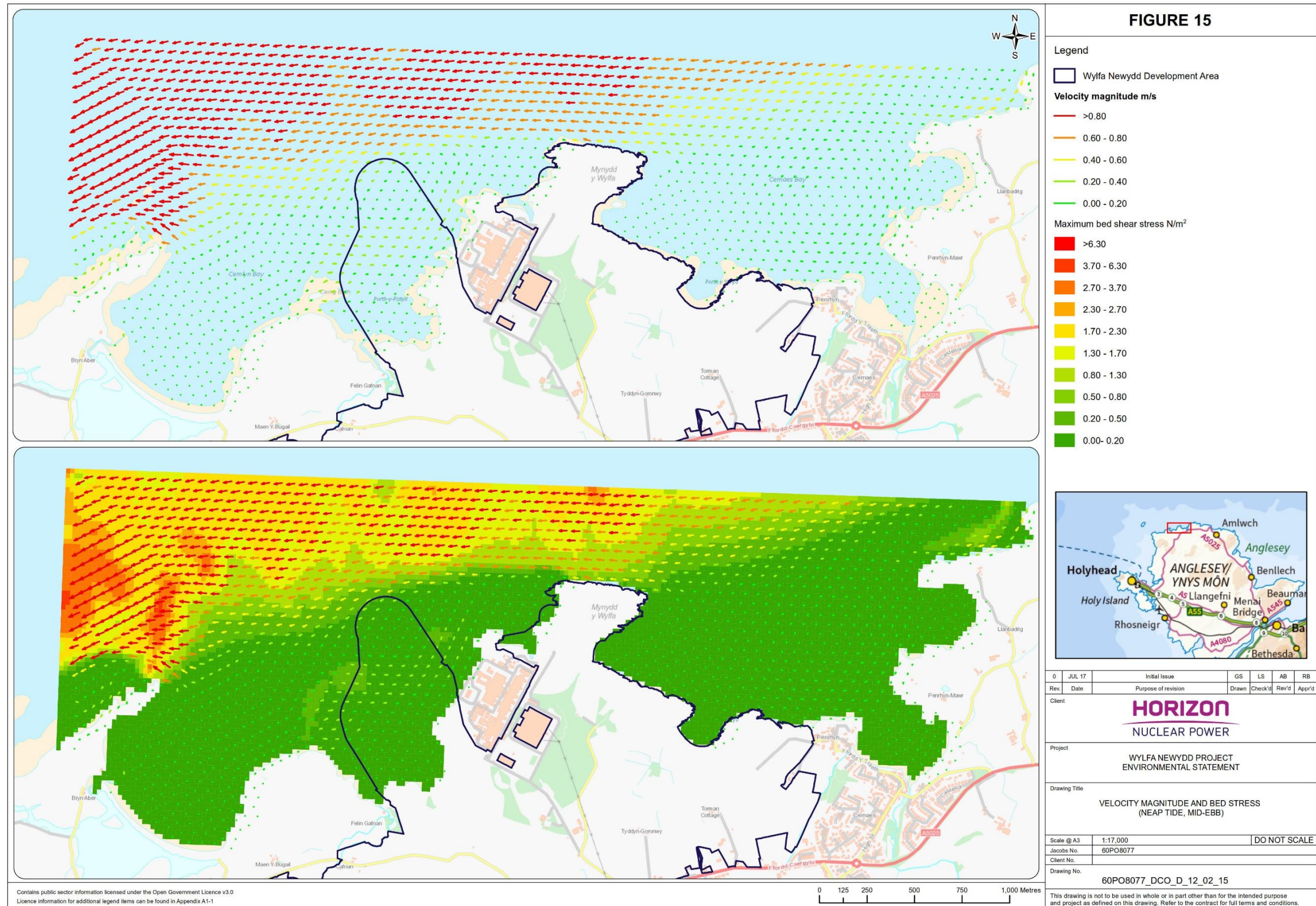


Figure 15. Depth averaged velocity vector plot (upper panel) showing the current velocity magnitude (and direction) at neap tide, mid ebb; the corresponding tidal bed stresses are shown in the lower panel.

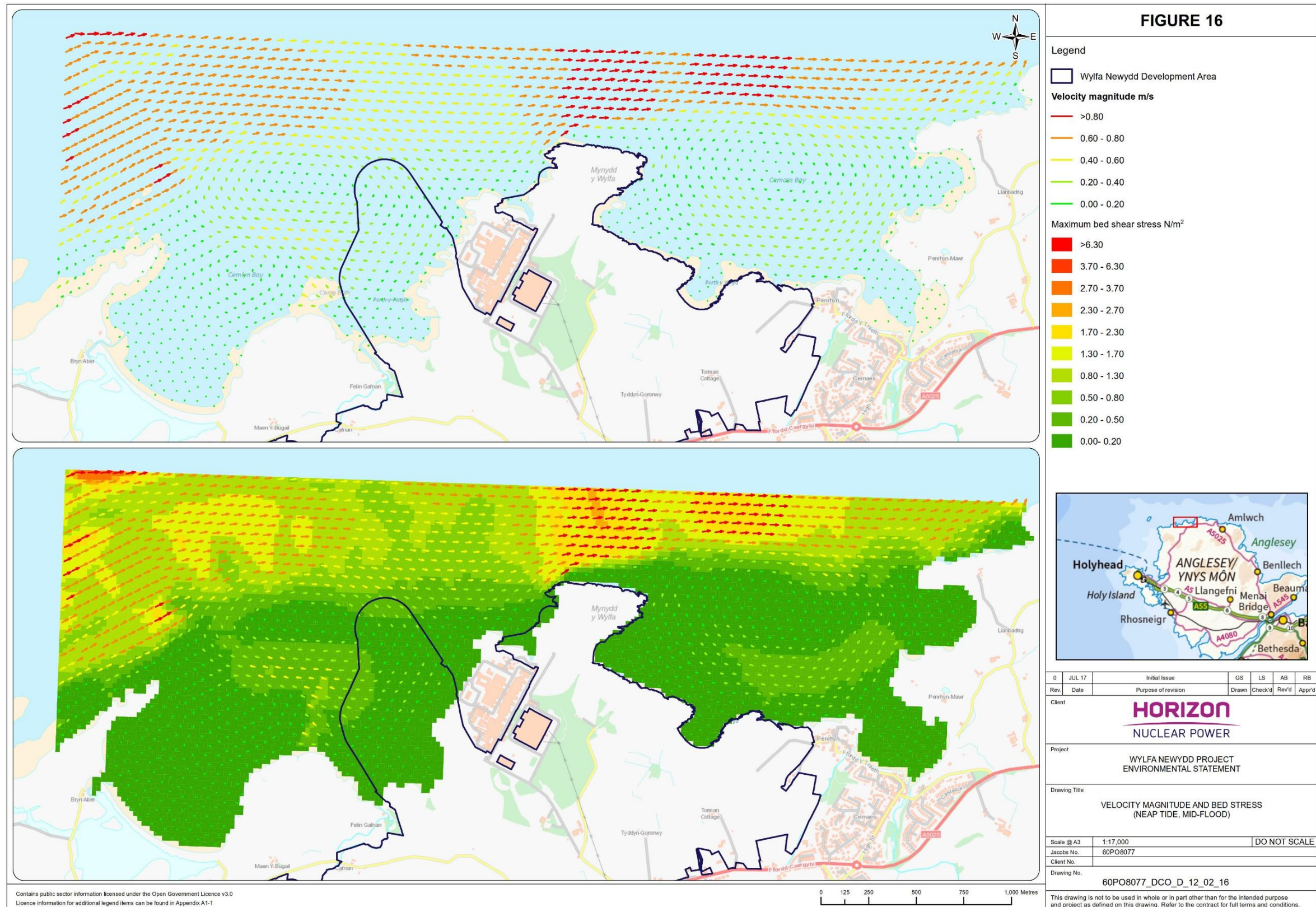


Figure 16. Depth averaged velocity vector plot (upper panel) showing the predicted current velocity magnitude (and direction) at neap tide, mid flood; the corresponding tidal bed stresses are showing in the lower panel. .

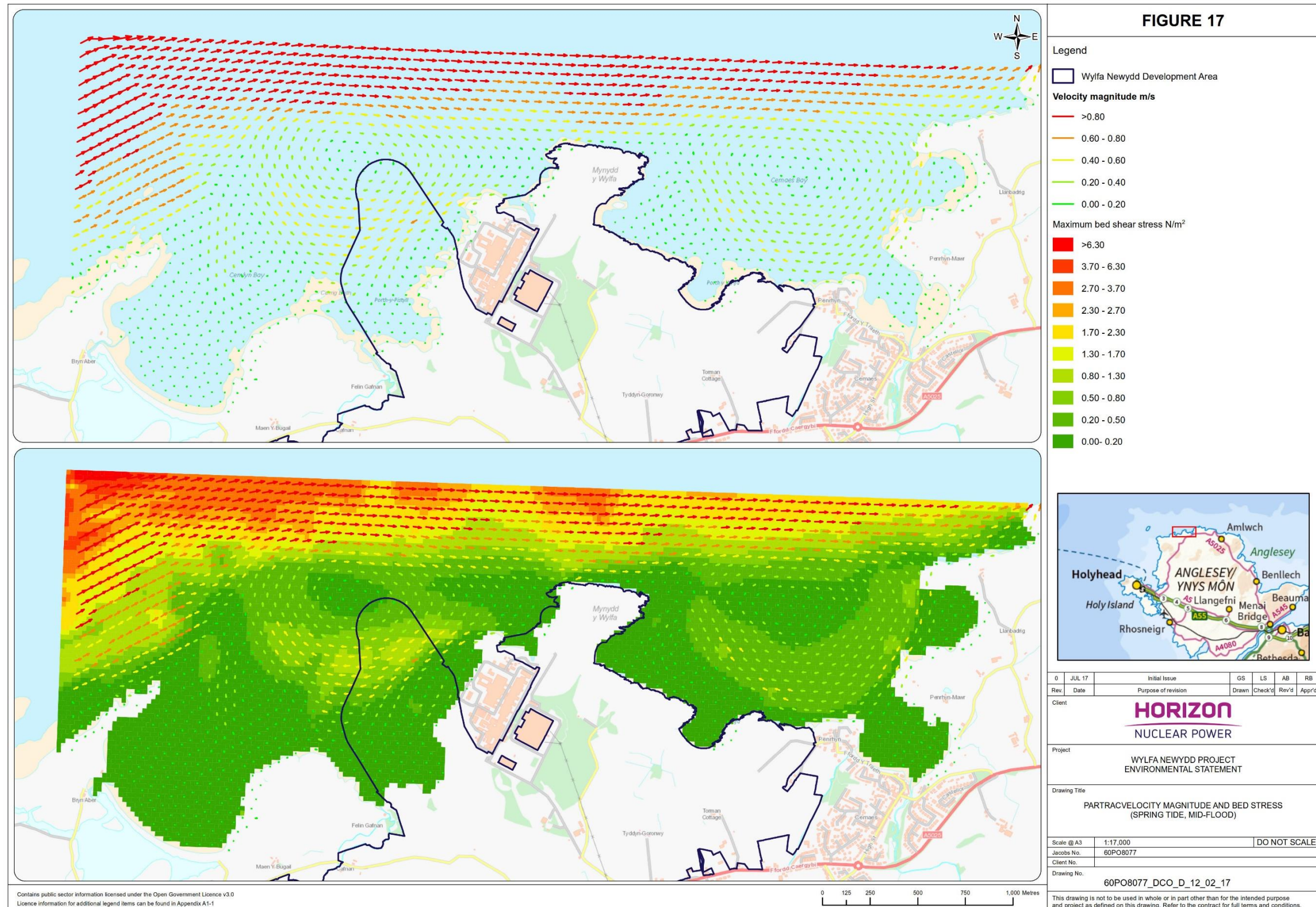


Figure 17. Depth averaged velocity vector plot (upper panel) showing the current velocity magnitude (and direction) at spring tide, mid flood; the corresponding tidal bed stresses are shown in the lower panel.

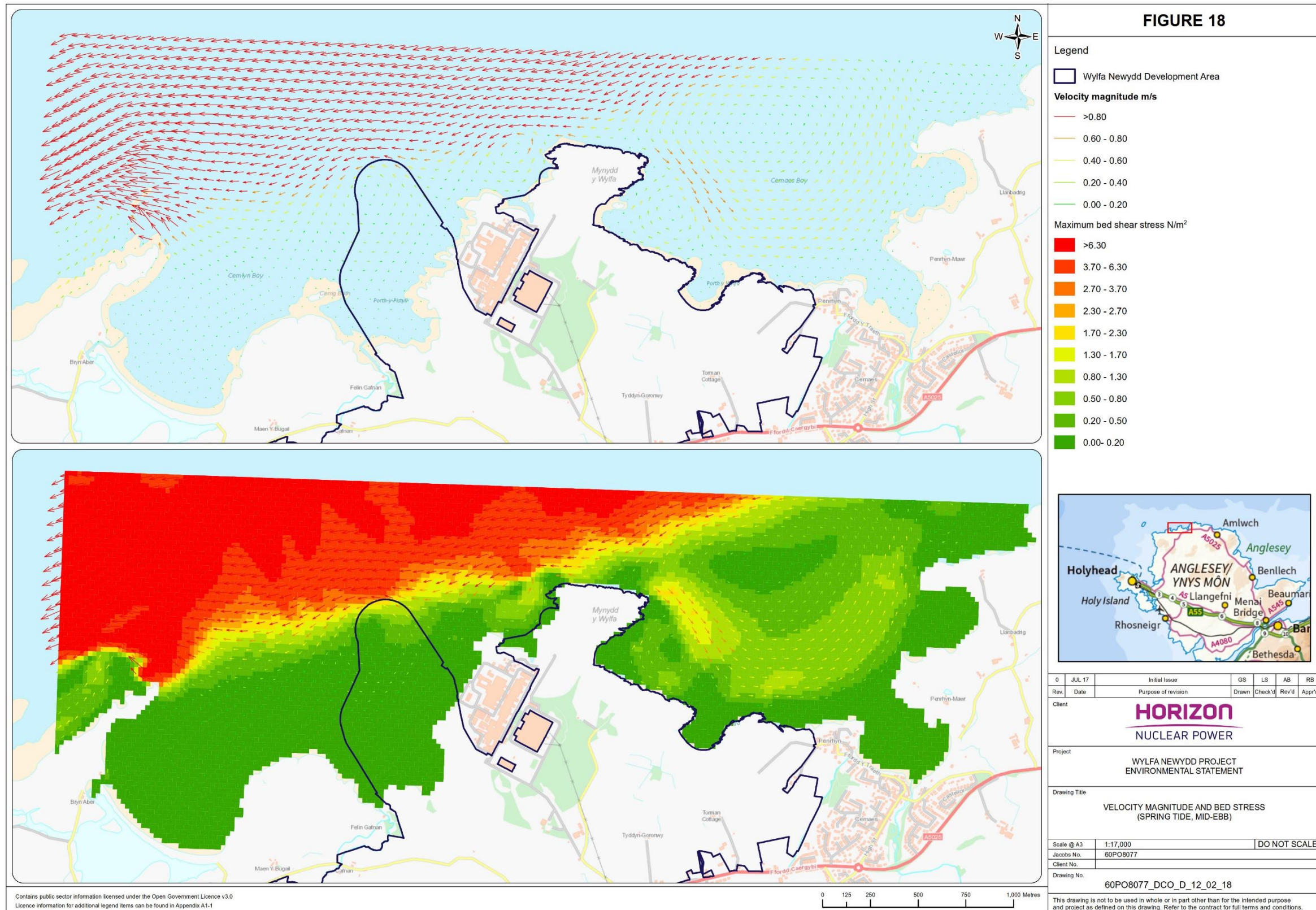


Figure 18. Depth averaged velocity vector plot (upper panel) showing the current velocity magnitude (and direction) at spring tide, mid ebb; the corresponding tidal bed stresses are shown in the lower panel.

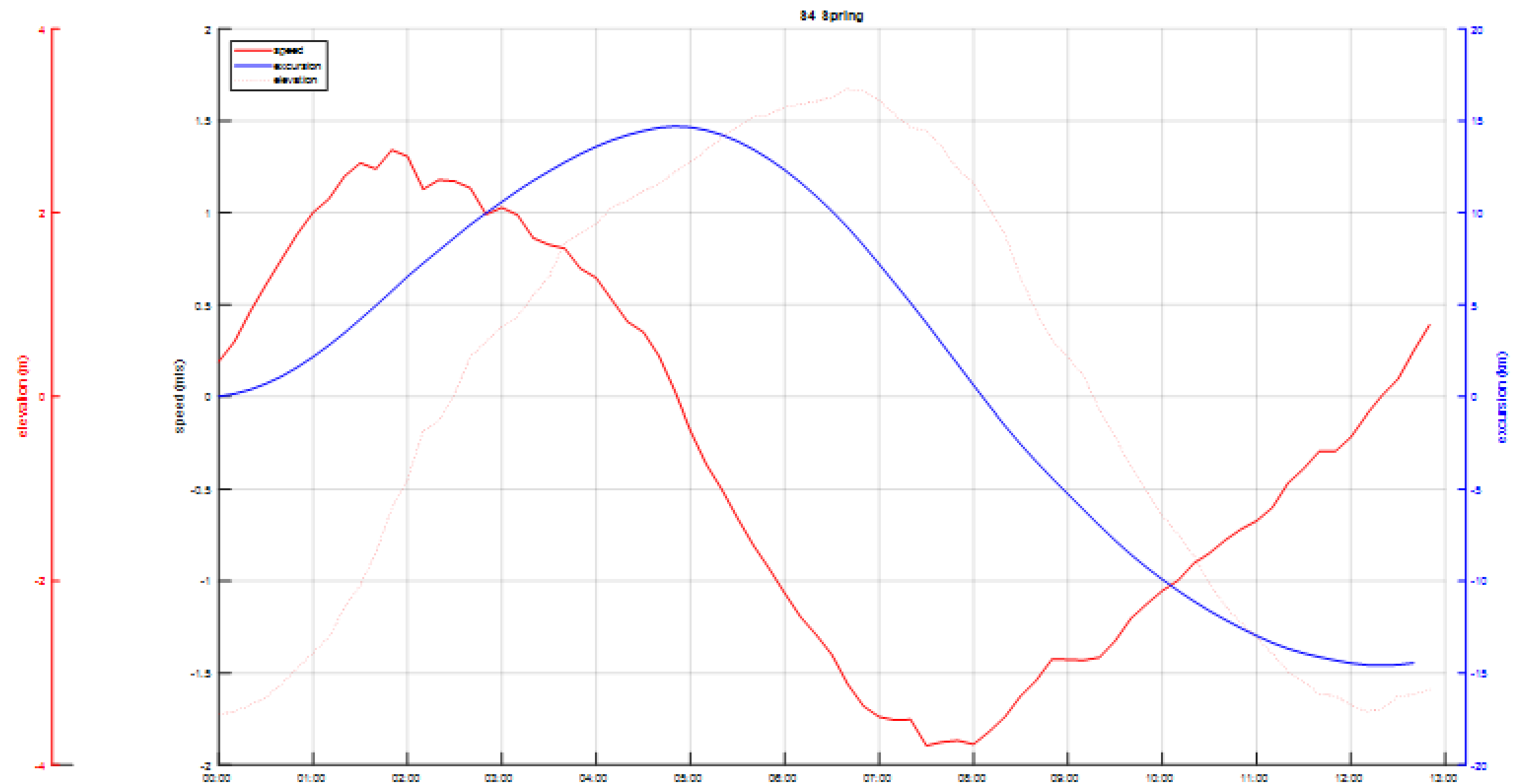


Figure 19. Illustration of tidal asymmetry at station s4 (offshore). This analysis reveal a longer (by approximately 2 hrs), and slightly stronger (by approximately 11%) ebb current phase. Data source: Horizon (2012).

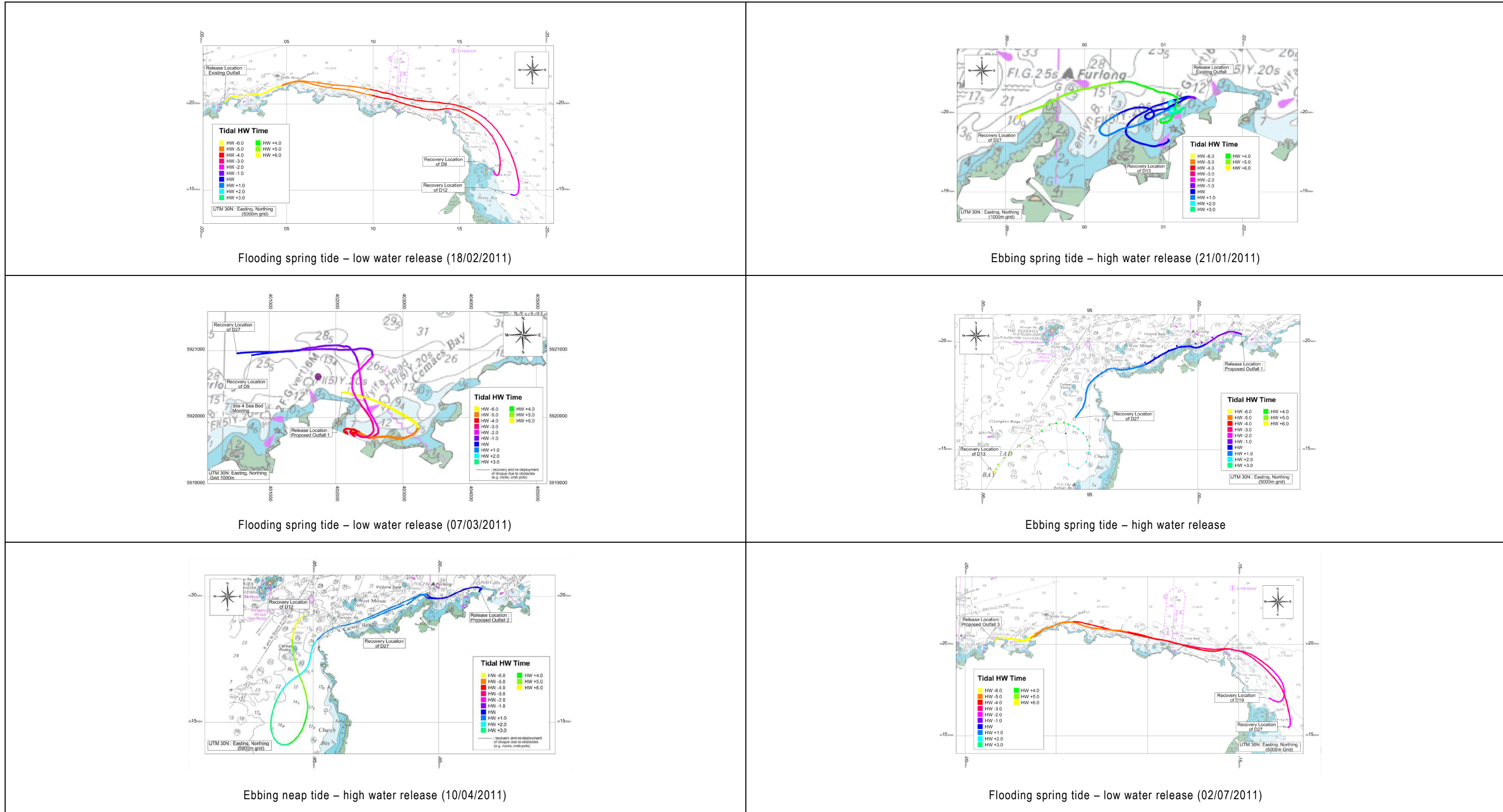


Figure 20. Lagrangian (continuous in time) trajectories of drogue releases made during the oceanographic survey. Data Source: Horizon (2012).

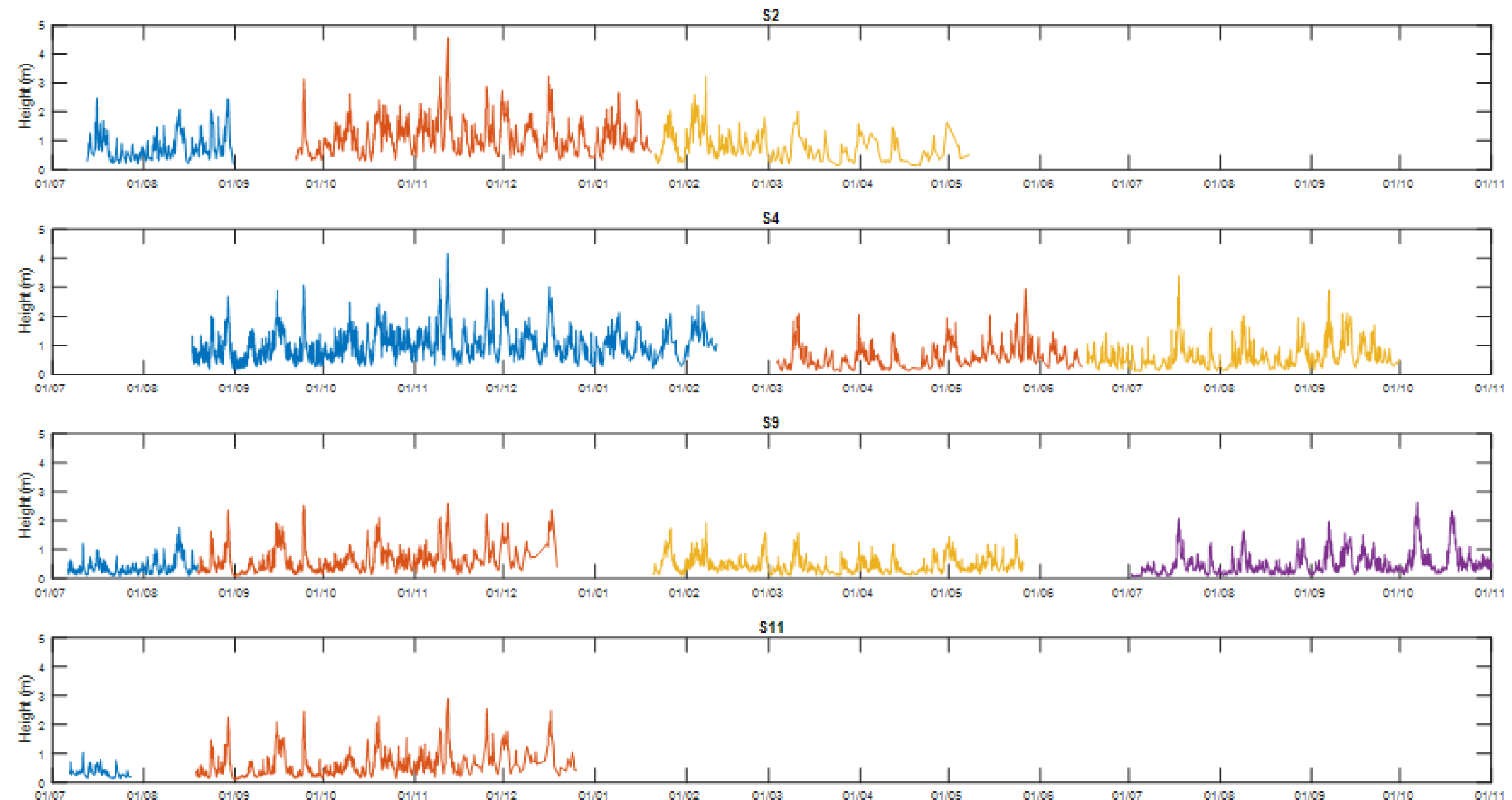


Figure 21. Time series showing the significant wave height (H_{s0}) observed at the four monitoring sites. Data Source: Horizon (2012).

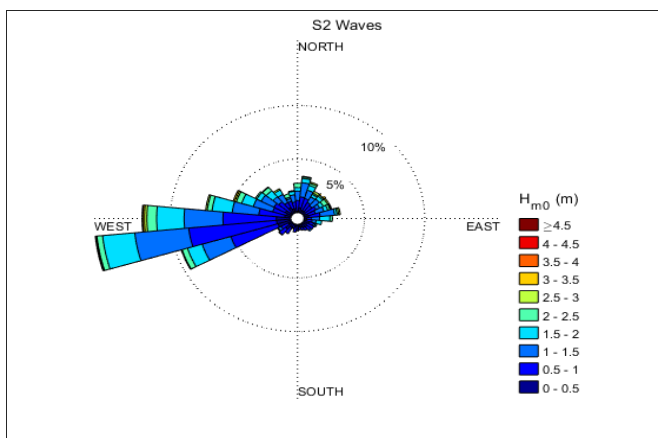
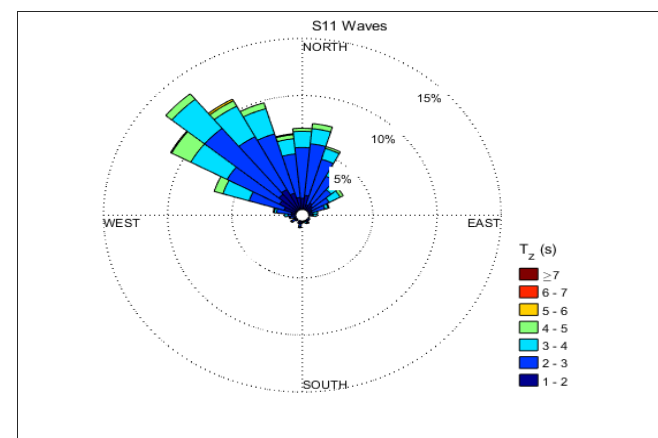
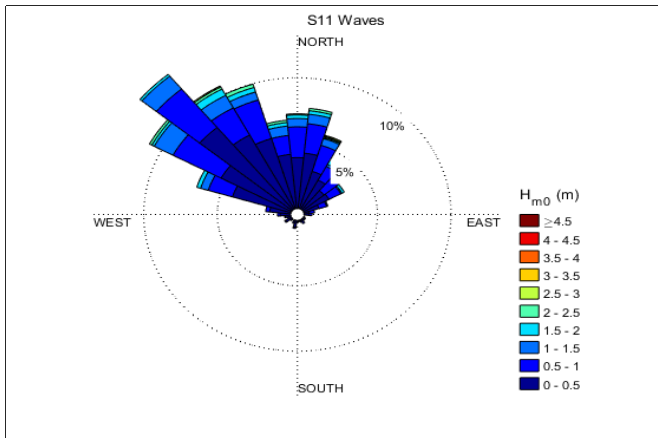
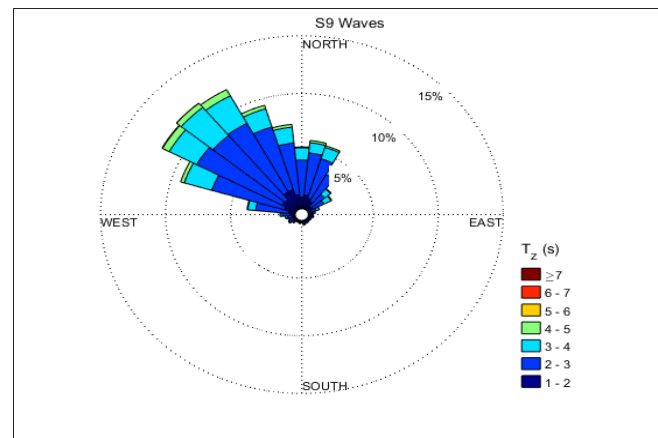
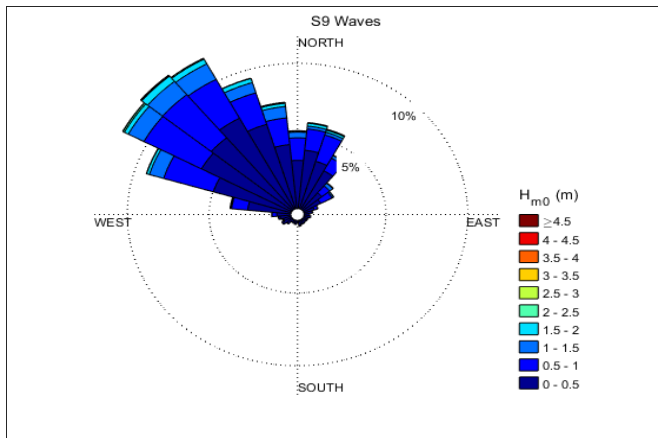
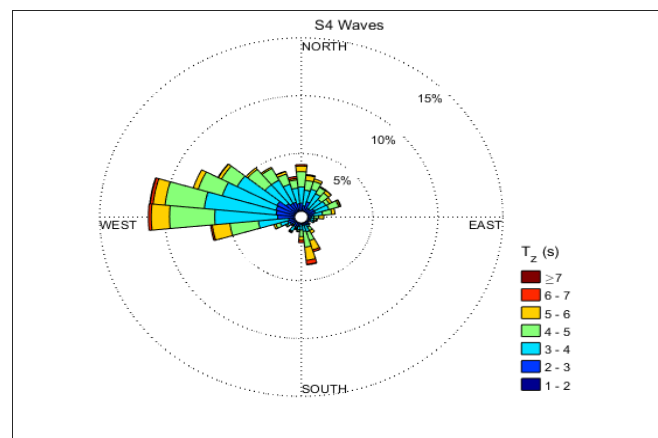
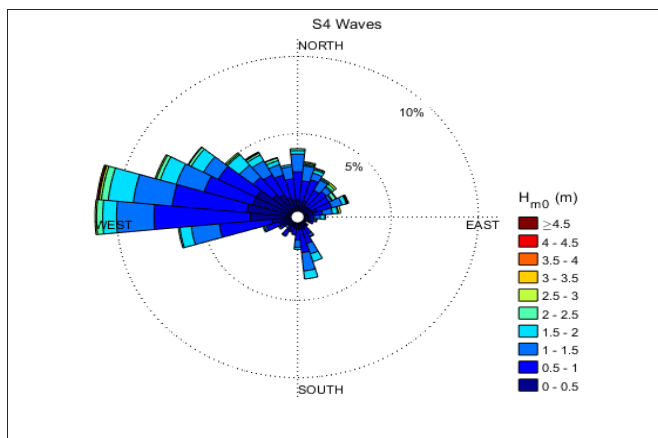
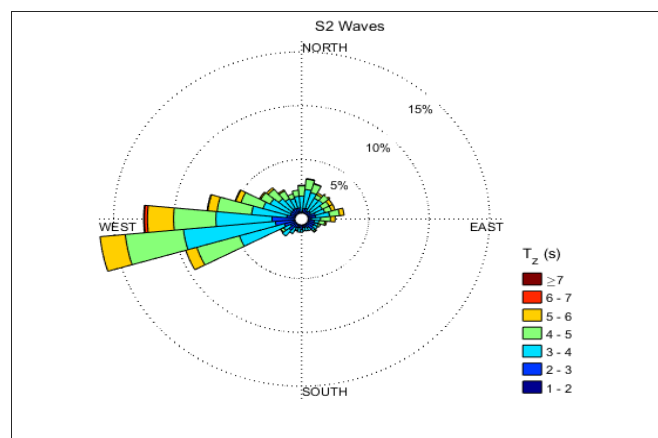
H_{m0} & direction

 T_z & direction


Figure 22. Wave roses for the four monitoring stations (July 2010 – November 2011) showing significant wave height (H_{m0}) (left column) and wave period (T_z) (right column) and the associated direction. Data Source: Horizon (2012).

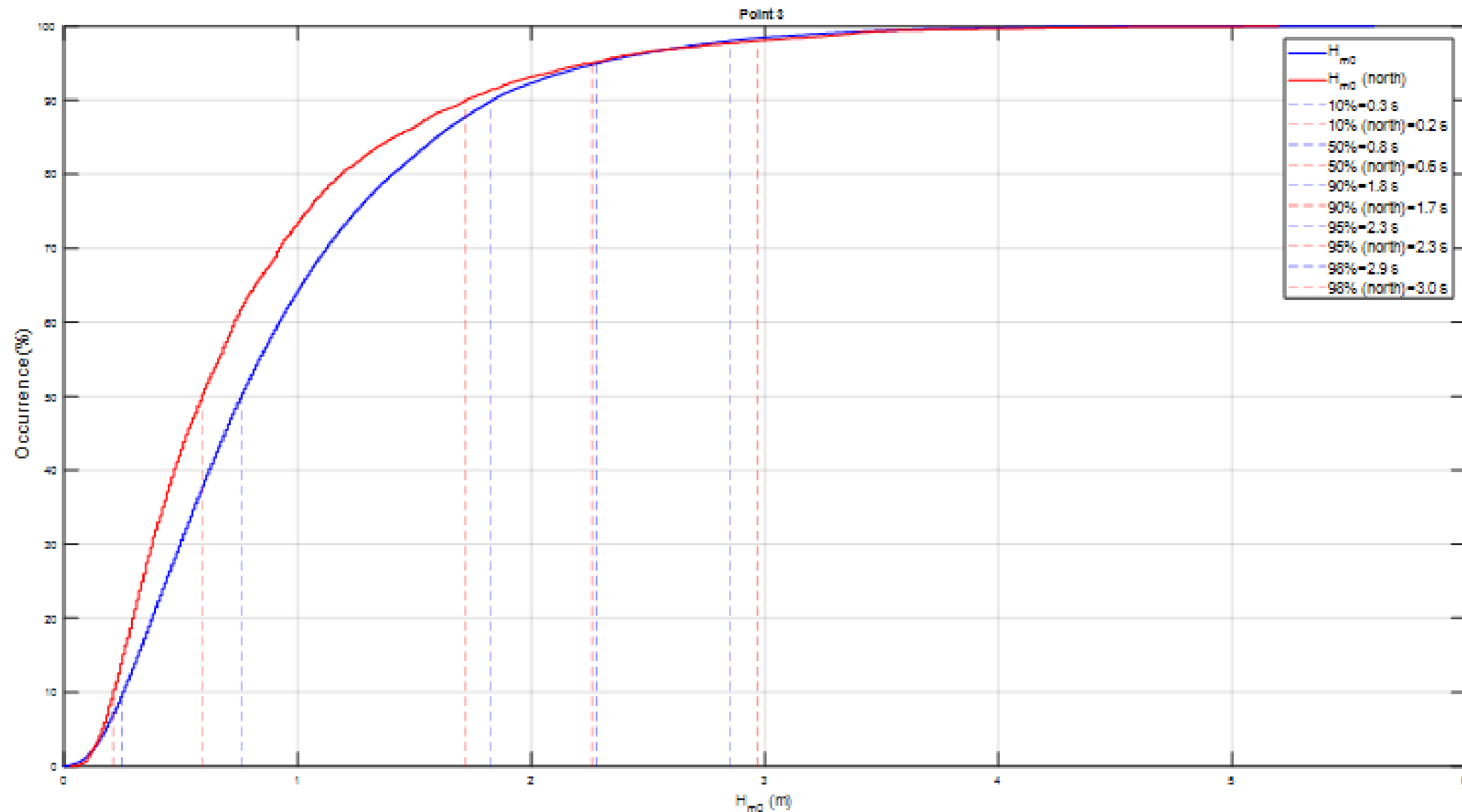


Figure 23. Frequency of predicted significant wave heights (H_{m0}) at model point 3 for the entire dataset ('all') and for the North sector only ('north'). Data Source: RWE (2017).

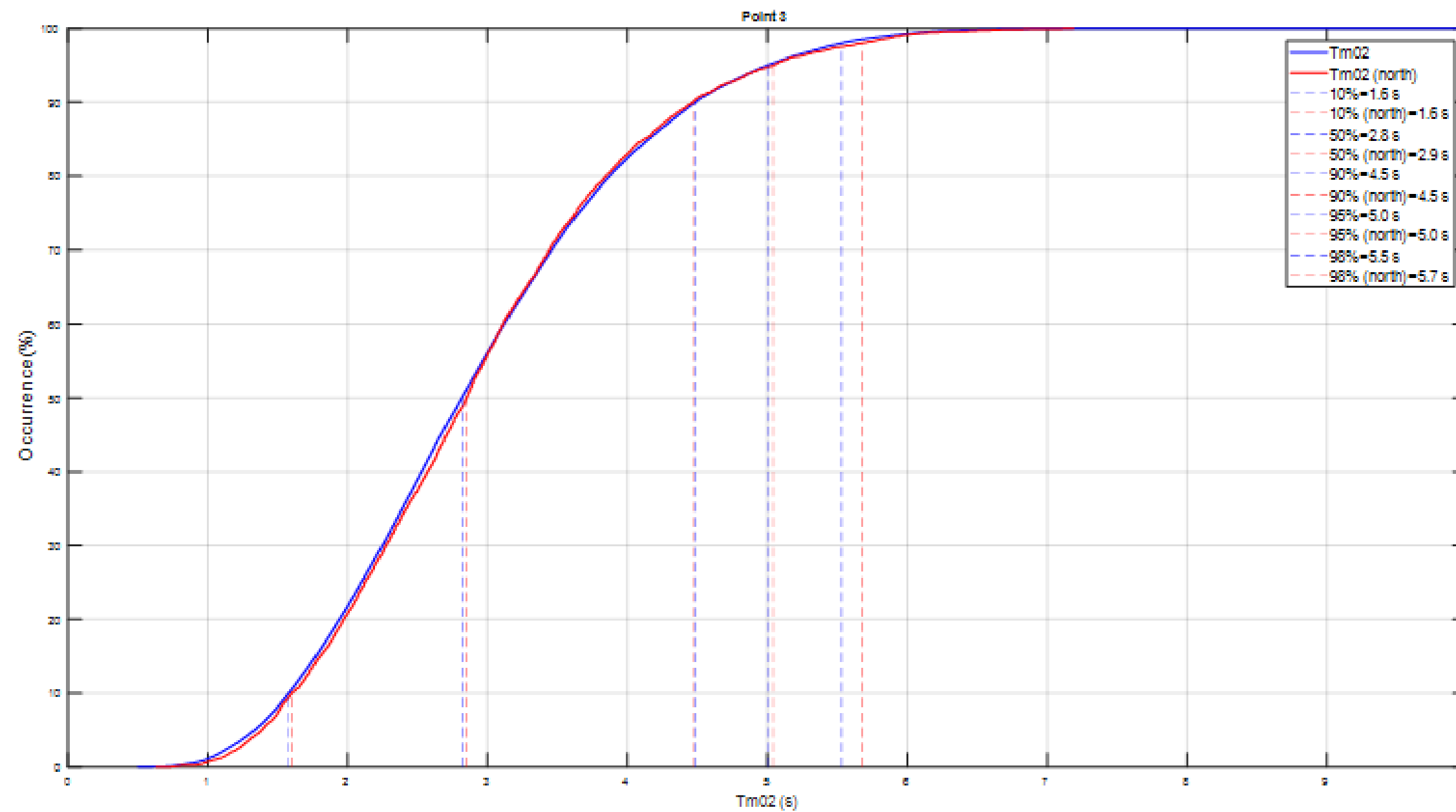


Figure 24. Frequency of predicted associated wave period at model point 3 for the entire dataset ('all') and for the North sector only ('north'). Data Source: RWE (2017).

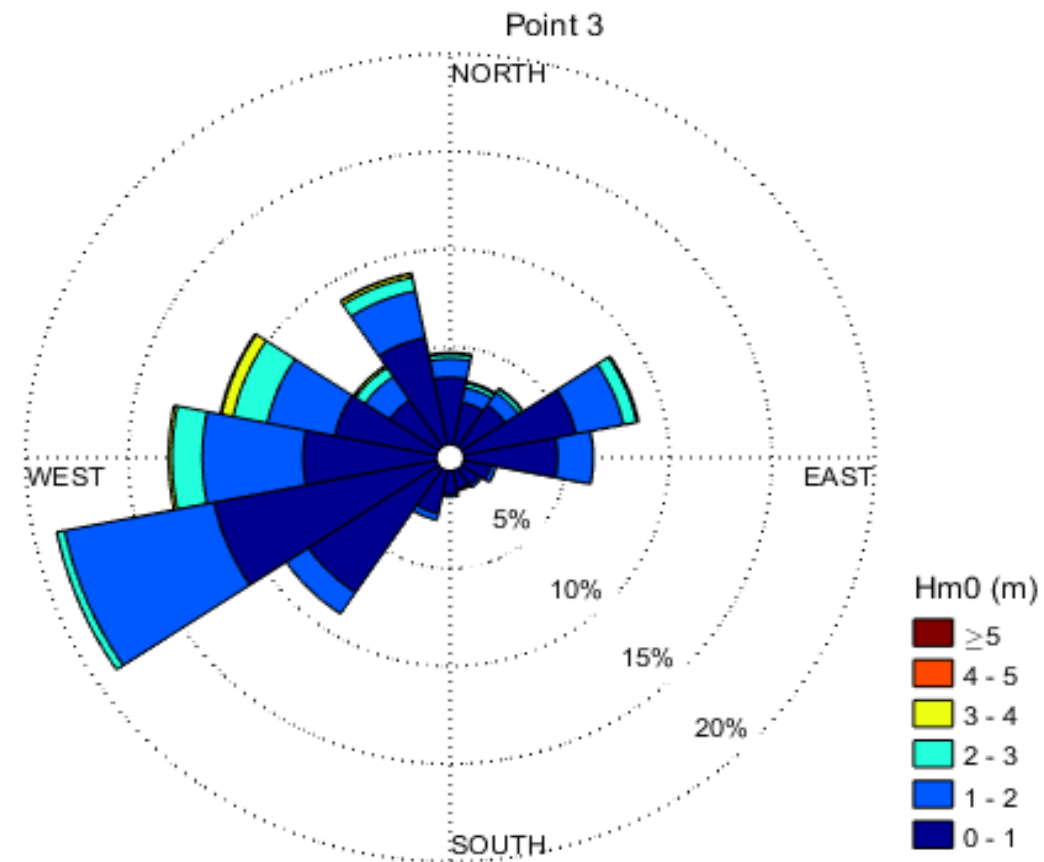
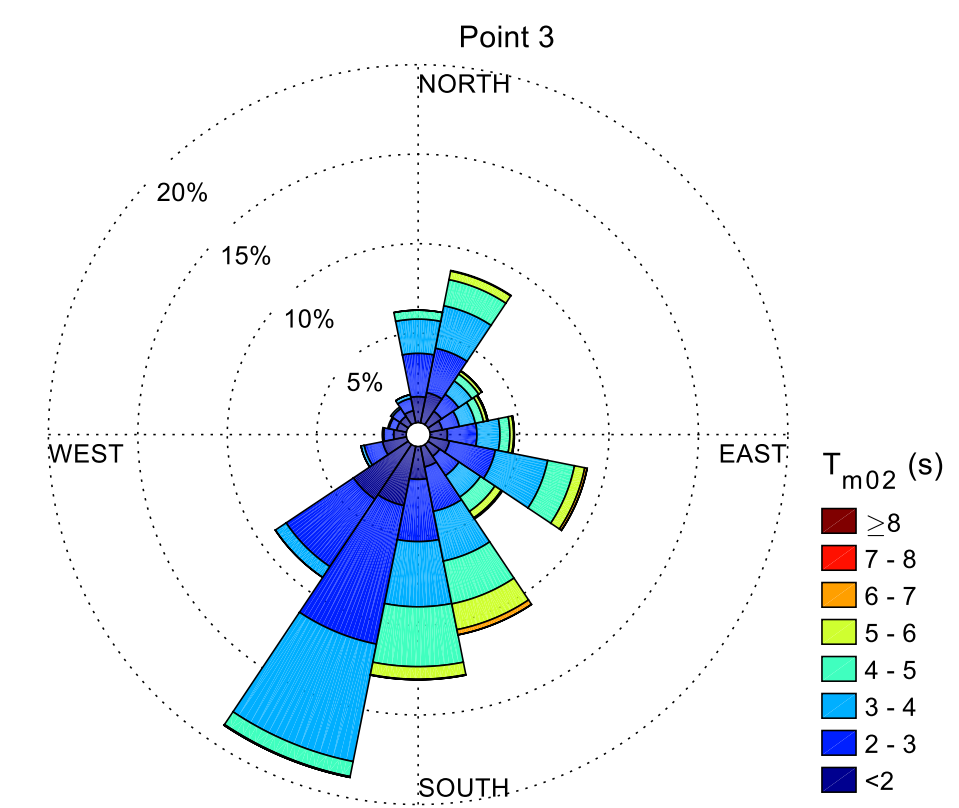
H_{m0} & direction

T_{m02} & direction


Figure 25. Wave roses showing significant wave height (H_{m0}) (left) and wave period (T_{m02}) (right) and the associated direction predicted at model point 3. Data Source: RWE (2017).

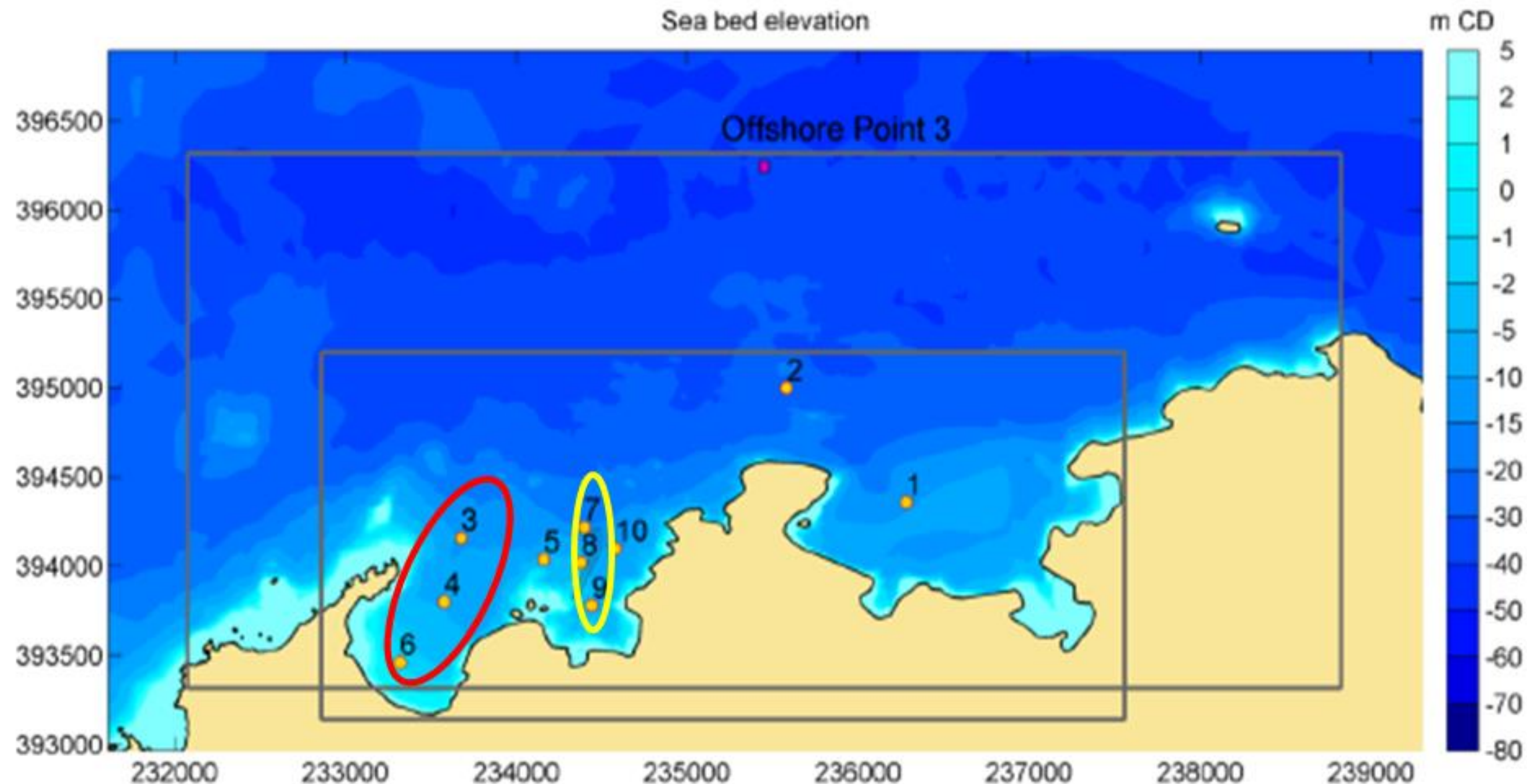


Figure 26. The position of the nearshore prediction points (1 -10) and 'offshore' model point 3 in relation to the Anglesey coastline. Prediction points 3, 4 and 6 (marked 0) and points 7, 8 and 9 (marked 1) provide two shore-normal gradients useful for examining wave modification at the site. Source: HR Wallingford (2017).

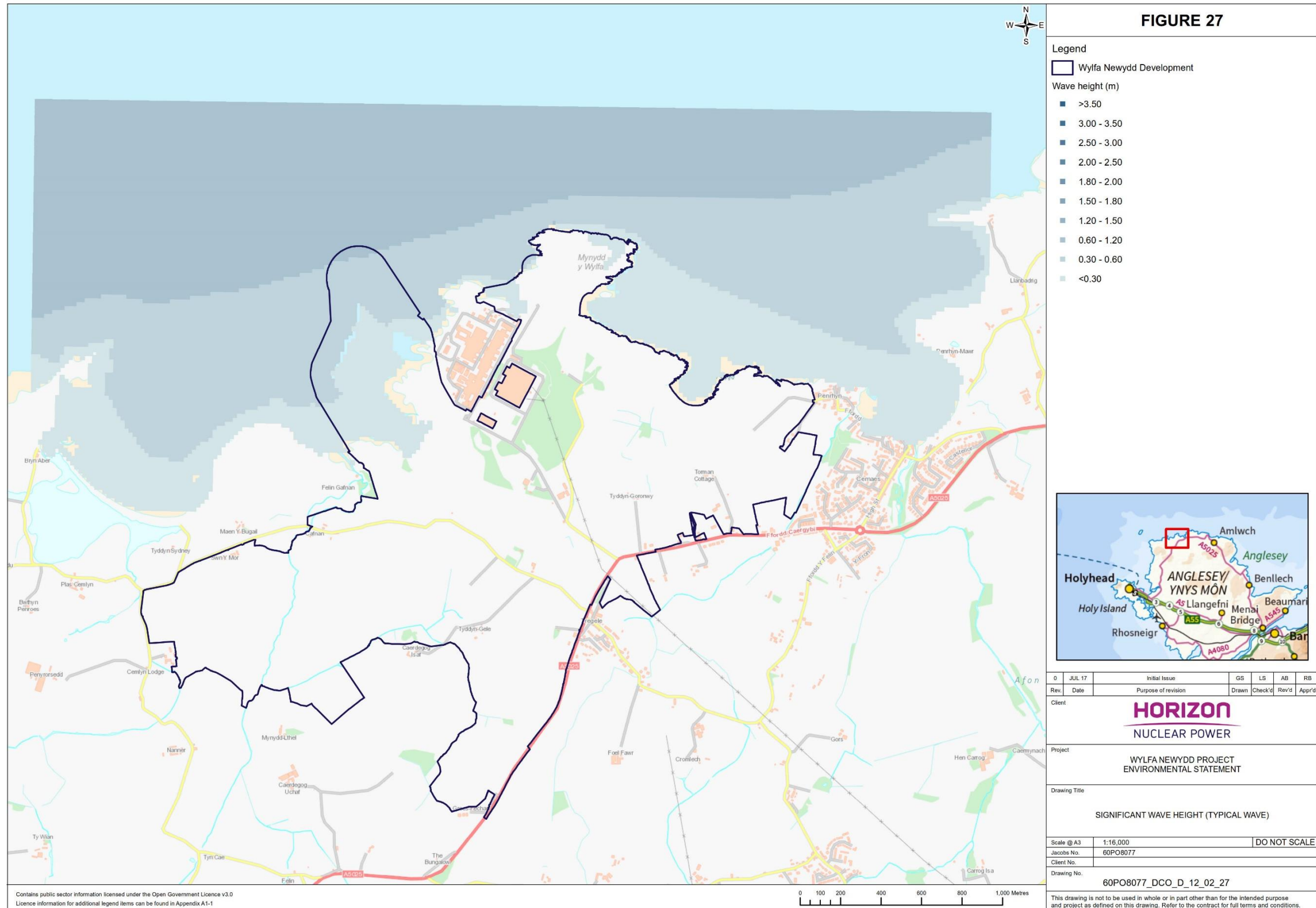


Figure 27. The predicted wave height across the site for a typical wave scenario (H_m0 0.9 m, 228°) on a Spring tide.

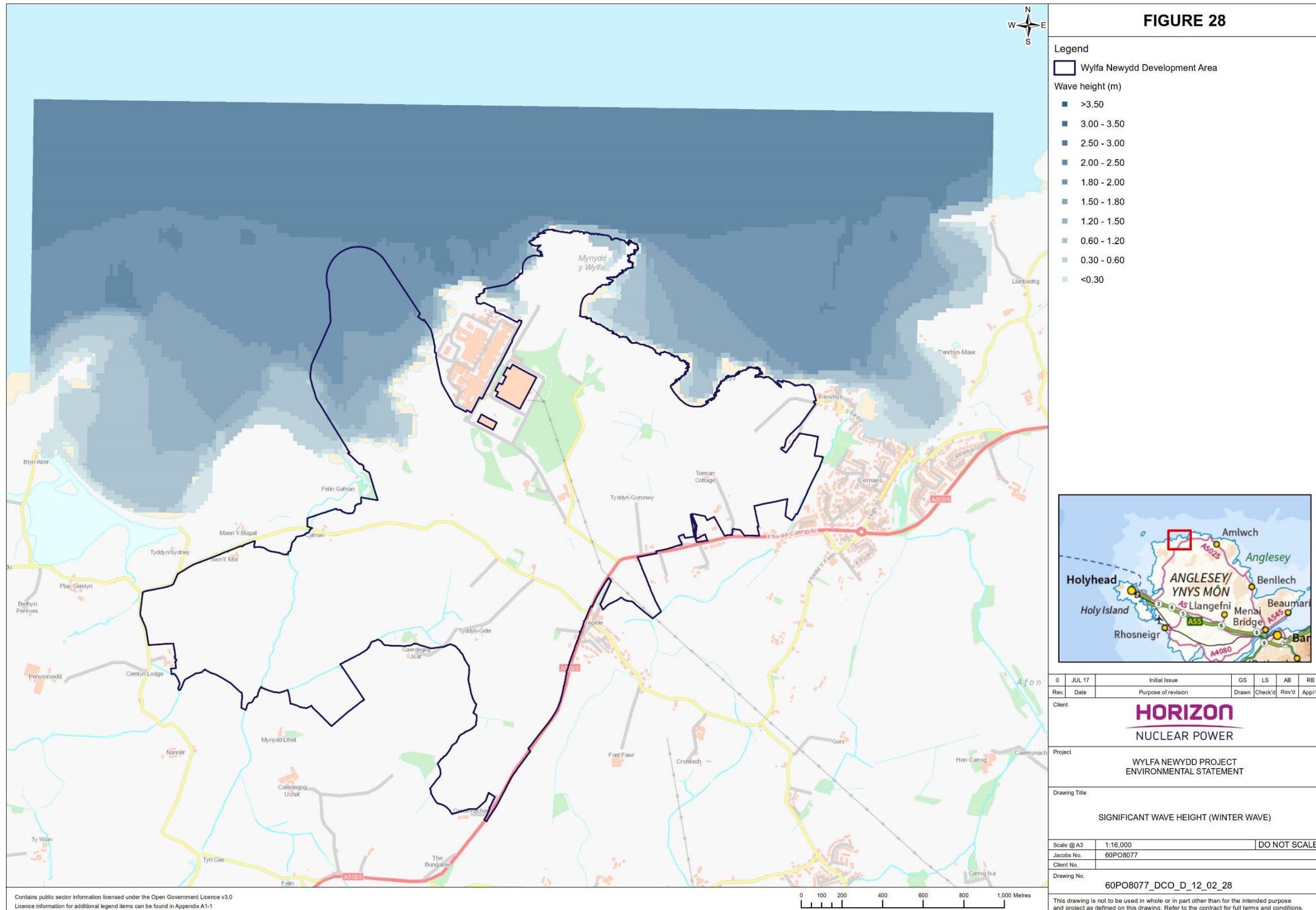


Figure 28. The predicted wave height across the site for a winter wave scenario (H_{m0} 2.0 m, 228°) on a Spring tide.

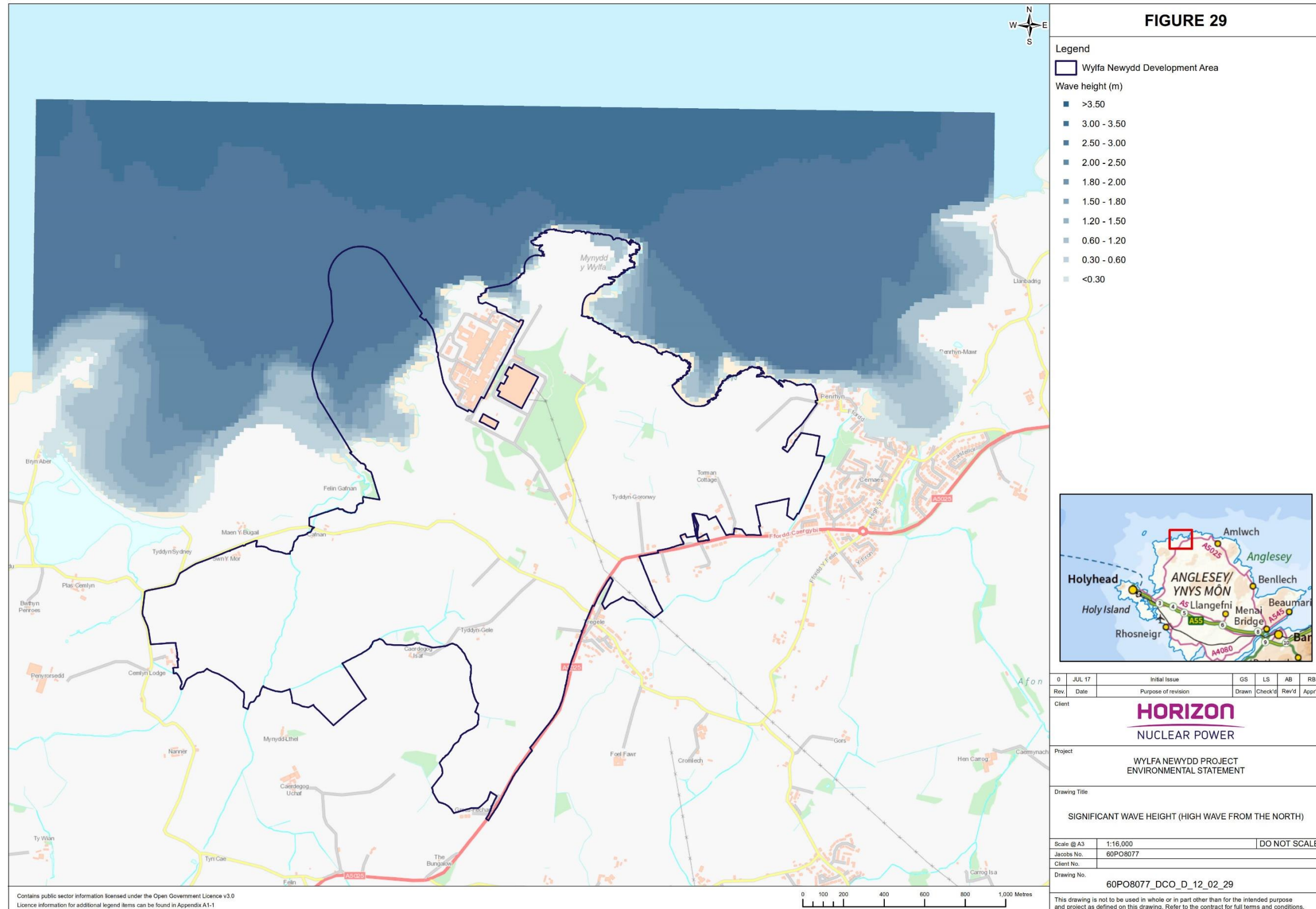


Figure 29. The predicted significant wave height across the site for a high (98%ile) wave from the north scenario (H_m0 2.85 m, 346°) on a Spring tide..

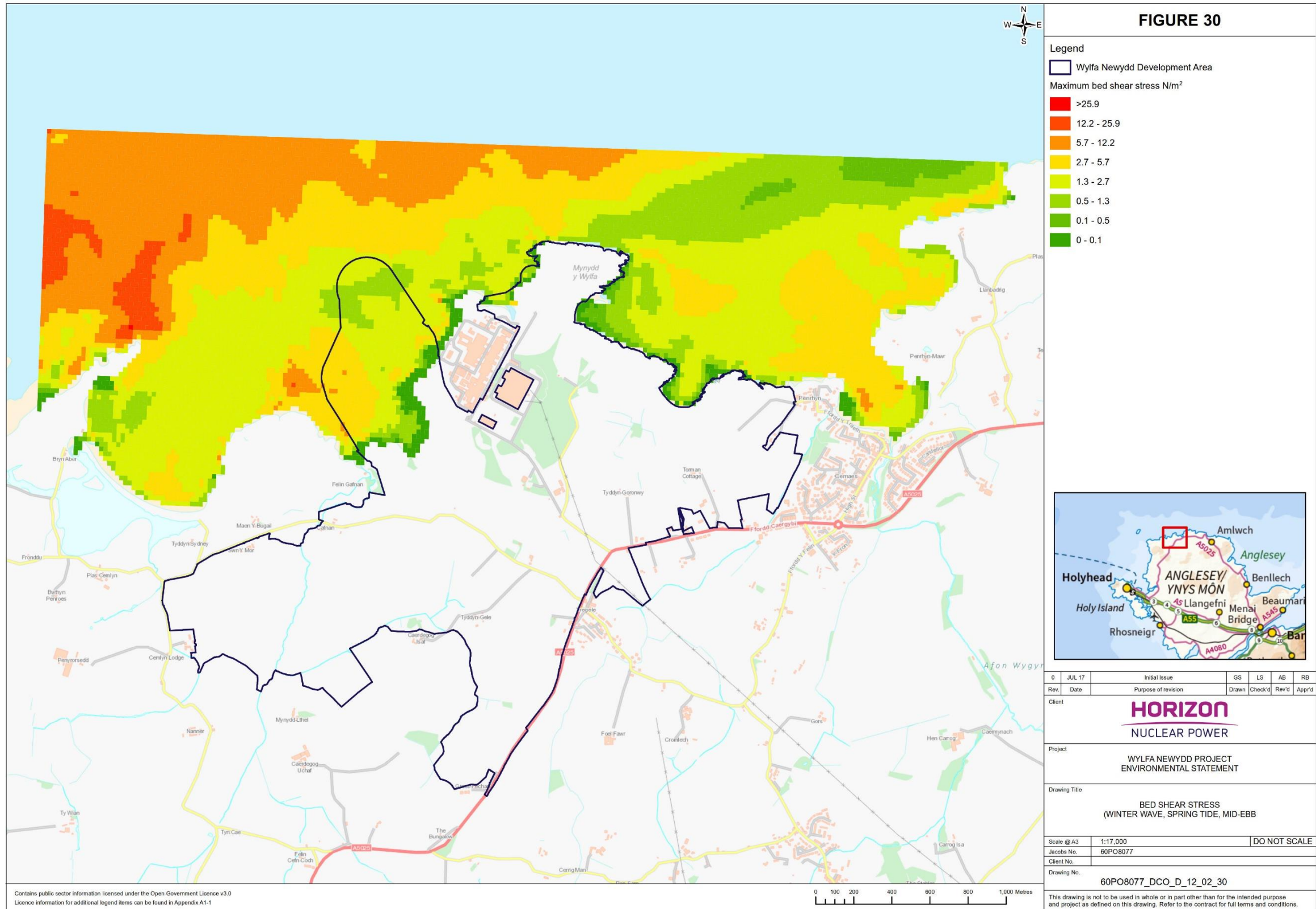


Figure 30. Geospatial distribution of maximum bed shear stress acting upon the bed during a Spring tide, mid-Ebb condition (the strongest currents) with a typical winter wave scenario (H_{mo} 2.0m, 343°).

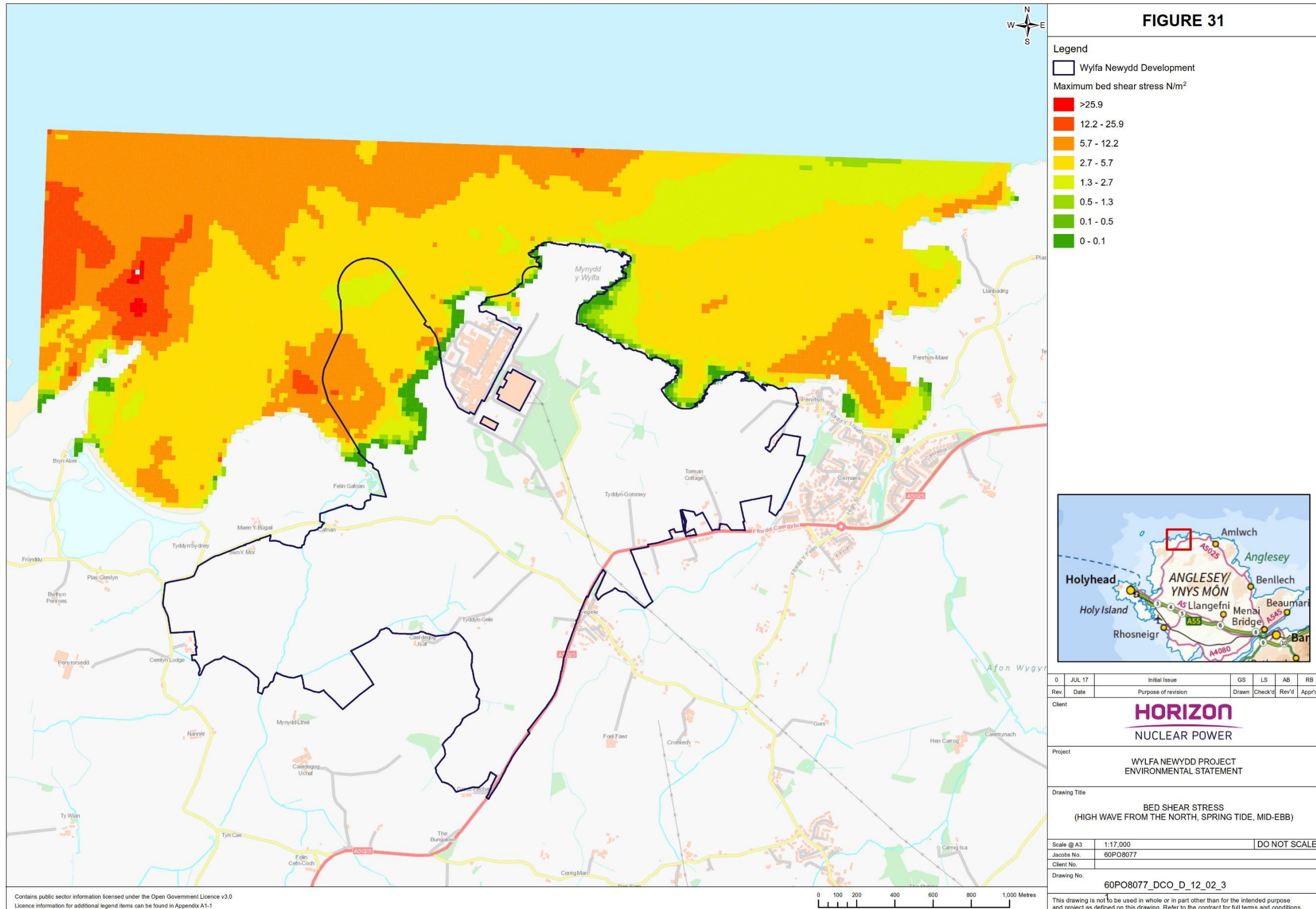


Figure 31. Geospatial distribution of maximum bed shear stress acting upon the bed during a Spring tide, mid-ebb condition (the strongest currents) with an high wave (98%ile) from the north scenario (H_{mo} 2.85m, 358°).



PARTRAC

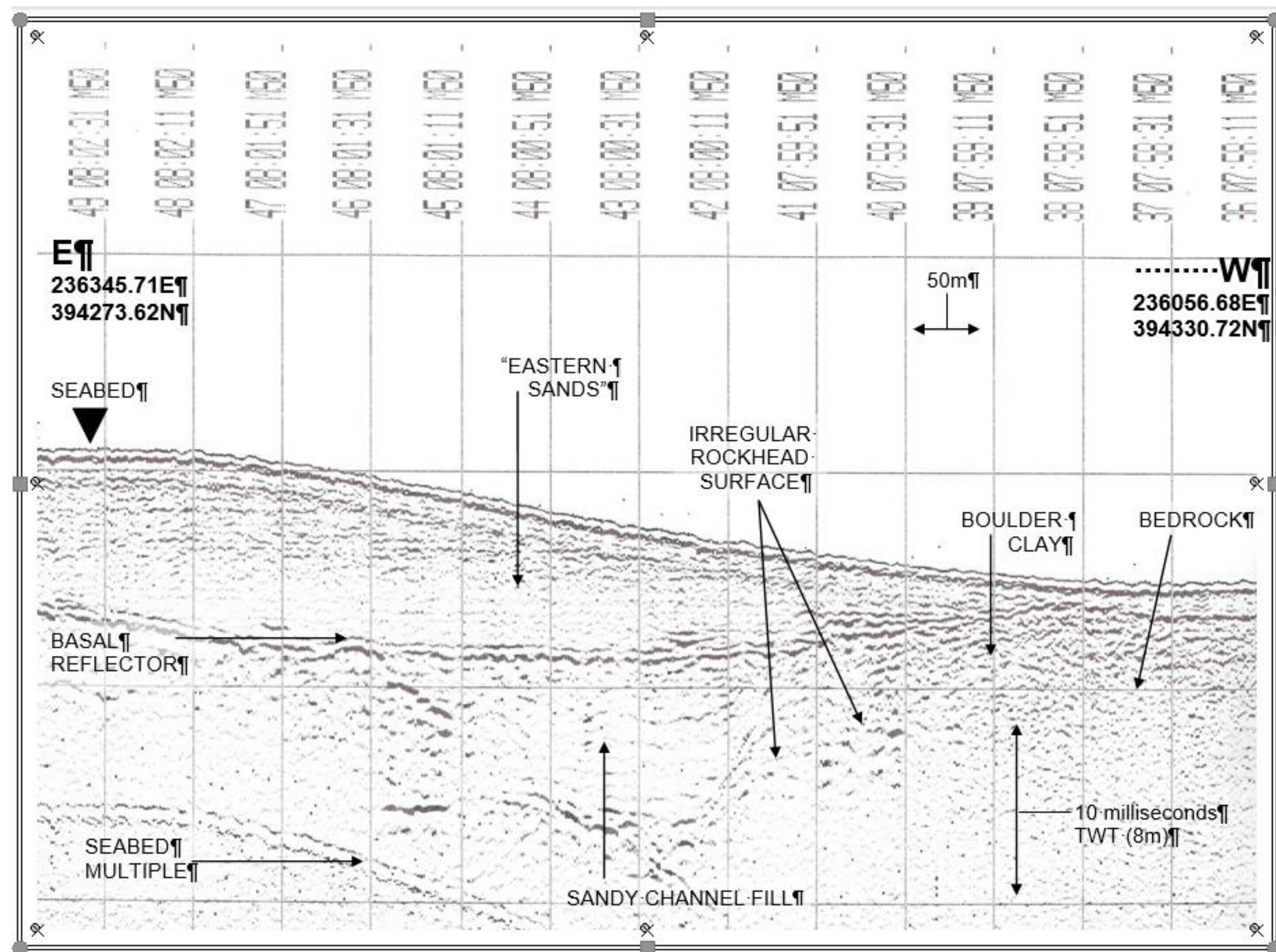


Figure 32. Boomer record showing typical conditions in Cemaes Bay. The sediment lenses within Cemaes bay are clearly visible (Source: Titan, 2009).

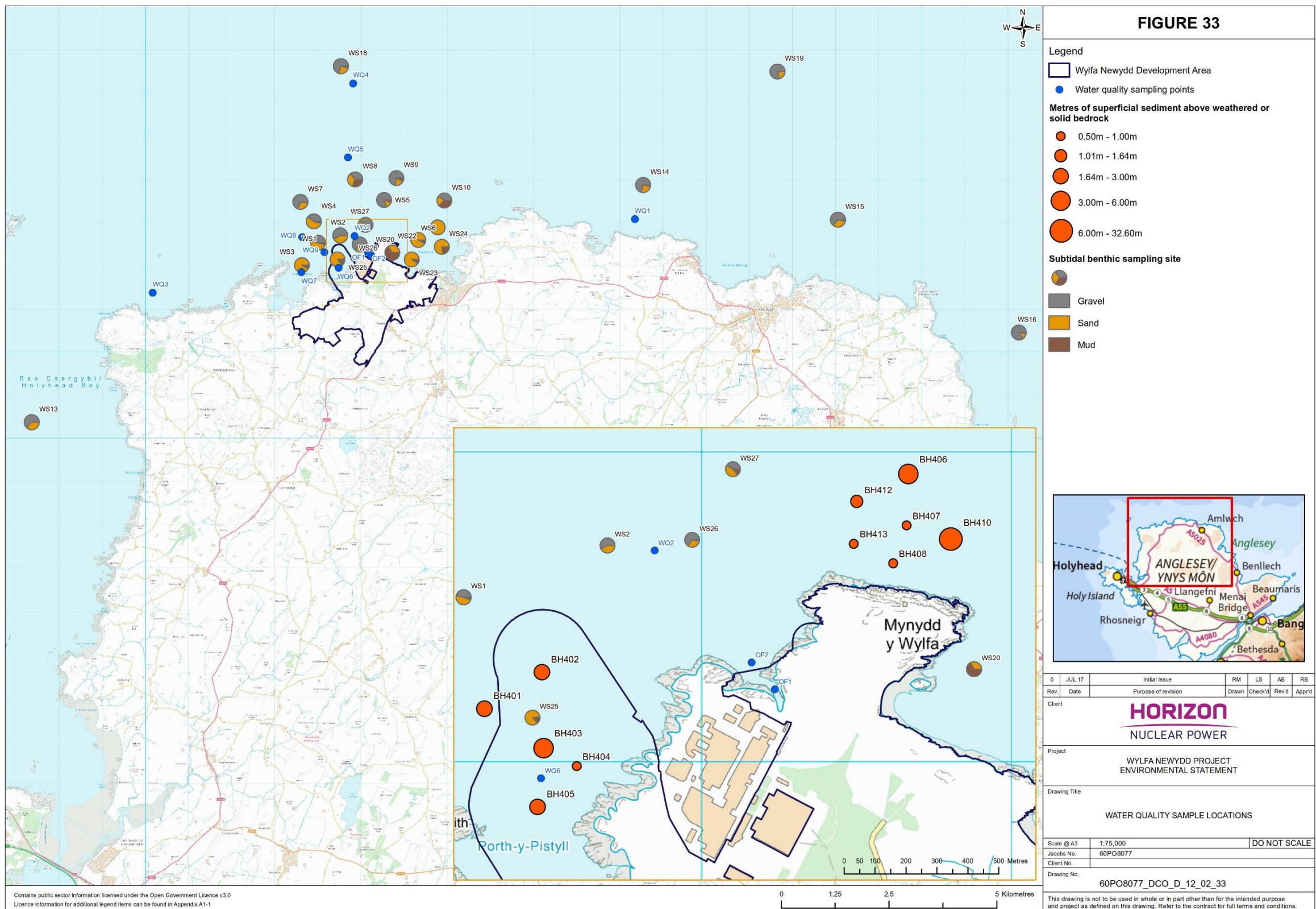


Figure 33. The locations of the samples collected in 2010 (grab, borehole, water). Source: Jacobs UK Ltd (2011)

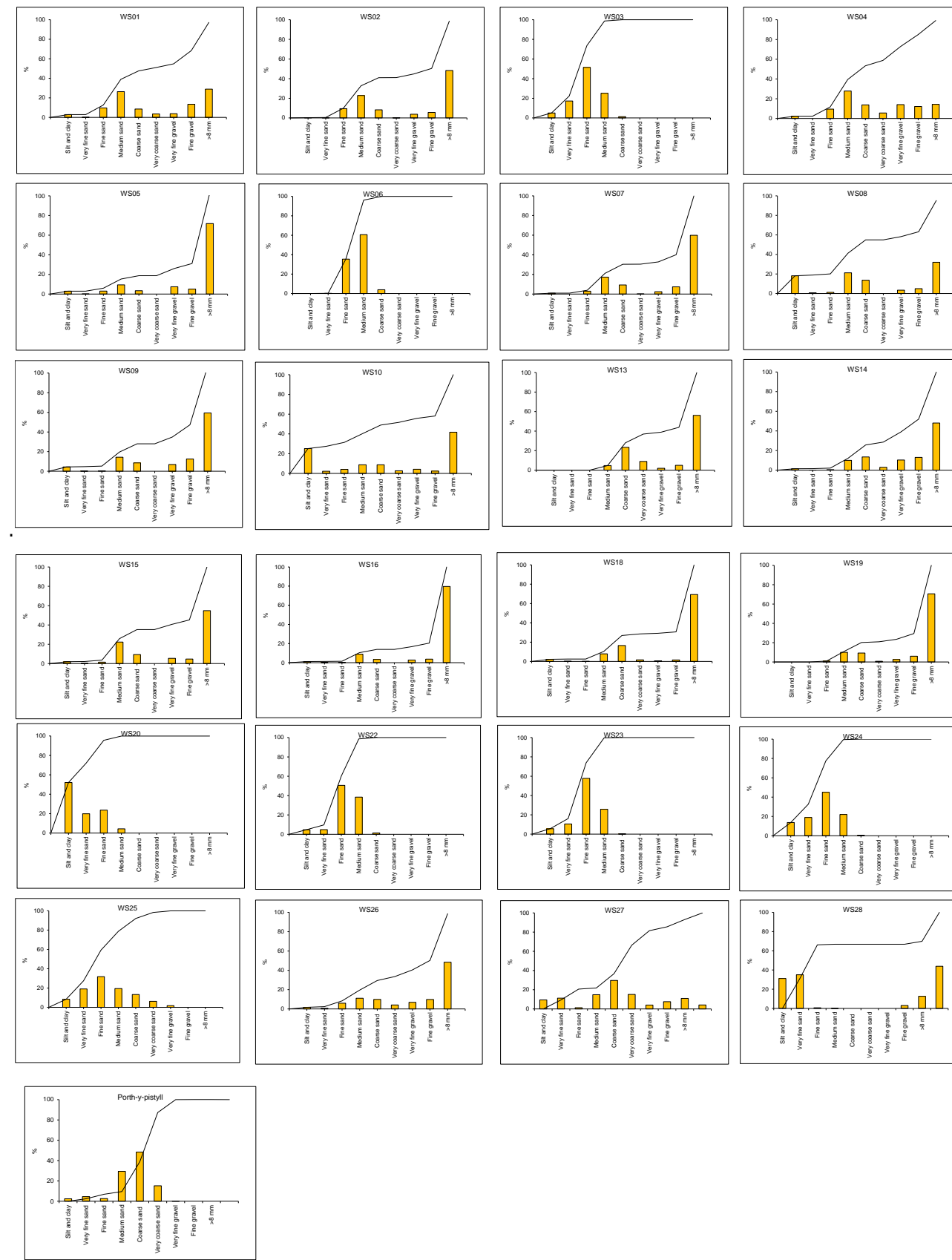


Figure 34. Particle size data from samples collected at various locations across the site during the benthic sampling campaign in 2011. Data source: Jacobs UK Ltd (2011).

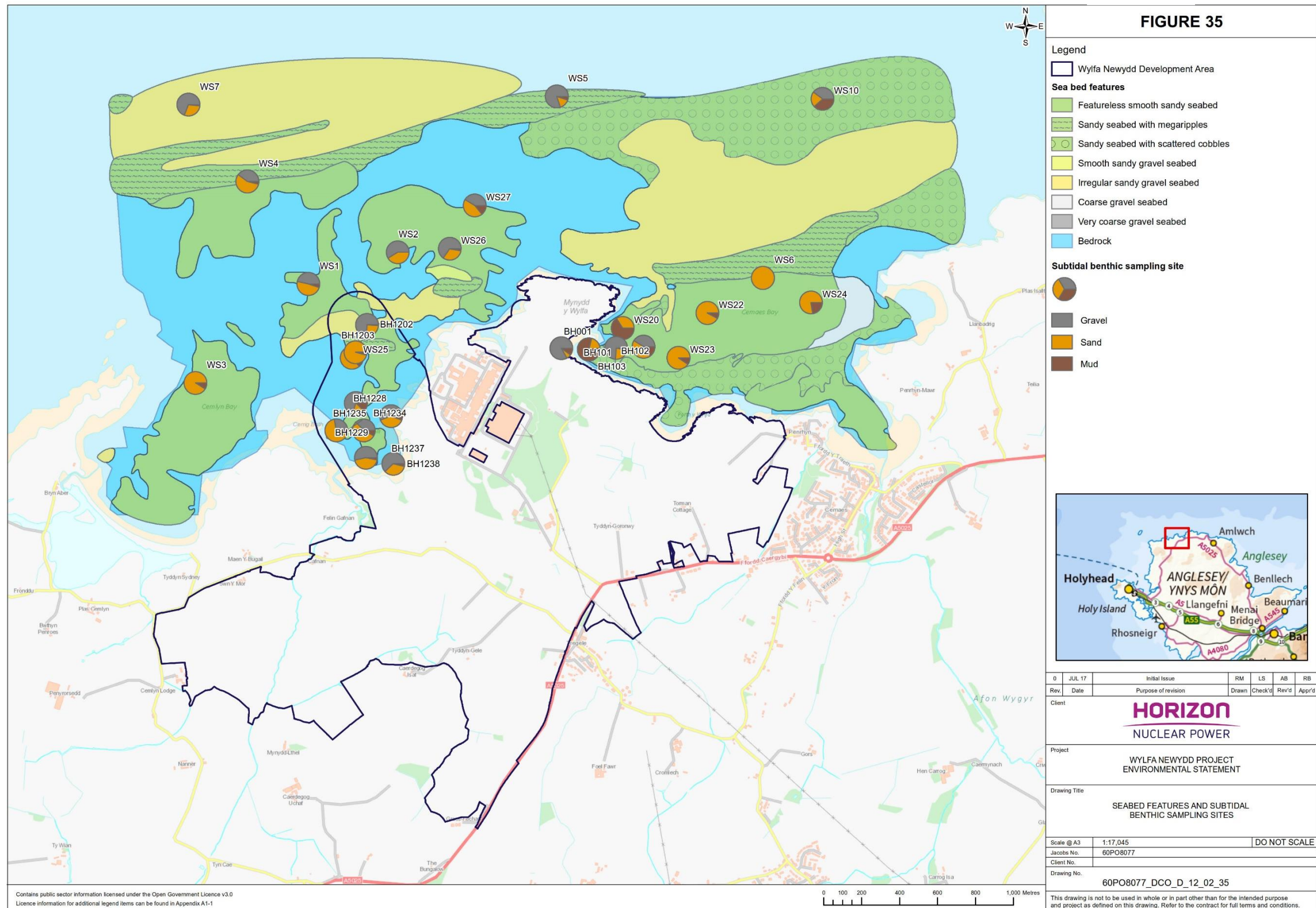


Figure 35. Seabed features plot with grain size data presented in the form of gravel: sand: mud [$> 2 \text{ mm}$: $2 \text{ mm} - 0.063 \text{ mm}$: $< 0.063 \text{ mm}$] ratio data, superimposed on the sediment type determined from geophysical survey (AGDS). Source: Jacobs (2015).

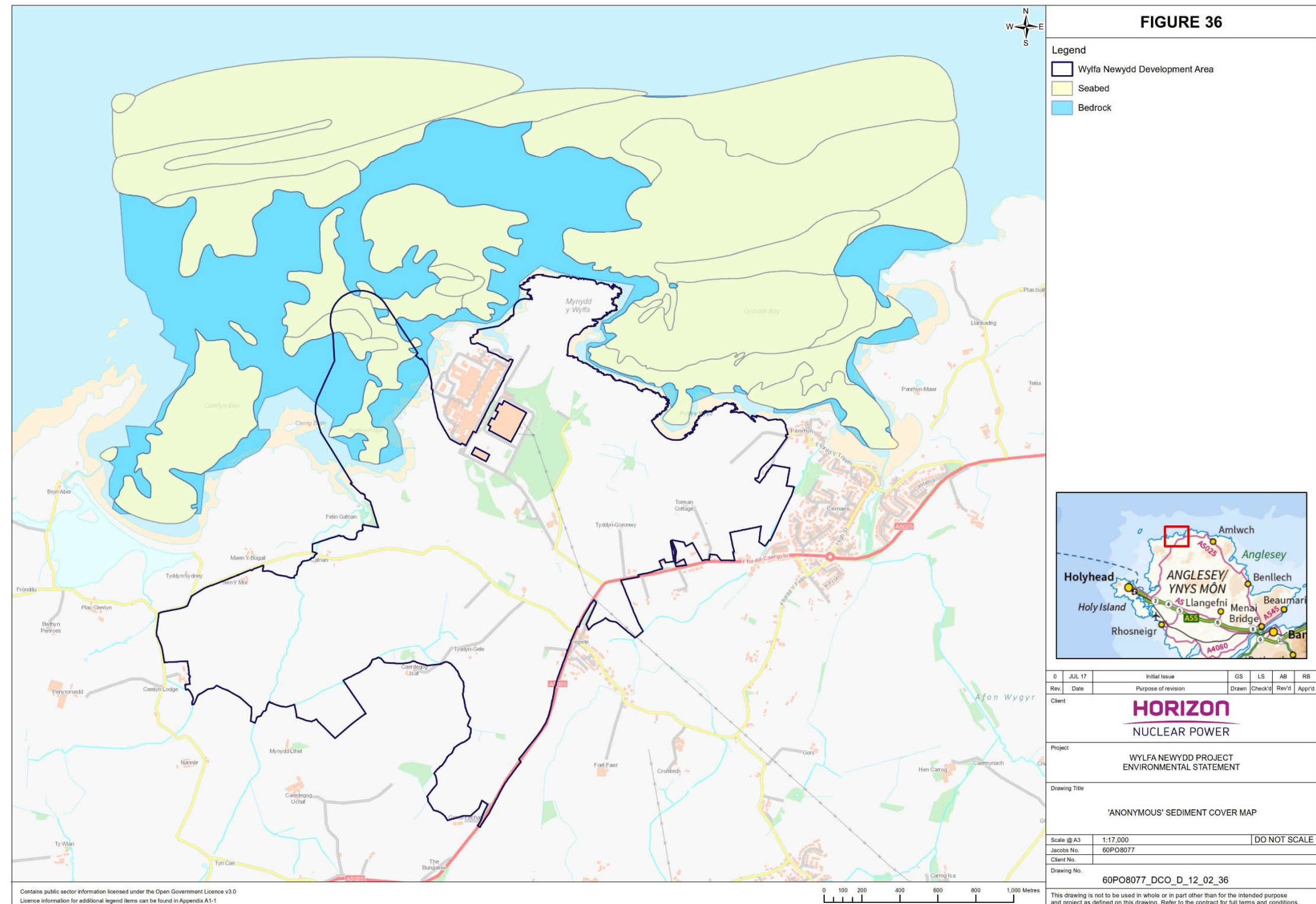


Figure 36. The 'anonymous' sediment map which distinguishes between the two principal seabed components (sediment and bedrock).

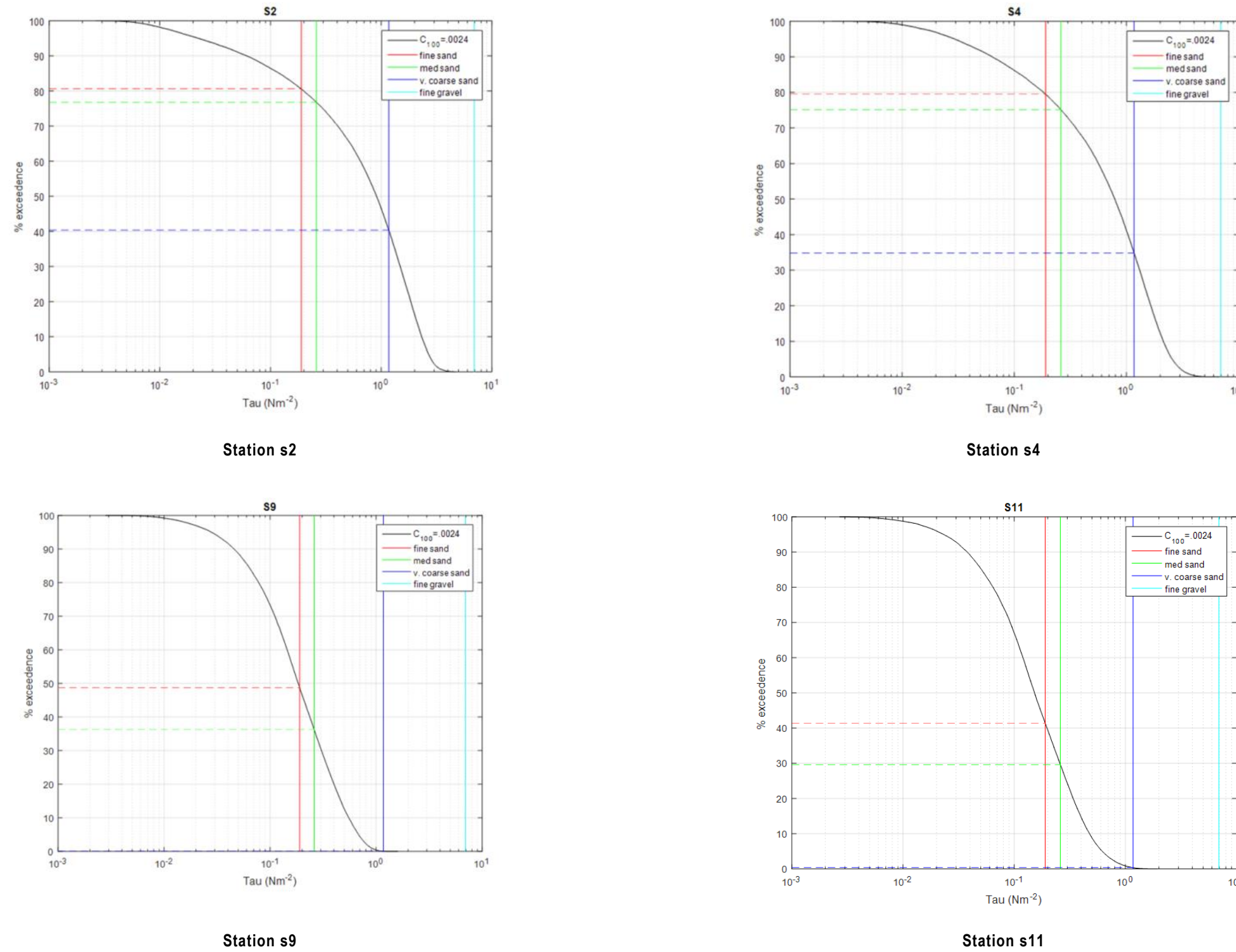


Figure 37. Tidal stress exceedance plots, by station, for various size fractions in Table 27

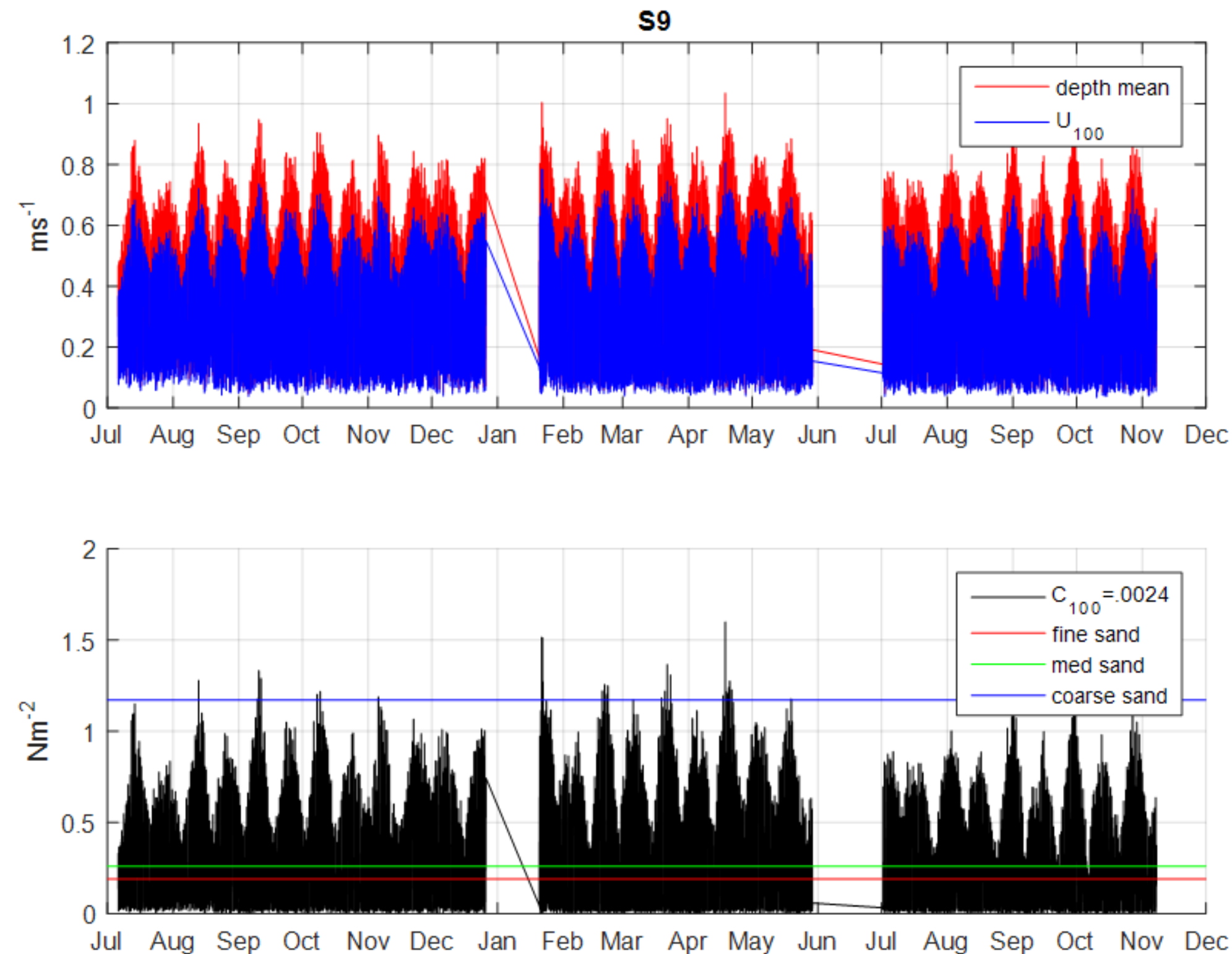


Figure 38. Time series overlay showing the fraction-specific critical stress values for sand in relation to stress amplitude at station s9. Data Source: Horizon (2012).

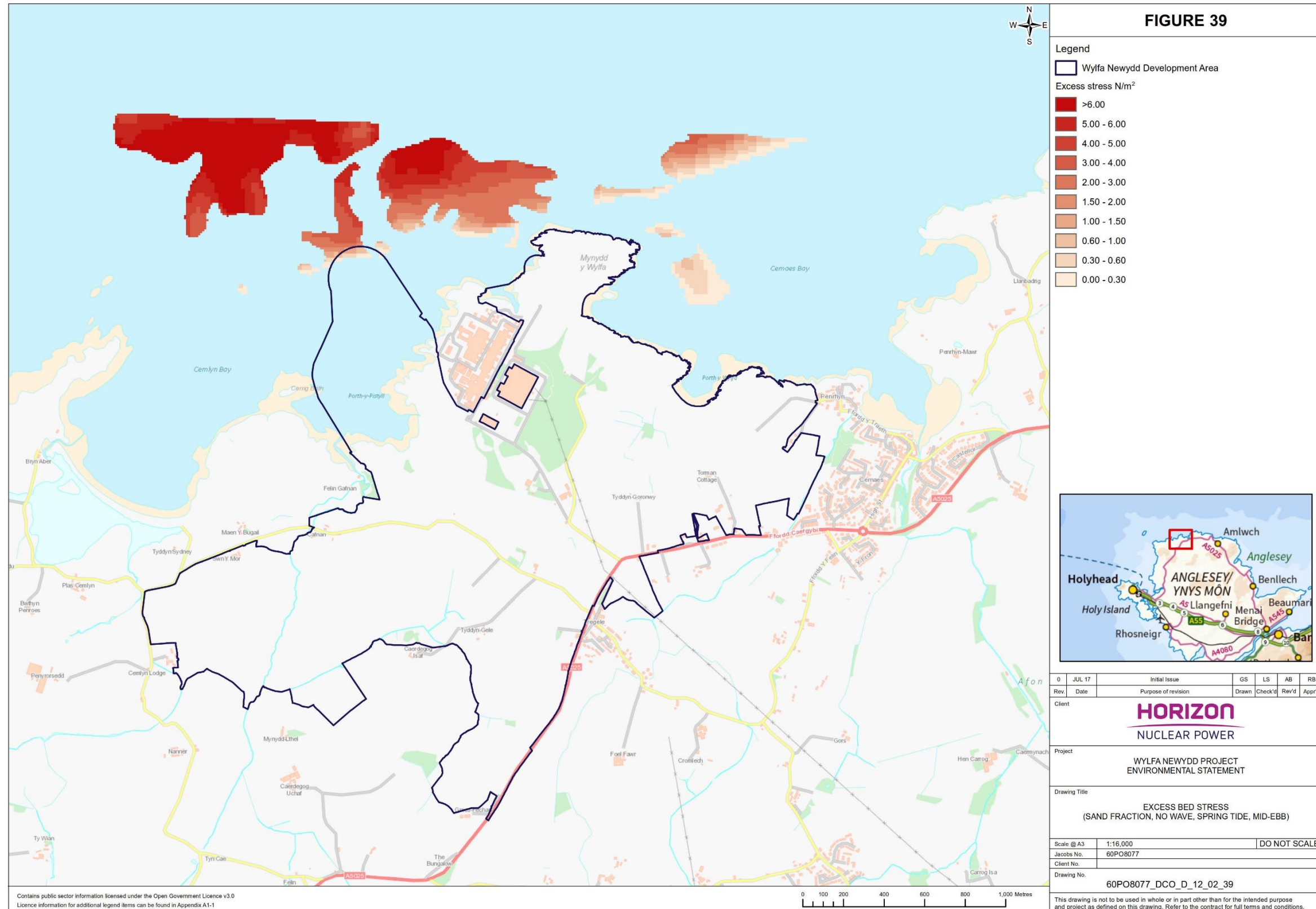


Figure 39. Geospatial excess bed stress plots for the sand fraction for a Spring tide, mid-ebb condition.

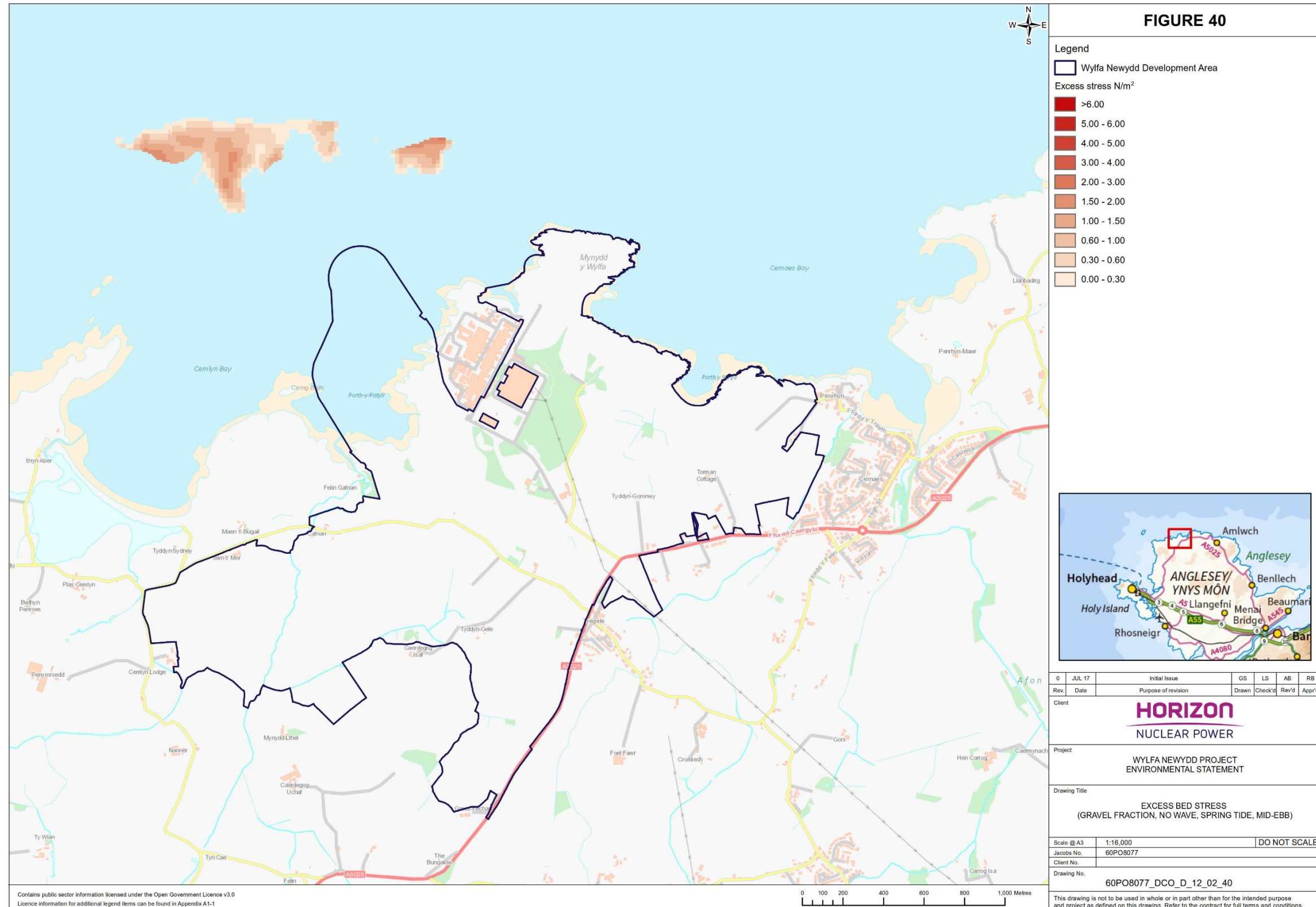


Figure 40. Geospatial excess bed stress plot for the fine gravel fraction for a Spring tide, mid-ebb condition (the strongest currents).

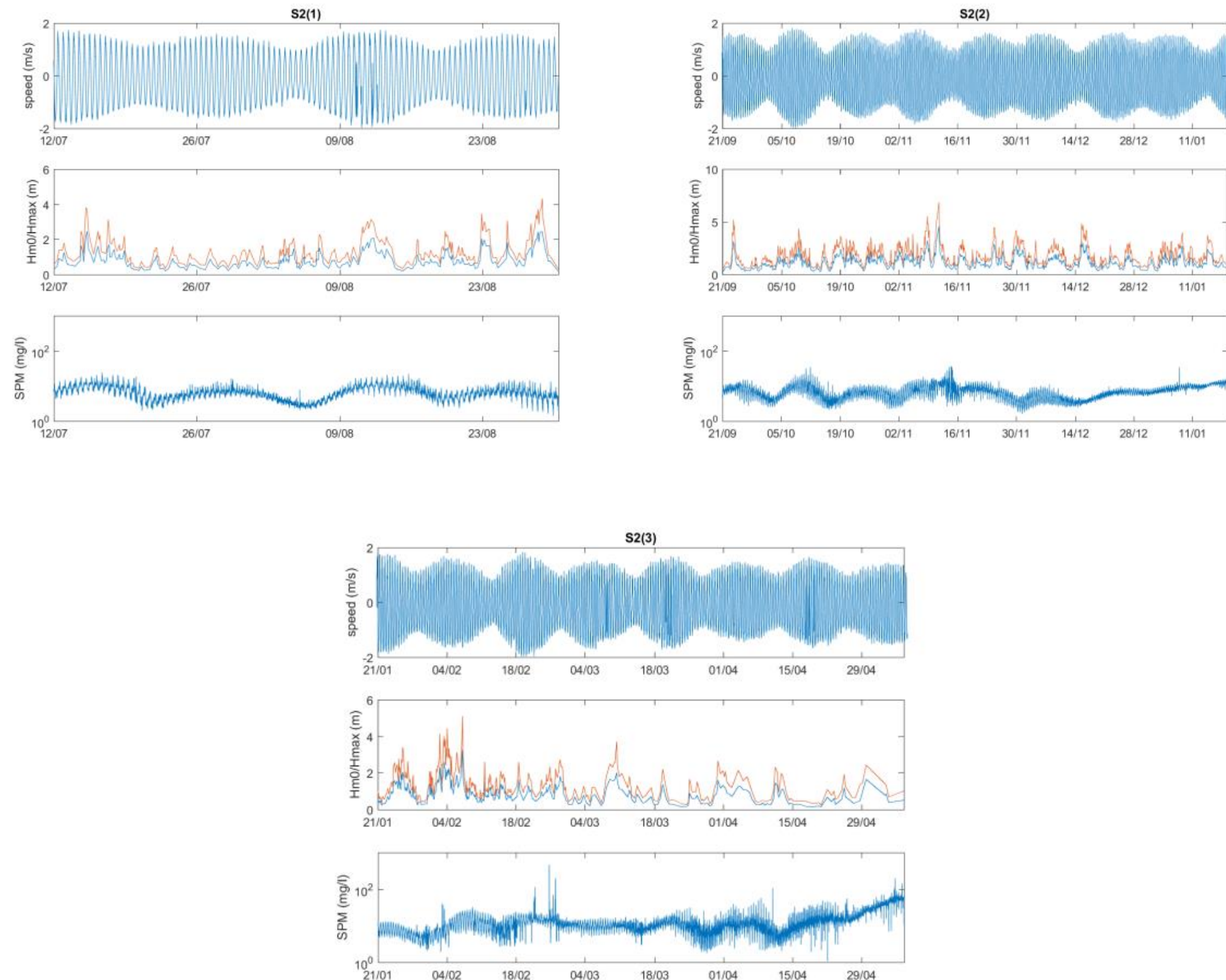


Figure 41. Time series of SPM concentration, significant wave height (H_{m0}) (orange), maximum wave height (H_{max}) (orange), and current velocity for all deployments at monitoring station, s2. Data Source: Horizon (2012).

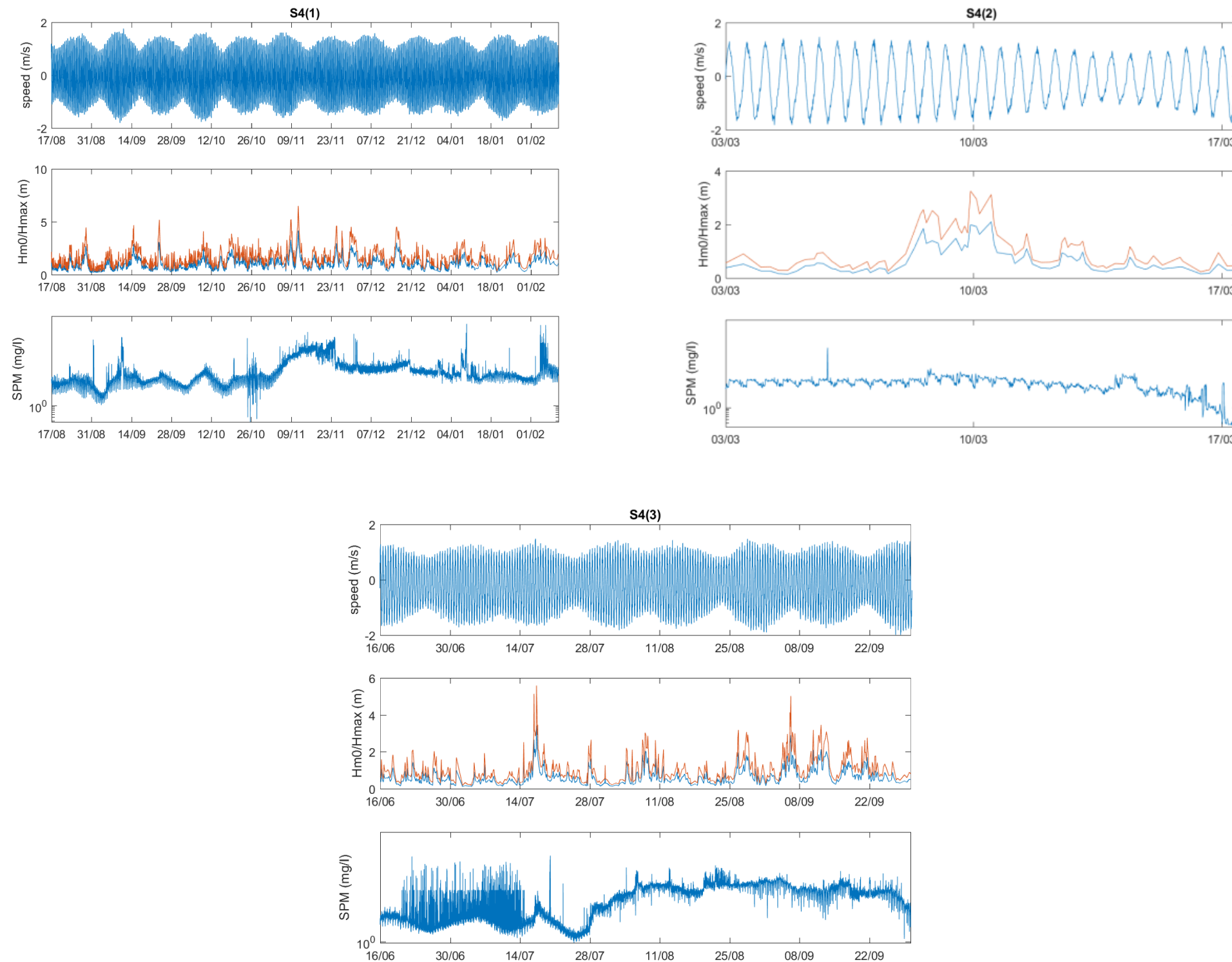


Figure 42. Time series of SPM concentration, significant wave height (H_{s0}), maximum wave height (H_{max}) (orange), and current velocity for all deployments at monitoring station, s4. Data Source: Horizon (2012).

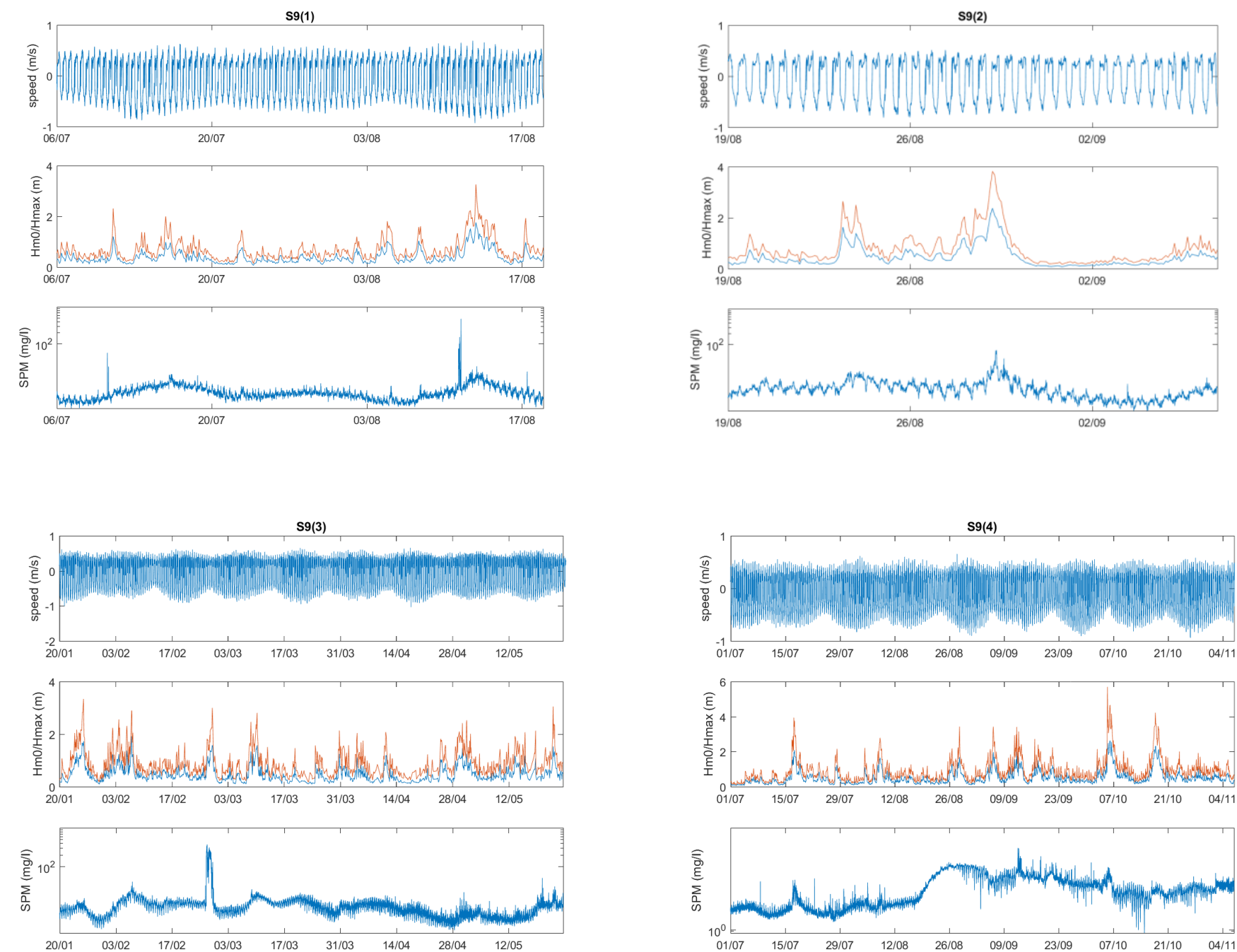


Figure 43. Time series of SPM concentration, significant wave height (H_{m0}), maximum wave height (H_{max}) (orange), and current velocity for all deployments at monitoring station, s9. Data Source: Horizon (2012).

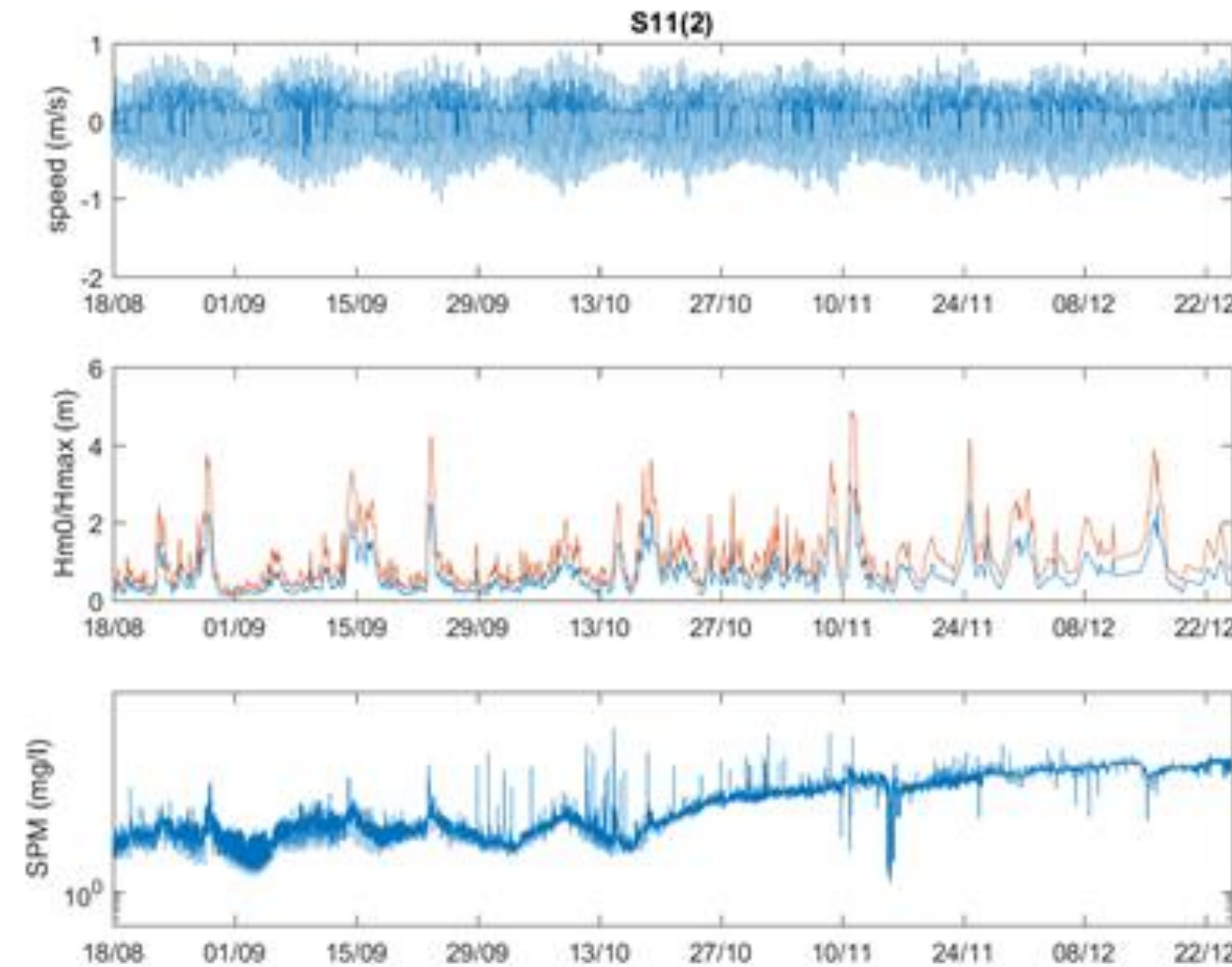


Figure 44. Time series of SPM concentration, significant wave height (H_{m0}), maximum wave height (H_{max}) (orange), and current velocity for all deployments at monitoring station, s11. Data Source: Horizon (2012).

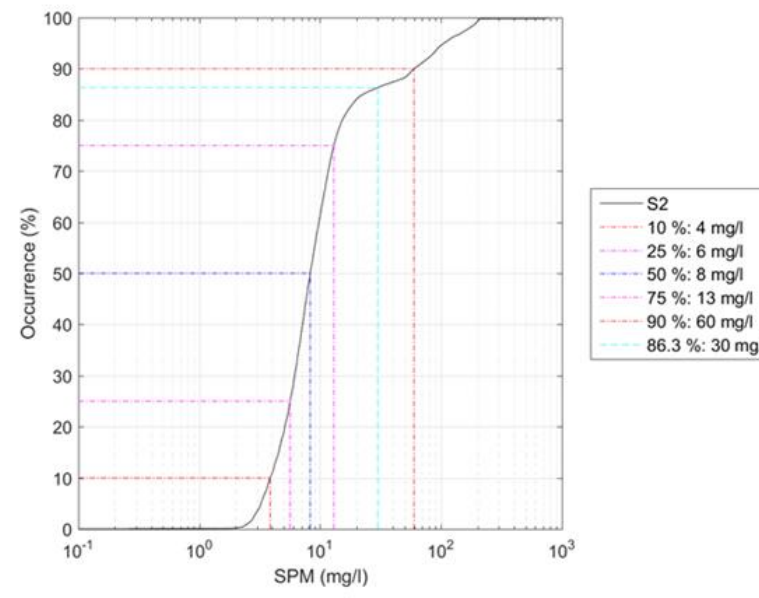
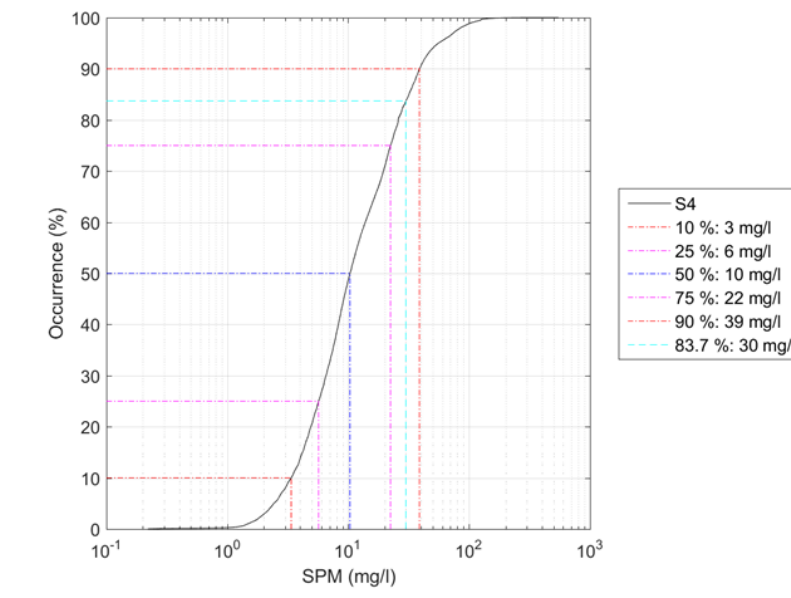
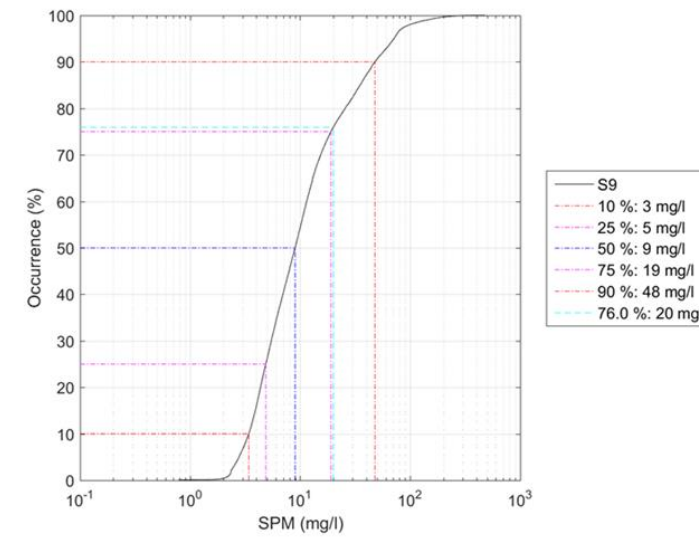
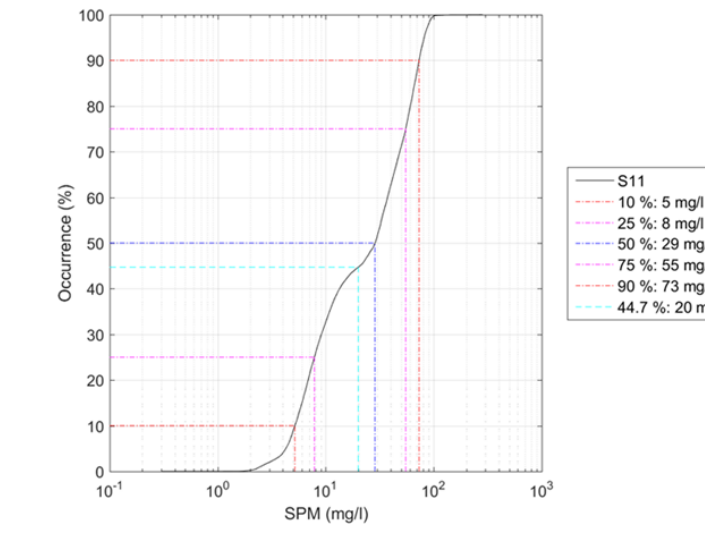

Station s2

Station s4

Station s9

Station s11

Figure 45. SSC exceedance plots, by station. The background suspended sediment concentration values for offshore sites (30 mg l^{-1}) and inshore sites (20 mg l^{-1}) are marked. Data source: Horizon (2012).

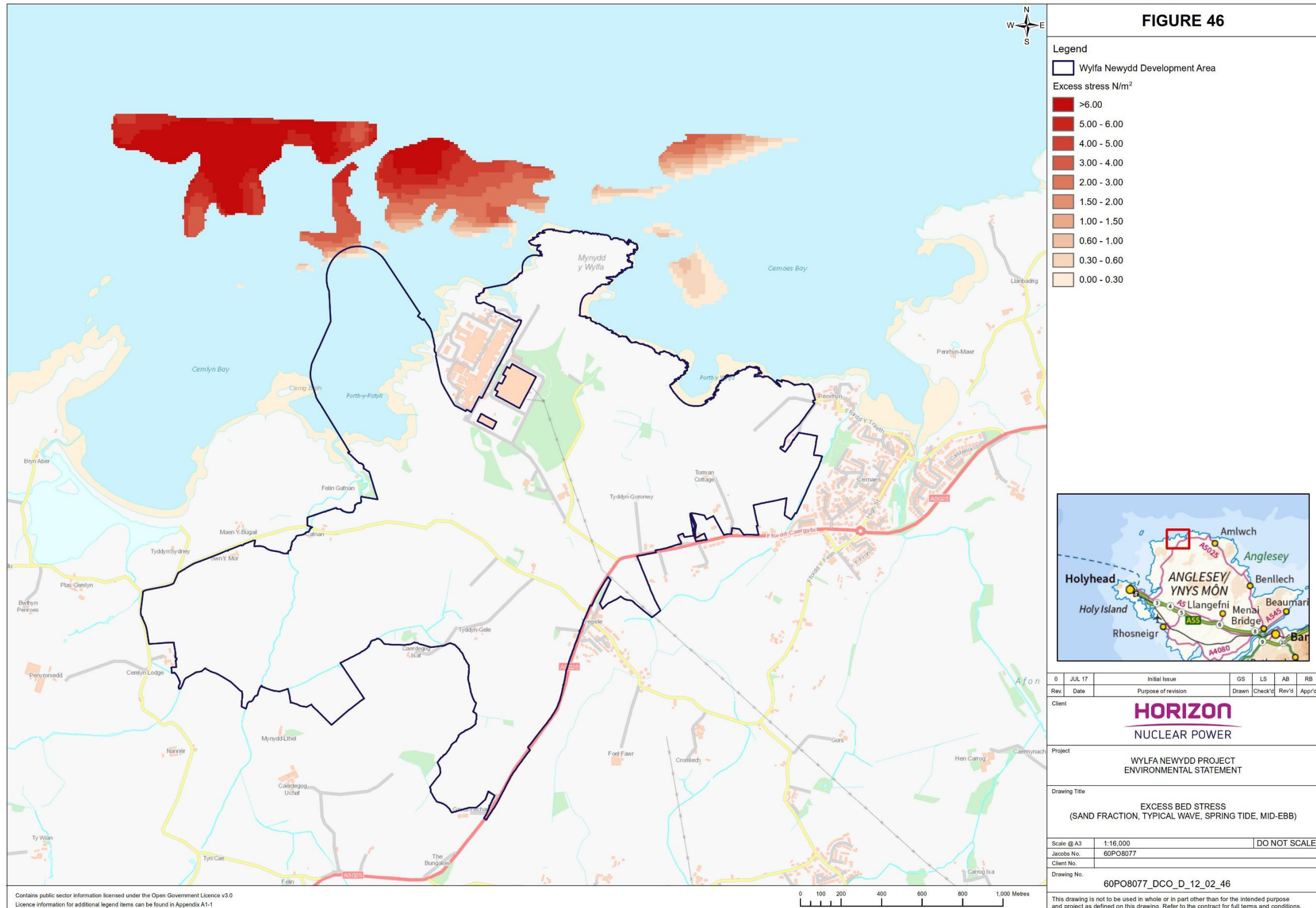


Figure 46. Geospatial excess bed stress plot for the sand fraction for a Spring tide, mid-ebb condition (the strongest currents) with a typical wave scenario (H_{mo} 0.9 m, 228°).

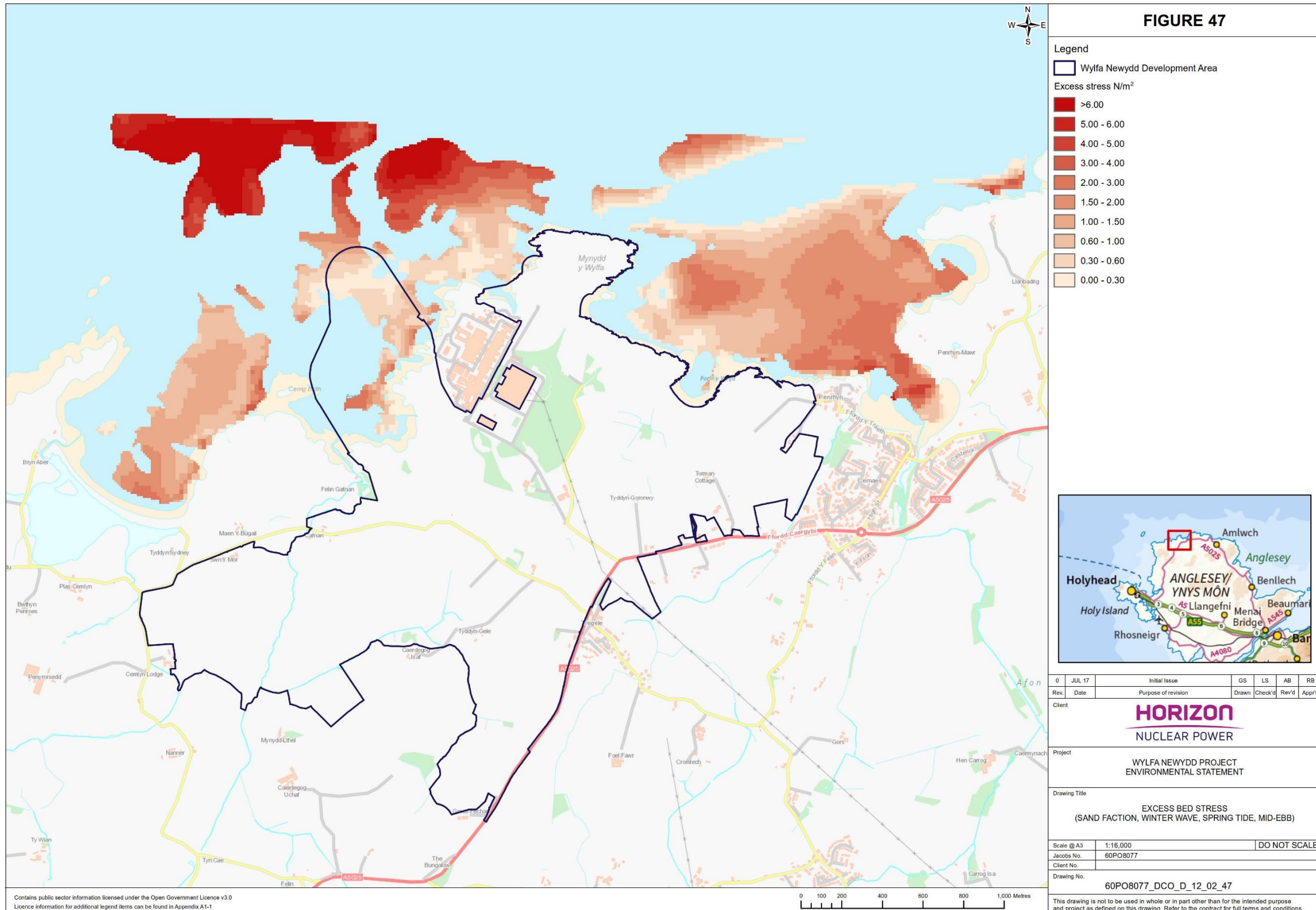


Figure 47. Geospatial excess bed stress plot for the sand fraction for a Spring tide, mid-ebb condition (the strongest currents) with a winter wave scenario (H_{mo} 2.0 m, 228°).

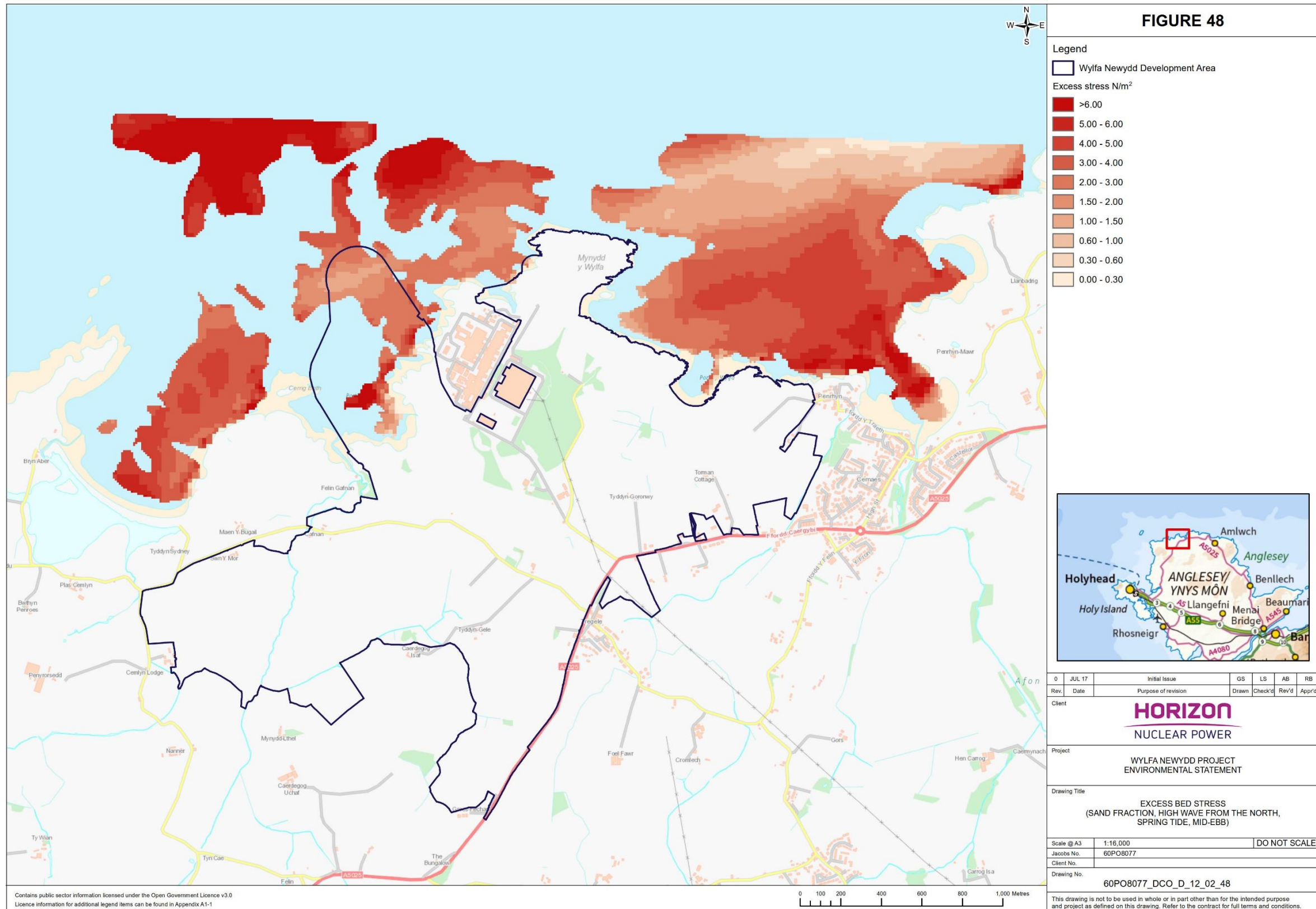


Figure 48. Geospatial excess bed stress plot for the sand fraction for a Spring tide, mid-ebb condition (the strongest currents) with an high wave from the north (98%ile) (H_{m0} 2.85 m, 358°).

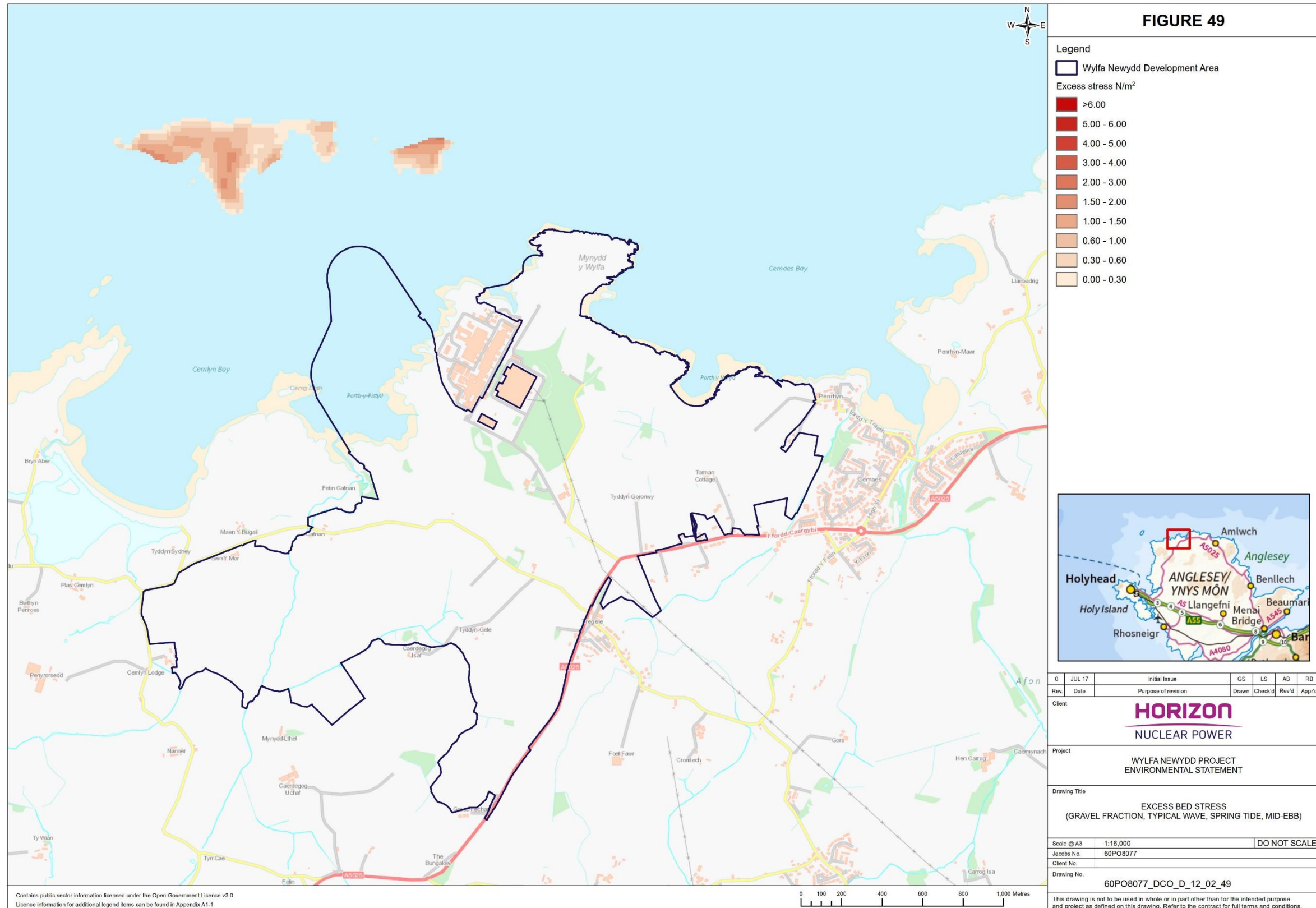


Figure 49. Geospatial excess bed stress plot for the fine gravel fraction for a Spring tide, mid-Ebb condition (the strongest currents) with a typical wave scenario (H_{m0} 0.9 m, 228°).

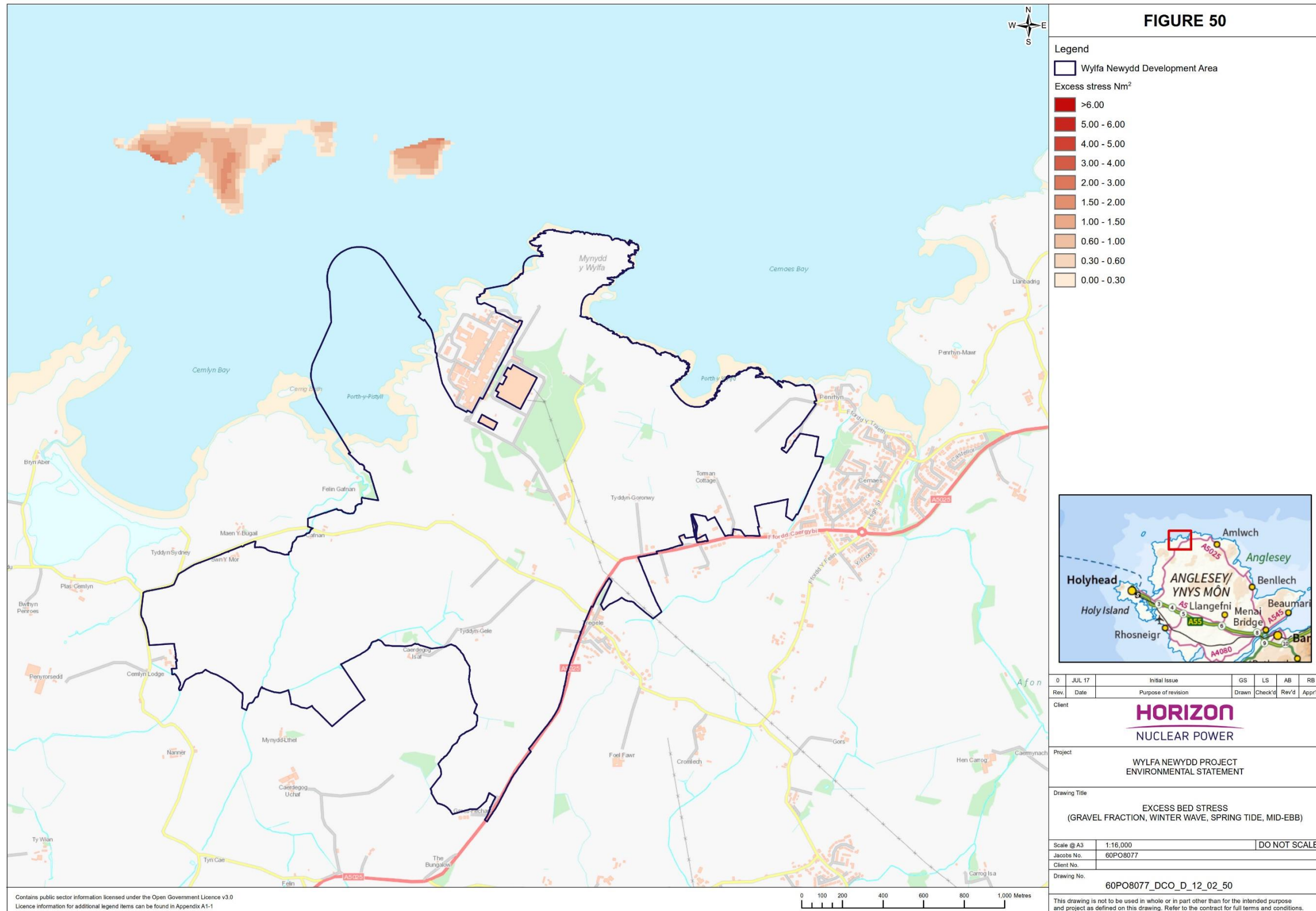


Figure 50. Geospatial excess bed stress plot for the fine gravel fraction for a Spring tide, mid-ebb condition (the strongest currents) with a winter wave scenario (H_{m0} 2.0 m, 228°).

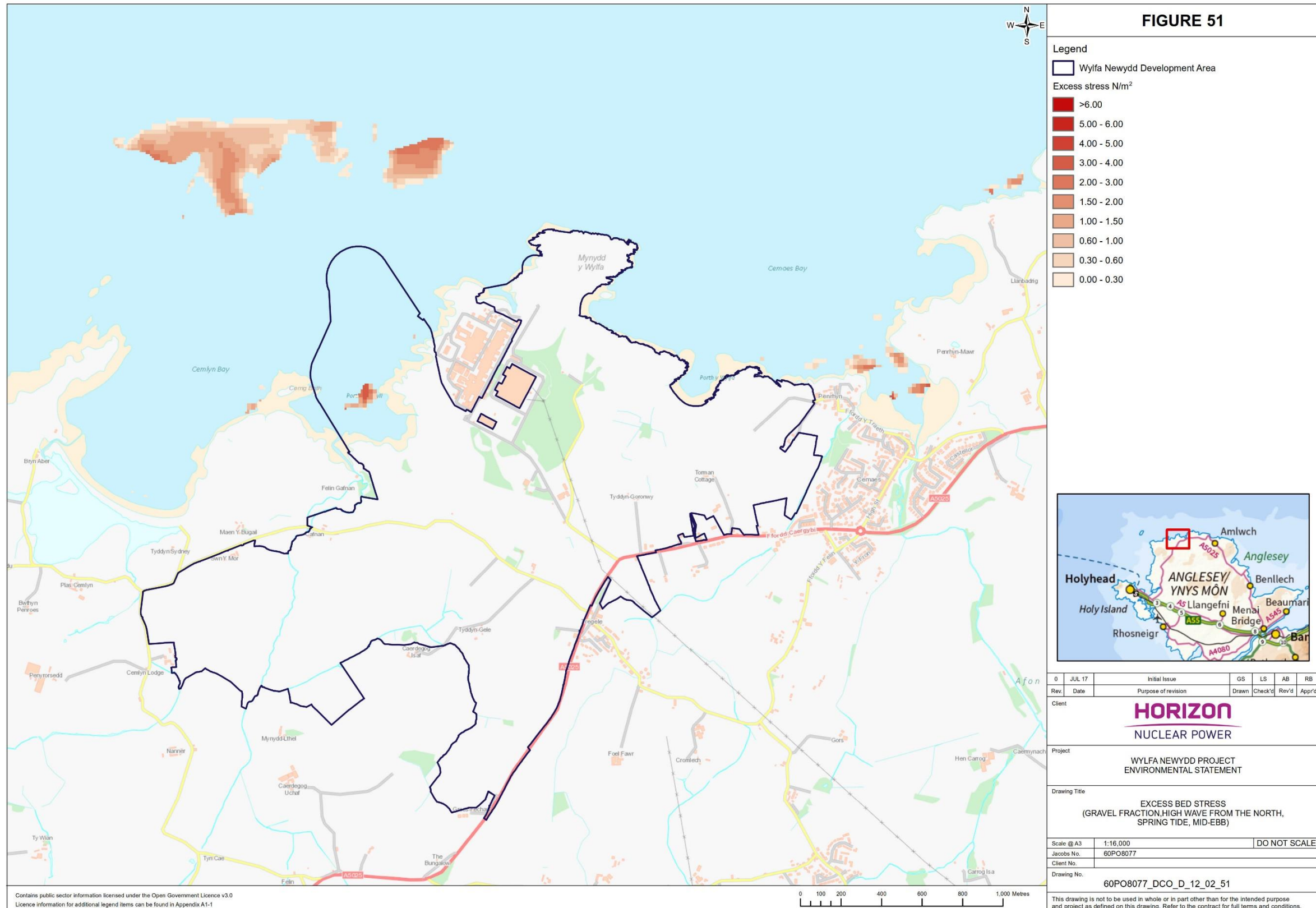


Figure 51. Geospatial excess bed stress plot for the fine gravel fraction for a Spring tide, mid-ebb condition (the strongest currents) with an high wave from the north scenario (H_{m0} 2.85m, 358°).

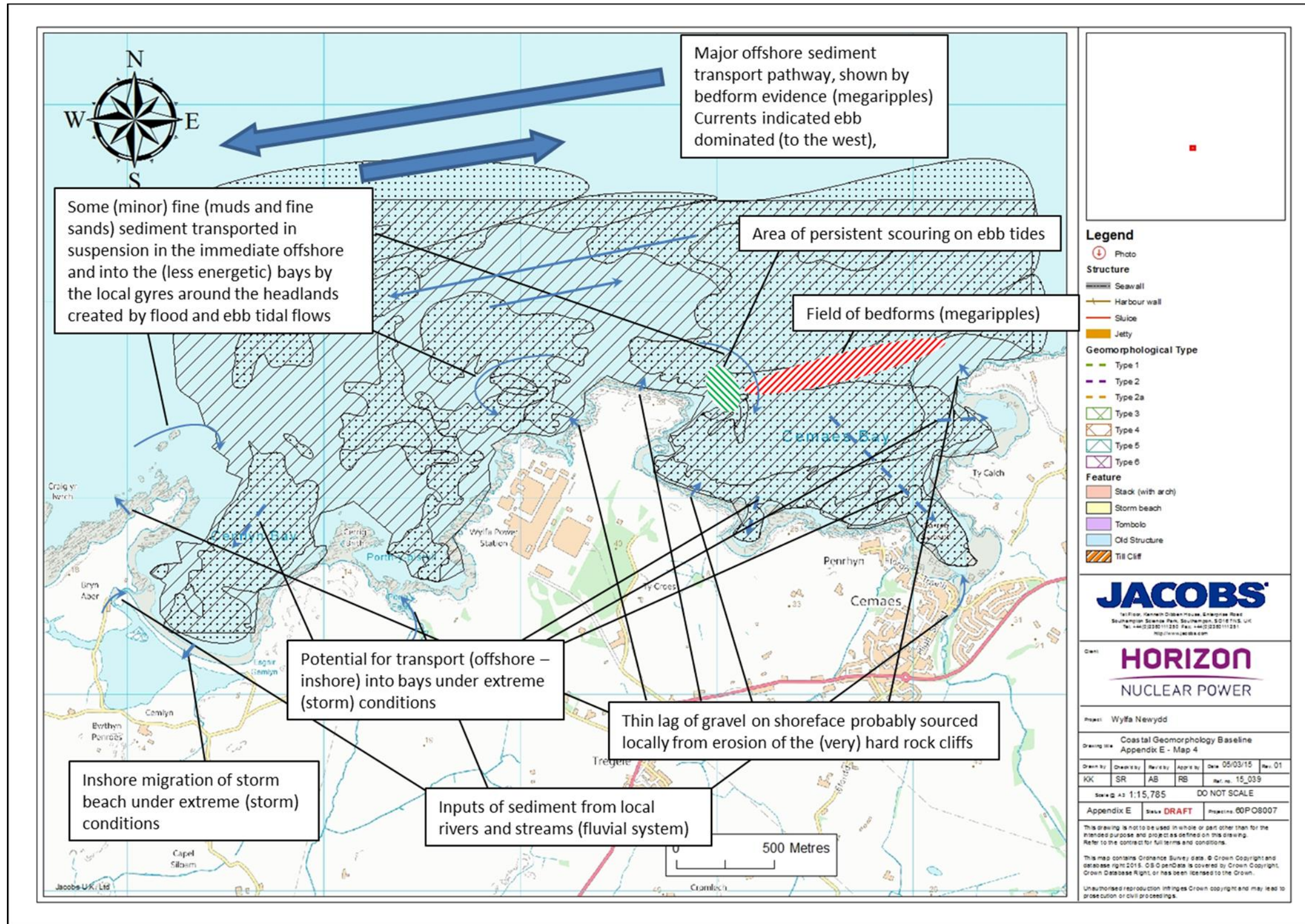


Figure 52. The conceptual understanding of the local sediment regime in proximity to Wylfa head. It has been collated from a variety of sources and informed by expert judgement. The transport pathways are indicative and the arrows represent inferred magnitudes of transport.

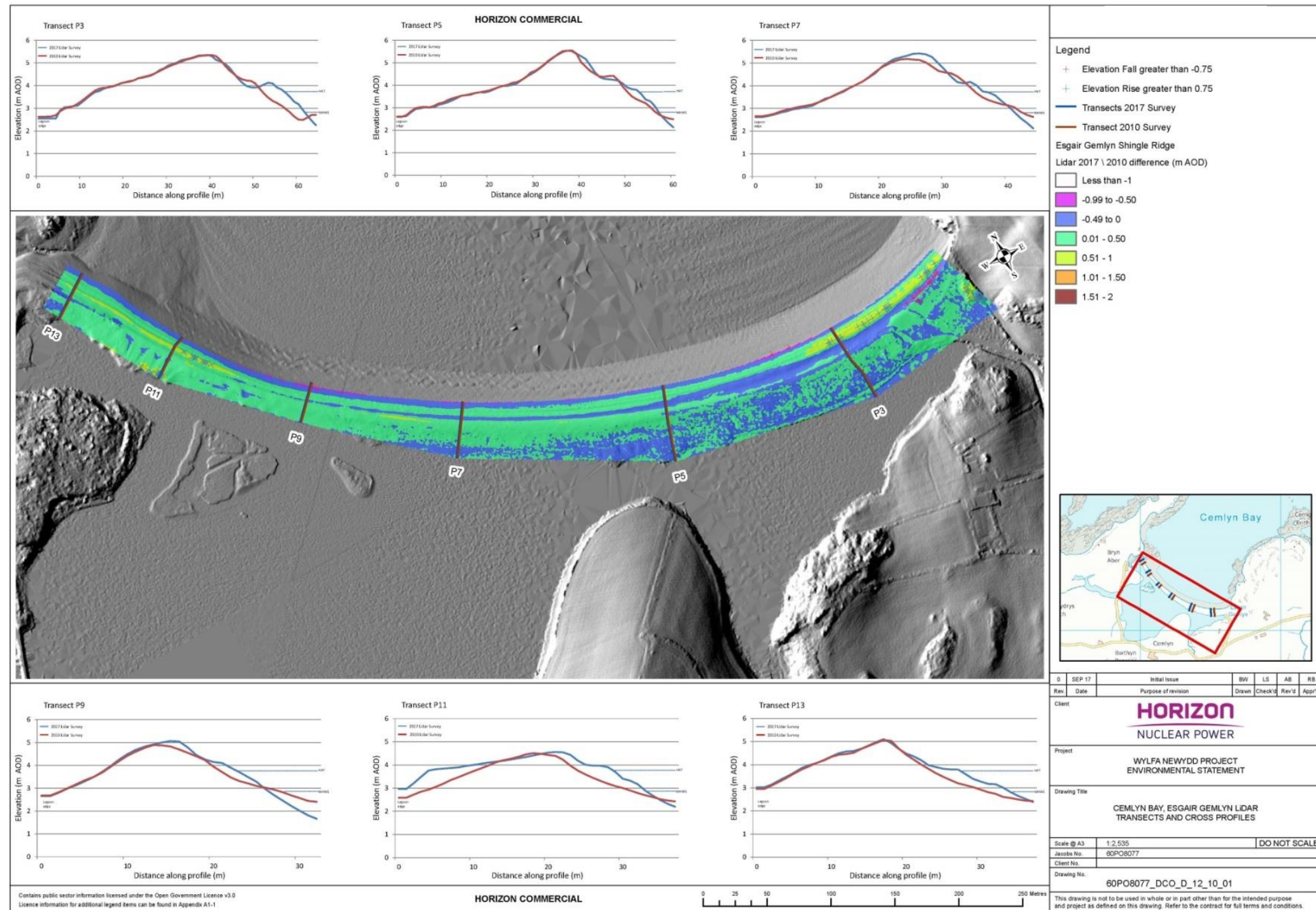
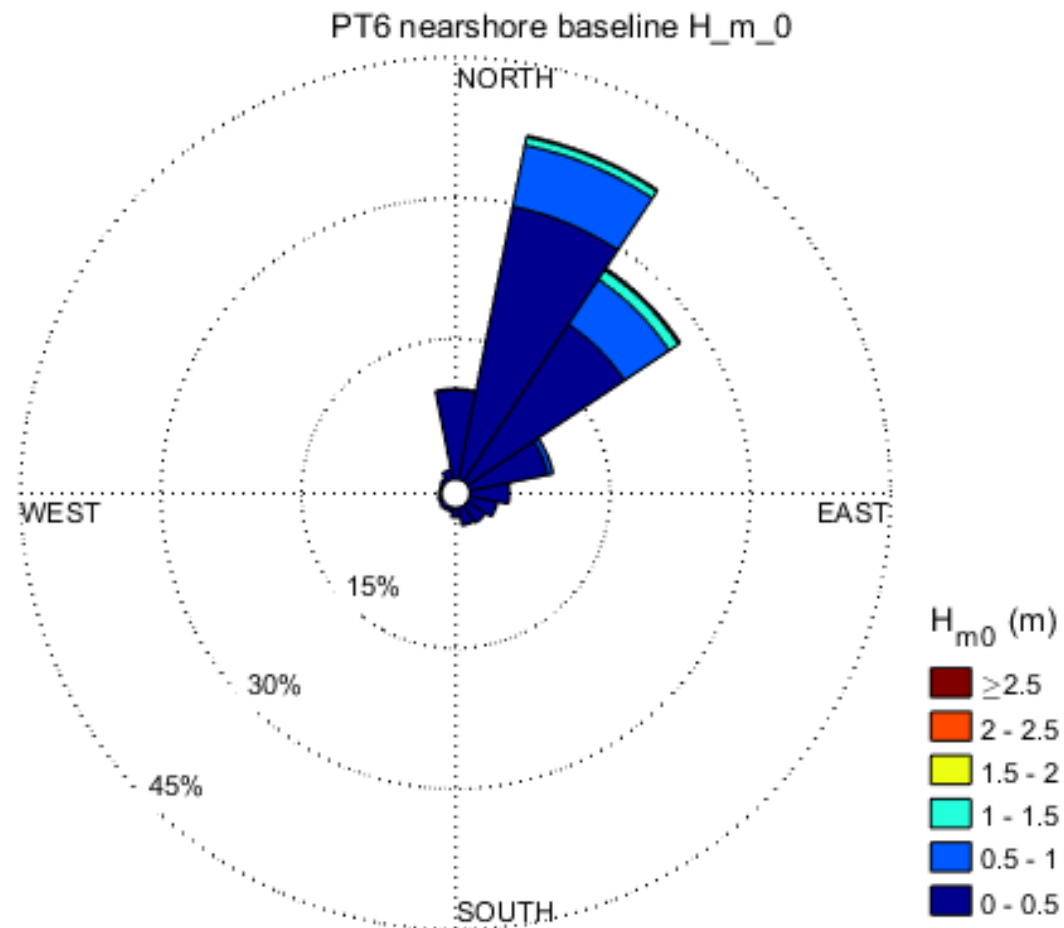


Figure 53. Comparison of 2010 and 2017 aerial LiDAR data. Data source: Jacobs UK Ltd (2017)

a)



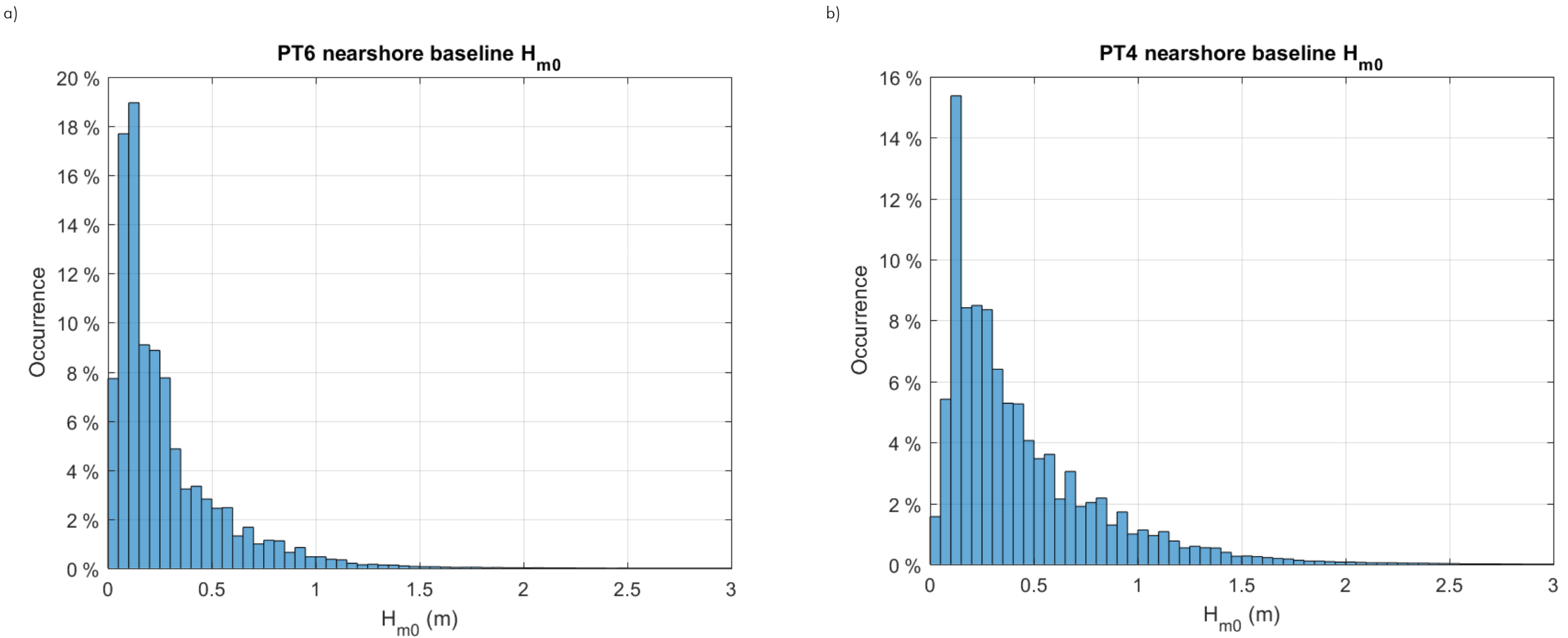


Figure 55. Frequency of occurrence of significant wave heights (H_{m0}) for the 30 year hind-cast modelled wave data at points 6 (a) and 4 (b).